Natural Ventilation Driven by Wind and Temperature Difference

Larsen, Tine Steen

Publication date:
2006

Document Version
Publisher's PDF, also known as Version of record

Natural Ventilation Driven by Wind and Temperature Difference

Ph.D. thesis by Tine Steen Larsen

ISSN 1901-7294
DCE Thesis No. 2

AALBORG UNIVERSITY
Department of Civil Engineering

Aalborg University
Department of Civil Engineering
Group of Architectural Engineering

DCE Thesis No. 2

Natural Ventilation Driven by Wind and Temperature Difference

PhD Thesis defended public at Aalborg University 020206

by

Tine Steen Larsen

June 2006

SCIENTIFIC PUBLICATIONS AT THE DEPARTMENT OF CIVIL ENGINEERING

Technical Reports are published for timely dissemination of research results and scientific work carried out at the Department of Civil Engineering (DCE) at Aalborg University. This medium allows publication of more detailed explanations and results than typically allowed in scientific journals.

Technical Memoranda are produced to enable the preliminary dissemination of scientific work by the personnel of the DCE where such release is deemed to be appropriate. Documents of this kind may be incomplete or temporary versions of papers—or part of continuing work. This should be kept in mind when references are given to publications of this kind.

Contract Reports are produced to report scientific work carried out under contract. Publications of this kind contain confidential matter and are reserved for the sponsors and the DCE. Therefore, Contract Reports are generally not available for public circulation.

Lecture Notes contain material produced by the lecturers at the DCE for educational purposes. This may be scientific notes, lecture books, example problems or manuals for laboratory work, or computer programs developed at the DCE.

Theses are monograms or collections of papers published to report the scientific work carried out at the DCE to obtain a degree as either PhD or Doctor of Technology. The thesis is publicly available after the defence of the degree.

Latest News is published to enable rapid communication of information about scientific work carried out at the DCE. This includes the status of research projects, developments in the laboratories, information about collaborative work and recent research results.

Published 2006 by
Aalborg University
Department of Civil Engineering
Sohngaardsholmsvej 57,
DK-9000 Aalborg, Denmark

Printed in Denmark at Aalborg University

ISSN 1901-7294
DCE Thesis No. 2

PREFACE

This thesis represents a part of the fulfilment for acquiring the Ph.D. degree. The thesis was presented at Aalborg University on February 2, 2006

The work made in connection to this thesis has been carried out at the Hybrid Ventilation Center at Aalborg University and on a 5 month visit at the Japanese Building Research Institute.

The work has been supervised by Professor Per Heiselberg whom I would like to thank for guidance and good advice during my work.

I would like to thank Carl Erik Hyldgård, associate professor and Torben Christensen, assistant engineer for their help with my experiments at AAU.

I would also like to thank Dr. Eng. Takao Sawachi and the staff at the Japanese Building Research Institute for their hospitality and friendliness which made me feel very welcome during my stay there.

Finally, I would like to thank my husband Ole for his great support during my PhD work and especially during my work in Japan where he was a great help in the laboratories.

Aalborg, 2006

Tine Steen Larsen

ABSTRACT

Natural ventilation is a commonly used principle when buildings are being ventilated. It can be controlled by openings in the building envelope, which open or close depending on the need of air inside the building. It can also be the simple action of just opening a door or a window to let the fresh air in.

In both cases it is often necessary to have an idea of the amount of air coming through the window. Therefore, expressions for this prediction have been developed through the last decades.

In cross-ventilation, the expressions are rather well defined and here the difficulty lies within the definition of the discharge coefficient that describes the characteristics of the opening, since it seems to fluctuate depending on the incidence angle of the wind.

In single-sided ventilation where openings only exist in one side of the building, the flow through the opening is harder to predict. The main driving forces are still wind pressure and temperature differences as with cross-ventilation, but here the turbulence in the wind and the pulsating flow near the opening also affect the flow through the opening.

From earlier work, some design expressions already exist, but none of these include the incidence angle of the wind, which is an important parameter in this type of ventilation.

Several wind tunnel experiments are made and from the results of these, a new design expression is made which includes the wind pressure, temperature difference, incidence angle of the wind and the fluctuations in pressure at the opening. A discussion is made regarding the correctness of using wind tunnel measurements for a design expression to be used outdoors, but here it is concluded from analysis of the different types of wind that this can be done with some knowledge of the differences.

Finally, the new expression is compared to results found from outdoor full-scale measurements with good agreement.

CONTENTS

NOMENCLATURE

SYMBOLS:

A	Area of the opening	[m²]
Ar	Archimedes number	[-]
C	Concentration	[m³/m³]
C_0	Background conc.	[m³/m³]
C_D	Discharge coefficient	[-]
C_p	Pressure coefficient	[-]
f_p	Effective ventilation rate	[-]
g	Gravitational acceleration	[m/s²]
h	Height	[m]
H	Height	[m]
K_β	Constant depending on β	[-]
L	Length	[m]
$\dot{m}$	Massflow of tracergas	[m³/h]
P	Pressure	[Pa]
Q	Airflow	[m³/s]
S_x	Power spectral density	
t	Time	[sec]
T	Temperature, chapter 1 & 2	[K]
T	Temperature	[°C]
U	Velocity	[m/s]
V	Volume	[m³]
W	Nondimensional parameter	[-]
W	Width	[m]
$x[\,]$	Samples in frequency domain	
$X[\,]$	Samples in time domain	
z	Height above ground	[m]

GREEK LETTERS:

β	Slope in log PSE (chapter 3)	
β	Incidence angle	[°]
δ	Non-dimensional width	[-]
Δ	Difference	
γ	Polytrophic exponent	[-]
ω	Decrease in volume of the original air inside the enclosure	[m³]
ρ	Density	[kg/m³]
$\sigma_{\Delta Cp}$	Standard deviation of ΔC_P	[-]
$\sigma_{\Delta P}$	Standard deviation of ΔP	[-]

SUBSCRIPTS:

a	Atmospheric
e	External
eff	Effective
H	Height = h
i	Internal
in	Ingoing
L	Local
m	mean value
ref	Reference height
V	Volume
0	Reference level or neutral plane (ch.1+2)
0	Time=0
10	Height = 10 m

CHAPTER 1

Introduction to natural ventilation

As an introduction to this thesis, some of the characteristics of natural ventilation are described. At first a general introduction to natural ventilation is made. Afterwards, the weather conditions are described together with a small description of the differences between wind measurements made in a wind tunnel (mechanical wind) and outdoors (natural wind). Finally, the driving forces in natural ventilation are described. A more detailed description of the main aim of this work will be presented in chapter 2.

1. INTRODUCTION TO NATURAL VENTILATION

In Denmark approximately half of the energy consumption is used for heating and ventilating buildings. During 2006 the Danish building regulations will be changed and thereby the energy consumption in new buildings will be reduced by 25-30%, but still it is necessary to consider alternative ways to save energy with the unstable oil prices and the uncertain political situation in the oil producing countries.

An average person today spends about 90% of his time indoors. Therefore, it is important to maintain focus on a good and healthy indoor environment, but this does not exclude saving energy. To be more independent of the oil as an energy source and also to reduce the damaging outlets to the environment, an increasing use of sustainable technologies such as solar energy, better use of daylight and use of natural ventilation is more and more often discussed when new buildings are built or old ones are renovated. Unfortunately, not all sustainable technologies can be used in all climates, since the weather conditions are an important factor in these technologies.

Considering natural ventilation it can be difficult to keep stable indoor conditions, since outside weather conditions often change. Also, not all types of buildings are suitable for natural ventilation, since this type of ventilation sets some requirements for e.g. internal heat load in the building, depth of the rooms, room height and surroundings.

In the field of natural ventilation there are typically two types of ventilation named after the position of the openings in the outer walls. In *cross-ventilation* (see Figure 1.1) there are openings in more than one wall so that the air crosses the room. In *single-sided ventilation* (see Figure 1.2) there are only openings in one wall.

The driving forces in natural ventilation are temperature differences and wind pressure differences. For cross-ventilation, the main driving force will be the wind as long as the openings are in the same height. With a difference in height the thermal buoyancy will also influence the airflow rate. In single-sided ventilation the air-change rate is much dependent on the shape of the opening. High openings will be more affected by temperature differences than low openings. Wide openings will be more affected by the wind than small and narrow openings. In single-sided ventilation also the size of the turbulent eddies and pulsations in the flow is of great importance.

Figure 1.1. *The principle in cross-ventilation. /By og Byg 202/*

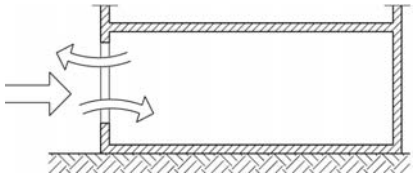

Figure 1.2. *The principle in single-sided ventilation. /By og Byg 202/*

1.1 OUTDOOR WEATHER CONDITIONS

Since the driving forces in natural ventilation are temperature and wind, the outdoor conditions are an important factor when talking about natural ventilation.

For building simulations made under Danish conditions, the Danish "Design Reference Year" (DRY) is applied. DRY is a database with artificially made weather data. The data in DRY are found from analysis of data measured in the period between 1975 and 1990. The criterion for the weather data in DRY was that it should represent the general weather characteristics from the different months.

The average temperature found from DRY and the typical variation during 24 hours are shown in Table 1.1.

Month	Average temperature [°C]	Typical variation during 24 h [°C]
January	-1	5.0
February	-0.5	6.0
March	1.9	7.5
April	5.9	9.0
May	10.9	11.5
June	15.2	12.0
July	16.1	12.0
August	15.9	11.0
September	12.9	9.0
October	8.9	7.0
November	4.5	5.0
December	0.8	5.0

Table 1.1. *Weather data taken from DRY.*

To give an idea of the temperature and wind distribution in Denmark, the duration graphs for the temperatures and wind speeds are plotted for all the hours in DRY. This is done in Figure 1.3.

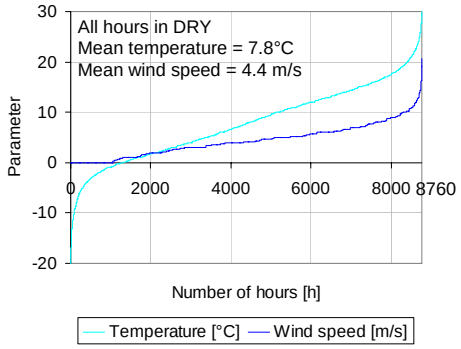

Figure 1.3. *Duration graphs for temperature and wind speed in DRY calculated for all hours during a year.*

Since natural ventilation is most often used in office buildings and other buildings where people are only present during an 8 hour period every day, the duration graph is also made for the hours in the time interval between 8 and 16. This is done in Figure 1.4.

If the results in Figure 1.3 and Figure 1.4 are compared it is seen that the mean temperature is higher during daytime which doesn't come as any surprise, since the lowest temperatures always occur during the night. It is also seen that the highest wind speeds appear during the day, which is quite practical since you need the highest air changes and thereby the highest pressures during daytime.

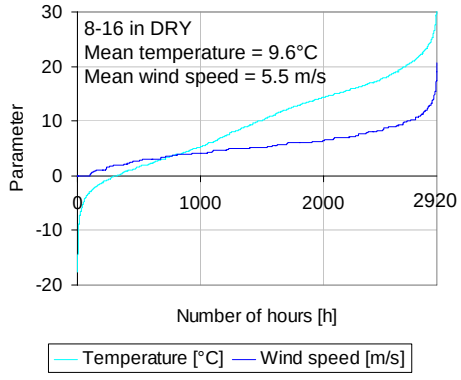

Figure 1.4. *Duration graphs for temperature and wind speed in DRY calculated for the period between 8 and 16 o'clock during a year.*

Another important parameter when talking about weather data is the wind direction, since this also will affect the pressure difference and the air flow though an opening. The wind rose for all hours during the year (in DRY) is shown in Figure 1.5. Here it is seen that the main part of all wind in Denmark blows from west to south west. This fact became a problem during the measurements for this thesis since almost all measurements made outdoors have this wind direction. This is described in more detail in *chapter 5*.

Today DRY is used for all simulations in Denmark disregarding the geographical position of the building. It can be discussed whether this estimation of the same weather in the entire country is correct. To give an idea of the local differences, weather data from five different locations are compared with DRY. The locations consist of both coastal areas and country areas. The locations are shown in Figure 1.6.

The results of the measured mean temperature and wind speed at the five different locations are shown in Table 1.2. Here it is seen that the temperature is varying slightly around the value used in DRY, but the average wind speeds differ much. Since the square of the wind speed is used when the pressure difference is calculated (see more in section 1.3), the results from simulation with wind speed data from DRY should be considered with care especially in the cases where the building is situated close to coastal areas.

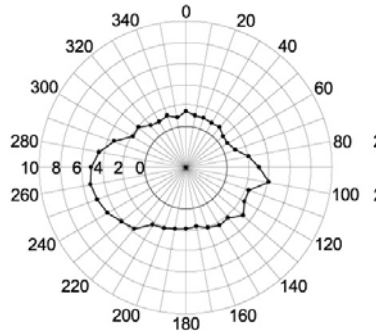

Figure 1.5. *The wind rose found from DRY for all hours during a year. /By og Byg 202/*

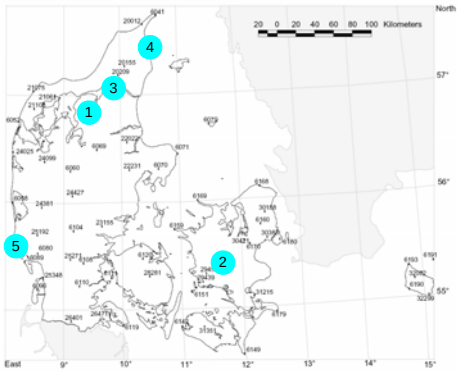

Figure 1.6. *Location of the different weather stations. /DMI 99/*

Station	Name	Average temperature [°C]	Average wind speed [m/s]
DRY	-	7.8	4.4
1	Hornum	8.0	*3.0*
2	Alstedgård	8.4	*4.7*
3	Aalborg	7.8	*5.3*
4	Frederikshavn	7.6	6.1
5	Blåvandshuk	8.5	7.2

Table 1.2. *Weather data calculated for the period 1987-2002 at the five locations.*

1.2 WIND CHARACTERISTICS

During calculations of air flows in natural ventilation, knowledge of the wind characteristics is an important factor. The level of the velocity and the direction of the wind set the amount of air coming through the opening(s). Especially in single-sided ventilation, knowledge of the fluctuations (turbulence) in the wind also becomes important, since the main air exchange happens through pulsating flows in the opening if only wind is considered. This is discussed further in section 1.2.1 where the problem with wind tunnel measurements compared to outdoor measurements is introduced.

If the wind velocity is taken from meteorological data it is often measured in large open spaces and a recalculation is therefore necessary to find the level of the wind velocity, e.g. in the middle of an urban area. This calculation of the correct velocity profile can be made from the expression in (1.1). /By og Byg 202/

$$U_h = U_{10} \cdot k \cdot h^{\alpha} \qquad (1.1)$$

where the parameters k and α depend on the terrain in the following way:

	k	α
Open, flat terrain	0.68	0.17
Terrain with scattered growth	0.52	0.20
Suburban area	0.35	0.25
Urban area	0.21	0.33

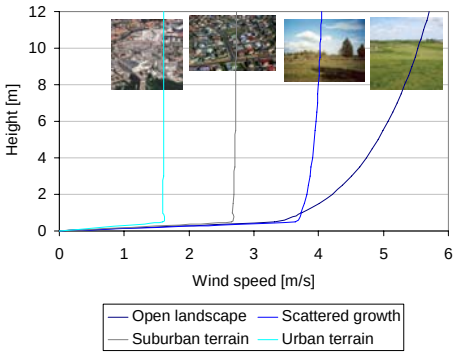

Figure 1.7. *Wind profiles with U_{10} = 5.5 m/s*

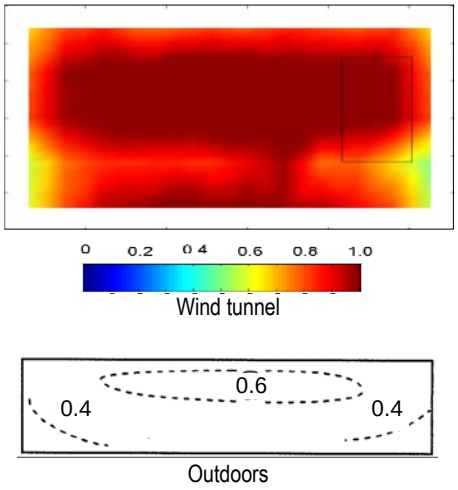

Figure 1.8. *The pressure distribution found in the wind tunnel and outdoors on the front wall of the building with incidence angle = 0°.*

An example of the different velocity profiles calculated for U_{10}=5.5 m/s is shown in Figure 1.7. Here it is seen how the shape of the boundary layer becomes steeper in urban areas compared to open landscape where the more traditional profile is found.

1.2.1 DIFFERENCES IN NATURAL AND MECHANICAL WIND

During the experiments made in connection with this thesis, measurements of wind velocities were made in a wind tunnel and outdoors. Since the results from these two locations will be compared, it is important to know the difference between them. A more detailed analysis of this is made in *chapter 3,* but the main differences will shortly be presented here.

In outdoor wind (natural wind) there will always exist a boundary layer shaped as described in the previous section. In the wind tunnel used in these experiments where the wind is created by mechanical fans (mechanical wind), the velocity profile that represents the wind will be uniform since all fans are working at the same frequency. The effect of this difference is unknown, but the difference in the results will be greatest in open flat landscapes, since the velocity profiles in urban areas, where these measurements are made, are rather flat outdoors too. If the pressure distributions in the two cases are compared (see Figure 1.8), the pressure distribution at the wind tunnel building differs from a normal pressure distribution by having a high pressure near the ground too. This is due to the flat wind tunnel velocity profile that also provides high velocities near the ground on the contrary to a normal profile outdoors. If only the pressure distribution at the opening area is considered, it looks the same as on the outdoor building and therefore it is assumed that the difference caused by the different velocity profiles in mechanical and natural wind is insignificant in this case.

Another difference in the natural and mechanical wind is the content of eddies in the wind. The size of these eddies depends on the surroundings and varies in scale from millimetres to kilometres. Outdoors, the limitation of these whirls can be other buildings, plantations or even a change in wind direction at a very large scale and down to the shape of a specific opening in a building. In the wind tunnel, the sides of the tunnel create the limits for the size of eddies. Here the wind always comes from only one direction which will not change during the measurements unless you rotate the entire building. Therefore, the size of the largest scale eddy is expected to be smaller in the wind tunnel than outdoors.

The level of turbulence intensity is also different in the two types of wind. In the wind tunnel, the turbulence intensity is less than 5% in front of the building, but in the outdoor experiments it is measured to 35%-45% on the roof of the building. The difference will especially influence on the airflow through the openings in single-sided ventilation since a main part of this airflow is driven by the turbulence in the wind.

1.3 DRIVING FORCES IN NATURAL VENTILATION

Natural ventilation is driven by pressure differences created by either temperature differences (thermal buoyancy), wind on the building or a combination of these two. The derivation of these pressure differences is made in the following sections.

From the pressure differences, an air flow rate through the opening(s) can be calculated. This calculation depends on the type of natural ventilation (cross-ventilation or single-sided ventilation) and a detailed presentation of the different expressions for calculations of flow rates is made in *chapter 2*.

1.3.1 THERMAL BUOYANCY

In the case where the natural ventilation is driven only by thermal buoyancy, the pressure difference is created by different densities in the warm and cold air, e.g. inside and outside a building. The exchange of air between inside and outside will happen through one or more openings in the outer wall. The pressure difference is increased with the height either between the openings or, if only one opening exists, the height of the opening itself.

The pressure at a single point at level *H* above the reference height (floor level) can be expressed as

$$P = P_0 - \rho_0 \cdot g \cdot H \tag{1.2}$$

If expression (1.2) is applied to the internal (*i*) and external (*e*) air, expressions (1.3) and (1.4) are found. In these expressions the temperature distribution is regarded as uniform and ρ_i and ρ_e are therefore constant.

$$P_i = P_{i,0} - \rho_i \cdot g \cdot H \tag{1.3}$$

$$P_e = P_{e,0} - \rho_e \cdot g \cdot H \tag{1.4}$$

The pressure difference between internal and external air can then be found by (1.5)

$$\Delta P = P_{e,0} - P_{i,0} - (\rho_e - \rho_i) \cdot g \cdot H \tag{1.5}$$

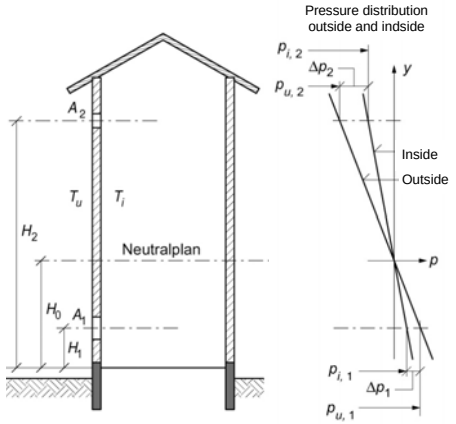

Figure 1.9. *Pressure difference around the neutral plane in a building ventilated only by thermal bouyancy. /By og Byg 202/*

Whether the air enters or exits a building at a certain height depends on the position of the opening compared to the neutral plane in the building, see Figure 1.9. At the neutral plane the pressure difference (ΔP) is zero. Above this plane an overpressure exists in the building that will generate an outgoing air flow. Below the neutral plane there will be an underpressure in the building compared to outside which will make the air flow into the building.

At the neutral plane ($H=H_0$) where $\Delta P=0$, expression (1.5) becomes

$$P_{e,0} - P_{i,0} = (\rho_e - \rho_i) \cdot g \cdot H_0 \tag{1.6}$$

From the equation of state it can be found that

$$\frac{\rho_e - \rho_i}{\rho_i} \cong \frac{T_i - T_e}{T_e}$$

and (1.7)

$$\frac{\rho_e - \rho_i}{\rho_e} \cong \frac{T_i - T_e}{T_i}$$

and (1.6) can therefore be rewritten to

$$P_{e,0} - P_{i,0} = \rho_i \cdot g \cdot H_0 \cdot \frac{T_i - T_e}{T_e} \tag{1.8}$$

Likewise the pressure in the height H_1 where $\Delta P \neq 0$ can be found as

$$\Delta P_{H=H_1} = P_{e,0} - P_{i,0} - \rho_i \cdot g \cdot H_1 \cdot \frac{T_i - T_e}{T_e} \tag{1.9}$$

If expression (1.8) is inserted into expression (1.9) the pressure difference in H_1 can be expressed only from the internal and external temperatures, the gravitational acceleration and the density of air. Positive values of the pressure difference in expression (1.10) (H_1 below the neutral plane) shows that the pressure outside the building is higher than inside.

$$\Delta P_{H=H_1} = \rho_i \cdot g \cdot H_0 \cdot \frac{T_i - T_e}{T_e} - \rho_i \cdot g \cdot H_1 \cdot \frac{T_i - T_e}{T_e} = \rho_i \cdot g \cdot (H_0 - H_1) \cdot \frac{T_i - T_e}{T_e} \quad (1.10)$$

From (1.10) it is seen that the pressure difference is increased with increasing height difference and/or increasing temperature difference.

1.3.2 WIND

When natural ventilation is driven only by wind, the pressure difference is created by the wind speed and the direction of the wind. The wind will then make an overpressure at the windward side of the building and an underpressure at the leeward side and the parallel sides of the building. This is illustrated in Figure 1.10.

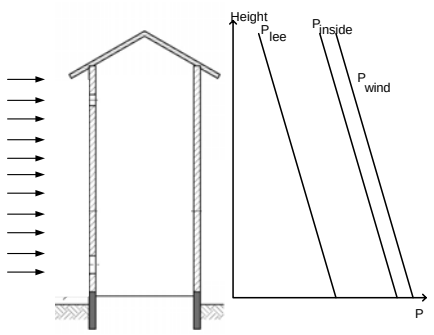

Figure 1.10. *Pressure differences created by wind on the building.*

The pressure created by the wind on the building is described in (1.11). It is calculated by multiplying a nondimensional pressure coefficient (C_p) with the dynamic pressure.

$$P_{wind} = C_p \cdot \frac{1}{2} \cdot \rho_e \cdot U_{ref}^2 \quad (1.11)$$

The C_p-coefficient is determined by the shape of the building, the wind direction and the surrounding terrain. An example of the distribution of C_P on a building is shown in Figure 1.11.

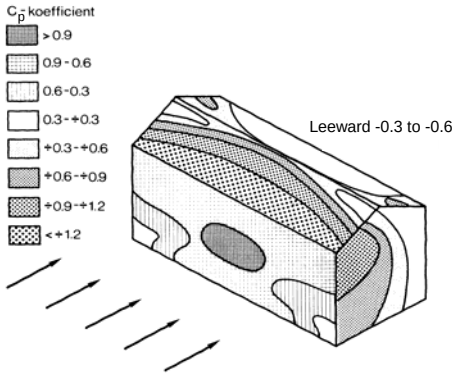

Figure 1.11. *Example of C_p-values on a building.*

The value can be calculated directly from the measurements if these are accurate enough. This is done in the first experiments made in this work, but in the full-scale outdoor experiments the calculations failed and table values are used instead.

From expression (1.11) the pressure difference between the inside and outside of the building can be calculated. This is done in expression (1.12).

$$\Delta P_{wind} = C_p \cdot \frac{1}{2} \cdot \rho_e \cdot U_{ref}^2 - P_i \quad (1.12)$$

If the pressure difference across the building is needed, the difference in C_p-values on the windward and leeward side are used instead. This is done in (1.13). By using this expression P_i disappears from the calculation of the pressure difference.

$$\Delta P_{wind} = (C_{p,windward} - C_{p,leeward}) \cdot \tfrac{1}{2} \cdot \rho_e \cdot U_{ref}^2 = \Delta C_p \cdot \tfrac{1}{2} \cdot \rho_e \cdot U_{ref}^2 \quad (1.13)$$

The reference velocity used in the expressions is normally the velocity at roof height, but since some sources instead use the velocity at 10 m's height, it is important always to make sure how U_{ref} is defined according to the source.

1.3.3 COMBINATION OF THERMAL BOUYANCY AND WIND

Most often the pressure differences in natural ventilation will be created as a combination of thermal buoyancy and wind. The total pressure across an opening is found as a summation of the pressure created by buoyancy (exp. (1.10)) and wind (exp. (1.12)). This is shown in (1.14).

$$\begin{aligned} \Delta P &= \Delta P_{wind} + \Delta P_{bouyancy} \\ &= \left(C_p \cdot \tfrac{1}{2} \cdot \rho_e \cdot U_{ref}^2 - P_i\right) + \left(\rho_e \cdot g \cdot (H_0 - H_1) \cdot \frac{T_i - T_e}{T_i}\right) \end{aligned} \quad (1.14)$$

CHAPTER 2

Calculation of natural ventilation

This chapter gives an insight into earlier work done in the field of natural ventilation. The chapter is written to give an idea of what kind of experiments and analytical ideas other researchers have used in their work and what might be a good idea to use or maybe improve or further develop in this work.

2. CALCULATION OF NATURAL VENTILATION

Through the last decades different research has been made with the aim of developing expressions for calculation of airflows in natural ventilation.

In calculations with cross-ventilation the expressions are reasonably well defined so in these calculations one of the main problem lies within the determination of the nondimensional pressure coefficient and discharge coefficient. The calculations with cross-ventilation are described in 2.1.

In the work with single-sided ventilation the calculation of airflows is more difficult because of the fluctuations in the airflow in this type of ventilation. The calculations and problems with this type of ventilation are described in section 2.2 together with some of the work made until now.

In section 2.3 a general approach with nondimensional parameters for design of natural ventilation is presented.

Finally, in section 2.4, the aim of this work is set up from some of the problems found during the reading of other researchers' work. This section will be used as a guideline for the work in this thesis.

2.1 CALCULATION OF CROSS-VENTILATION

Since cross-ventilation is much more used and also simpler to calculate than single-sided ventilation the knowledge of the airflow in this type of ventilation is more thorough. Here the flows induced by either thermal buoyancy, wind or a combination are presented together with other work made in this area. The theory with airflows driven by thermal buoyancy can also be applied in single-sided ventilation.

2.1.1 AIRFLOWS DRIVEN BY THERMAL BOUYANCY THROUGH MORE THAN ONE OPENING

The main importance with airflows driven by thermal buoyancy is to have openings at different heights in the building. In this case it is of no importance whether the openings are in different walls in the building and therefore this section is also valid for single-sided ventilation with more than one opening. The case with only one opening is described in 2.2.1.

The pressure difference generated by thermal buoyancy was derived in chapter 1 to be

$$\Delta P_{buoyancy} = \rho_e \cdot g \cdot (H_0 - H_1) \cdot \frac{T_i - T_e}{T_i} \qquad (2.1)$$

From the pressure difference an airflow can be found. The general way to calculate pressure driven airflows through an opening is written in (2.2). /Etheridge et al. 96/

$$Q_v = \pm C_D \cdot A \cdot \sqrt{\frac{2 \cdot |\Delta P|}{\rho}} \tag{2.2}$$

where C_D for window openings is often in the area between 0.6 and 0.75.

If (2.1) is inserted into (2.2), the airflow rate driven by thermal buoyancy through a single opening can be found from expression (2.3).

$$Q_v = \pm C_D \cdot A \cdot \sqrt{\frac{2 \cdot \left| \rho_e \cdot g \cdot (H_0 - H_1) \cdot \frac{T_i - T_e}{T_i} \right|}{\rho}} \tag{2.3}$$

If the direction of the flow is needed, $\Delta P / |\Delta P|$ can be added to expression (2.3). This is especially important if calculations with more than two openings are made and the level of the neutral plane is unknown. The neutral plane can be found through the mass balance in (2.4).

$$\begin{aligned} &\sum \textit{ingoing air} = \sum \textit{outgoing air} \\ &\Downarrow \quad \textit{two openings} \\ &\rho_e \cdot Q_{v,1} = \rho_i \cdot Q_{v,2} \end{aligned} \tag{2.4}$$

2.1.2 AIRFLOWS DRIVEN BY WIND

To calculate the airflow rate caused by wind driven natural ventilation, the pressure difference derived in chapter 1 is used. This is seen in expression (2.5) for the pressure difference across a single opening.

$$\Delta P_{wind} = C_p \cdot \tfrac{1}{2} \cdot \rho_e \cdot U_{ref}^2 - P_i \tag{2.5}$$

The pressure difference is inserted into the general expression in (2.2) and the airflow rate through a single opening is then found in (2.6).

$$Q_v = \pm C_D \cdot A \cdot \sqrt{\frac{2 \cdot \left| C_p \cdot \tfrac{1}{2} \cdot \rho_e \cdot U_{ref}^2 - P_i \right|}{\rho}} \tag{2.6}$$

Since P_i is unknown in expression (2.6), a mass balance is put up and P_i can be found from an iterative process. The mass balance for two openings is seen in (2.4).

EXPERIMENTAL WORK WITH WIND DRIVEN VENTILATION

To use expression (2.2), which originates from the Bernoulli equation, some assumptions are made. Some of the assumptions are that the flow through the opening is purely pressure driven and that pressure and velocity distributions are constant in the opening. It is also assumed that the kinetic energy in the flow is dissipated when it enters the room and therefore will not affect the airflow at the outlet opening in the building. In the work of J.P. Jensen True it is investigated whether these assumptions are correct, /True 03/ & /Heiselberg et al. 05/.

Wind tunnel experiments have been made with cross ventilated buildings with different opening sizes. The porosity φ was defined as the ratio between the opening area and the building surface area. Ratios from 0.12% to 9.1% were tested. During the experiments the flow was visualized by semolina powder at the floor of the building. The results are shown in Figure 2.1. Here it is seen how the powder is removed in areas with high velocities.

From the results it is seen that the small opening results in an airflow that is purely pressure driven. This is seen at the angle of the flow inside the building which is not affected by the wind direction outside the building.

In the experiments made with large openings it is seen that the flow direction outside the building continues inside the building and that the flow at the outlet is also affected by the flow at the inlet. In this case the kinetic energy in the "outdoor" airflow also affects the indoor airflow. In these cases expression (2.6) is not only dependent on the pressure difference as assumed when this expression is used.

In the work of Jensen True the flow can be regarded as purely pressure driven flow when φ is less than 1%.

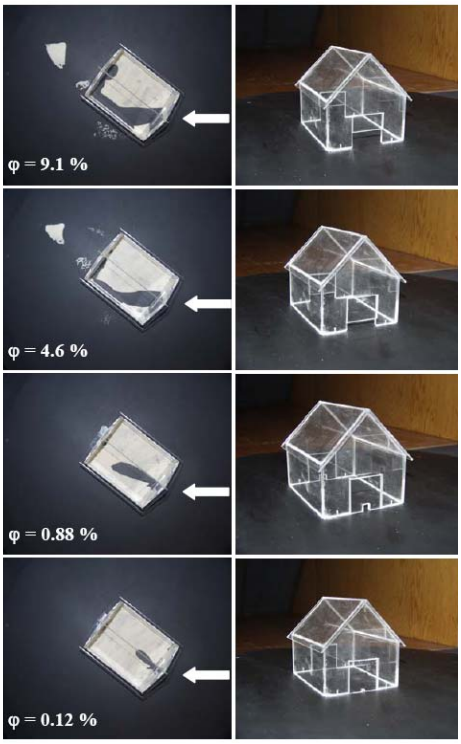

Figure 2.1. *Visualisation of the internal flow (left side pictures). Wind coming from the right of the picture. The right side figures show the corresponding openings in the model house./True 03/*

2.1.3 AIRFLOWS DRIVEN BY WIND AND THERMAL BUOYANCY

Most often the airflow in natural ventilation is affected both by wind and thermal buoyancy. In this case the pressure differences found from the separate cases (exp. (2.1) and (2.5)) are added to give the resultant pressure difference and thereby also the resultant airflow.

In the combined case the height of the neutral plane is found from the mass balance which can be reduced in the case where the C_D-values for the different openings are the same. In this case the neutral plane can be found from (2.7) /Heiselberg 05/

$$\sum_{j=1}^{n} A_j \cdot \left|H_o - H_j\right|^{1/2} \frac{H_o - H_j}{\left|H_o - H_j\right|} = 0 \qquad (2.7)$$

After the height of the neutral plane is found, the internal pressure can be found in (2.8) from an iterative solution of the mass balance. /Heiselberg 05/

$$\sum_{j=1}^{n} C_{D,j} \cdot A_j \cdot \rho_j \left(\frac{\Delta P_j}{½\rho} \right)^{½} \frac{\Delta P_j}{|\Delta P_j|} = 0 \tag{2.8}$$

With a known value of P_i and H_0 the airflow through the openings can be calculated from (2.9). /Heiselberg 05/

$$Q_V = ½ \sum_{j=1}^{n} C_{D,j} \cdot A_j \cdot \left(\frac{\left| ½ C_{p,j} \rho_e U_{ref}^2 - P_i + \frac{\rho_e \Delta T}{T_i} g(H_0 - H_j) \right|}{½\rho_j} \right)^{½} \tag{2.9}$$

EXPERIMENTAL WORK WITH CROSS-VENTILATION DRIVEN BY WIND AND THERMAL BUOYANCY

Normally, three different methods for estimating the ventilation rate in a room or building are used. These include tracer gas methods, calculation from measured velocity profiles in the openings and finally calculation of the airflow from either expression (2.3), (2.6) or (2.9) depending on whether the airflow is driven by buoyancy, wind or a combination of these two.

Figure 2.2. *The test structure in Silsoe used by M.P. Straw.*

The three methods are tested and compared in some full-scale experiments made by M.P. Straw in 2000, /Straw 00/. The work is described in his PhD-thesis “Computation and Measurement of Wind Induced Ventilation”. The thesis is made from experiments on a test structure in Silsoe, GB, see Figure 2.2. The structure is a cube (6x6x6 m) built in open landscape with two openings positioned on opposite sides each with an area of 1 m^2. The airflow is measured and calculated by both a single velocity measurement in each opening and tracer gas decay method and is also predicted by use of the expressions mentioned above. The largest difference between the three methods is between the decay method and the prediction from pressure difference, where the difference is found to be 61%.

In the thesis, predictions of the airflow are also made from CFD calculations and from two analytical techniques where he first looks at the measurements with a time domain approach, where the instantaneous pressure differences are considered together with the root mean square (rms) to give an expression for the total ventilation rate (mean and

fluctuating). The second method is a frequency domain approach where he uses Proper Orthogonal Decomposition to predict the turbulence induced wind driven ventilation. This method uses a number of analytical steps, which will not be covered here. The methods give good results although they are still lower than the airflow rate predicted by the tracer gas measurements.

In /Straw 00/ the thermal buoyancy is not included in the calculation of the airflow and it is stated that G. Papadakis have concluded that the effect of thermal buoyancy can be neglected when then wind speed is higher than 1.8 m/s. For the case where the ventilation is influenced by both wind and temperature difference he recommends that the effects are calculated separately and then the largest value is used to give an idea of the flow rate.

As it is seen in expression (2.9) it is possible to include the effect of both wind and thermal buoyancy to avoid this error.

2.2 CALCULATION OF SINGLE-SIDED VENTILATION

In the calculation of single-sided ventilation it is not possible just to look at the average wind velocity and pressure difference as often is done in the work with cross-ventilation. In single-sided ventilation the turbulence in the wind and the variation in the pressure differences induced by e.g. wind gusts results in the main part of the airflow through an opening. Since these parameters are unsteady, the airflow in single-sided ventilation is much more difficult to calculate. During the years some effort has been put into widening the knowledge of these parameters which has led to different empirical expressions found from wind tunnel experiments and/or full-scale outdoor experiments. Some of these expressions will be presented here together with a short review of the work made in connection to the development of the expressions.

2.2.1 AIRFLOWS DRIVEN BY THERMAL BUOYANCY IN A SINGLE OPENING

The airflow driven by buoyancy in a single opening differs from the flow when two or more openings are present since in this case the flow in the opening is bidirectional. This means that the direction of the velocity changes at the level of the neutral plane in the opening. This is illustrated in Figure 2.3.

The volume flow rate can be found from expression (2.10) derived in /Warren et al. 85/.

$$Q_v = \tfrac{1}{3} \cdot C_D \cdot A \cdot \sqrt{\frac{(T_i - T_e) \cdot g \cdot (H_t - H_b)}{\overline{T}}} \qquad (2.10)$$

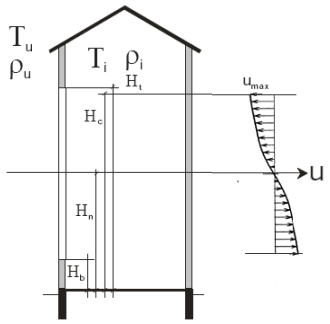

Figure 2.3. *Illustration of the bidirectional flow in a single large opening with airflow driven by thermal buoyancy. /Heiselberg 05/*

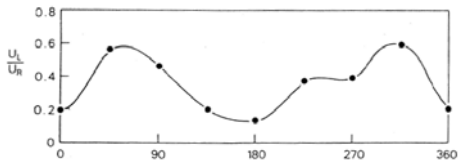

Figure 2.4. *The ratio between the local velocity (U_L) and the reference velocity (U_{ref}) seen as a function of the incidence angle. /Warren 77/*

2.2.2 AIRFLOWS DRIVEN BY WIND

As mentioned above, the ventilation rate in single-sided ventilation is not only driven by the mean wind velocity, but also by turbulence in the wind and fluctuations in pressure at the opening.

In 1977, P.R. Warren published some of his work with turbulent diffusion in airflows through a single opening, /Warren 77/. The main idea in turbulent diffusion is that only eddies sized smaller than or equal to the window size will contribute to the ventilation of the room.

The results in Warren's work are found from single-sided ventilation in both full-scale and wind tunnel tests. The results were improved in later work /Warren et al. 85/, but in this early work he among other things investigated how the ratio between the local wind velocity in front of the opening (U_L) and a reference velocity (U_R) depends on the incidence angle of the wind. The results are shown in Figure 2.4, where it is very easily seen that the local velocity is very much dependent on the wind direction. The reason for this is the different flow patterns on the wall that change from the leeward to the windward side.

Another analysis made by Warren is with the Archimedes number where a difference between the wind dominated and temperature dominated cases is found. From this he concludes that the best way to handle the combination of wind and buoyancy is to calculate the effect from each parameter separately and then use the largest of them. /Warren 77/

In the later work made by P.R. Warren and L.M. Parkins in /Warren et al. 85/ they improve the expressions found in /Warren 77/ which included theoretical considerations of both wind tunnel and full-scale experiments.

The *wind tunnel tests* were made with a small box that was built into one side of a wind tunnel with a cross sectional area of 1.0 x 0.8 m. The box was 0.5 x 0.5 x 0.5 m and the side towards the wind tunnel could be changed so that it was possible to test different openings. This construction means, that it was only possible to test wind directions parallel with the openings. The openings used in the experiments were:

- Square openings
- Slot openings (longest dimension perpendicular to the flow direction and equal to the box height)
- Single opening with vane. Three models of casement windows with different aspect ratios (1.0, 1.6 and 2.5) were tested with four different opening angles (0°, 30°, 60° and 90°), three directions of the flow (0°, 90° and 180°) and five or six different velocities in the tunnel
- Two openings with vane

The results showed that the flow through the square opening was significantly higher than through the slot. Also it is shown that an increase in turbulence in the free flow increased the ventilation rate by 60% for the slot and 40% for the square opening (see Figure 2.5). In the case with the single opening with vane it was shown that changes in the opening angle when the angle is larger than 50° have a low impact on the air change rate. Also it was shown that the air change rate was very sensitive to changes when the angle was lower than 30°.

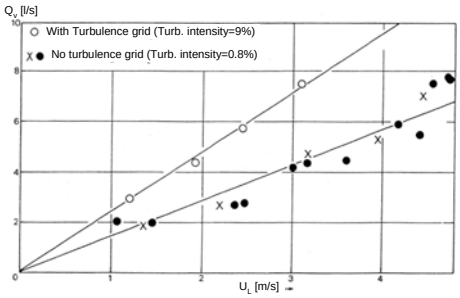

Figure 2.5. *Influence on the air change rate from the level of turbulence at the square opening. /Warren et al. 85/*

The full-scale experiments were carried out in two different buildings. In the first building, tests were made to compare with theoretical and wind tunnel data and in the second building, tests were made to find the effect of having more than one window open in the same room.

Building 1 was a single-storey building and the experiments were carried out in two different single-sided ventilated rooms with the following openings:

- Vertically sliding windows – both one and two openings (room A)
- Two side-mounted casement windows (room B)

The following measurements were made:

- Ventilation rates were measured by the tracer gas decay method (accuracy ±10%)
- Wind speed at a height of 10 m (±0.5 m/s)
- Wind direction at a height of 10 m
- Internal and external temperature (±0.25°C)

To be able to compare the results with the results made in the wind tunnel, a model of building 1 was made and tested in the wind tunnel to find the local velocity just in front of the opening. A good agreement between measurements in full-scale and wind tunnel was found.

Building 2 was a three-storey school building and the experiments were carried out in two different single-sided ventilated rooms at the second floor with the following openings:

- Seven vertically sliding windows – measurements with four different opening combinations (room A)
- Seven side-mounted casement windows open with an angle of 65° – measurements with four different opening combinations (room B)

The following measurements were made:

- Ventilation rates were measured by the tracer gas decay method (accuracy ±10%)
- Internal and external temperature (±0.25°C)
- Wind speed and wind direction were obtained from a meteorological site 8.5 km away from the site

From all the experiments described, two expressions are derived. These do not include the effect of temperature difference, and also it is noted that higher rates may be achieved for other combinations of windows, certain wind directions and tall buildings.

$$Q_v = 0.1 \cdot A \cdot U_L \tag{2.11}$$

$$Q_v = 0.025 \cdot A \cdot U_R \tag{2.12}$$

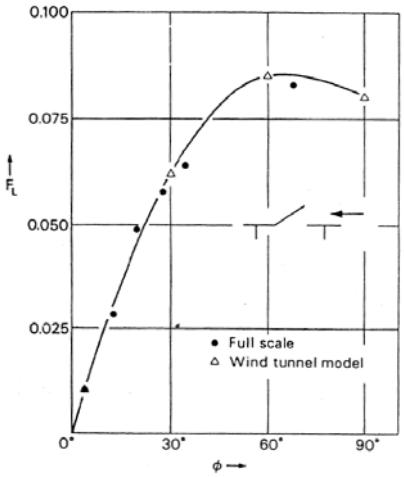

Figure 2.6. *Flow number found as a function of incidence angle in full-scale and wind tunnel experiments by Warren & Parkins. /Warren et al. 85/.*

As it is seen, both expressions are based on the same basic expression ($Q/(AU)$=constant). This expression is defined by Warren as the flow number F, which often is denoted F_L, F_T or F_R.

$$F = \frac{Q_v}{A \cdot U} \tag{2.13}$$

where the subscripts L, T and R refer to the point of the measured velocity. L stands for local, T stands for top of building and R stands for reference velocity (in expression (2.12) this reference velocity is measured at the height of 10 m).

Examples of flow numbers are shown in Figure 2.6.

MODELLING OF PULSATING FLOWS

In the work of J.P. Cockroft and P. Robertson a theoretical pulsation model is made from a study of a single opening pulsation flow, /Cockroft et al. 76/. It is only the low frequency pulsating airflow that is included in their model, which means that airflow caused by turbulence is disregarded in this work.

The expression was found through analysis and was tested in a wind tunnel experiment on a box sized 1.2 x 1.2 X 2.4 m with a single opening of 15.2 cm^2. The expression gives a suggestion on how the pulsating flow can be decided from the change in volume (ω) and is seen in (2.14).

$$Q_v = \frac{d\omega}{dt} = \pm C_D A \sqrt{\left| U^2 - \left(\frac{2\gamma P_a}{\rho V} \right) \omega \right|} \tag{2.14}$$

where γ is the polytrophic exponent which is equal to 1.4 for adiabatic flows and 1.0 for isothermal flows, /Haghighat et al. 00/. C_D is found to be 0.65. Cockroft and Robertson point out that the parameters in (2.14) depend on the shape and size of the opening, the external flow, the total flow through the opening and the internal volume. The dependence of the internal volume will later on be investigated in the work connected to this PhD-thesis.

Cockroft and Robertson also discuss whether all incoming air contributes to the effective ventilation, since some of the air soon after entering will leave the room again because of the fluctuations. They therefore define the effective ventilation rate as the ratio f_p multiplied by the air going into the room. Then the effective airflow can be calculated as

$$Q_{eff} = f_p \cdot Q_{in} = \tfrac{1}{2} f_p \cdot \overline{|Q_v|} \tag{2.15}$$

Cockroft and Robertson found that 37% of the airflow rate contributes to the effective air change, which was measured by the tracer gas decay method.

Other calculations for wind driven single-sided ventilation are some correlation methods made by R.D. Crommelin and E.M.H. Vrins, /Crommelin et al. 88/. They found a correlation between the standard deviation of pressure ($\sigma_{\Delta P}$) and the velocity and between the airflow and both the standard deviation of pressure, the velocity and the area of the opening.

The experiments have all been made in a wind tunnel and are found through measurements by the tracer gas decay method. All the expressions are based on empirical coefficients.

The results from their work with different wind velocities and different incidence angles of the wind are depicted in Figure 2.7 and Figure 2.8, respectively. From these results it is seen that increasing wind speed also results in an increasing airflow through the opening. The differences seen in Figure 2.7 in the airflow depending on the upstream length towards the fan are explained by the difference in turbulence in the two cases, since the short upstream length has a higher turbulence in the flow and thereby also an increase in the fluctuating airflow.

In the investigation of the variation in airflow rates caused by different incidence angles (Figure 2.8) dependence is shown, but this is not included in their final expression.

The expressions are as follows:

$$\sigma_{\Delta P} = \alpha_1 U^2 \tag{2.16}$$

and

$$Q = \alpha_2 \sigma_{\Delta P}^{\beta_1} = \alpha_1^{\beta_1} \alpha_2 U^{2\beta_1} \tag{2.17}$$

and

$$Q = \alpha_3 A^{\beta_3} \tag{2.18}$$

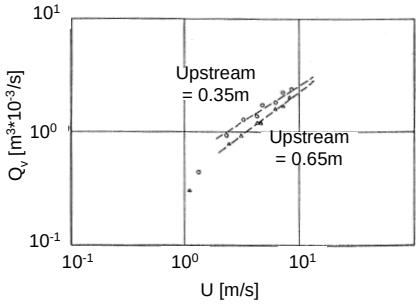

Figure 2.7. *The flow rate as a function of wind velocity found by Crommelin and Vrins. /Crommelin et al. 88/.*

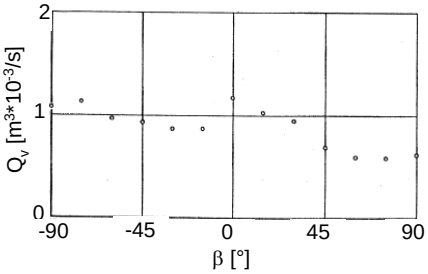

Figure 2.8. *The flow rate as a function of incidence angle found by Crommelin and Vrins. -90°: Wind towards opening, 0°: Wind parallel to opening, 90°: Wind at leeward side /Crommelin et al. 88/.*

Crommelin and Vrins found for an upstream length of 0.35 m that α_1 = 0.029, α_2 = 0.0018, α_3 = 0.0608, β_1 = 0.32 and β_3 = 0.92.

2.2.3 AIRFLOWS DRIVEN BY THERMAL BOUYANCY AND WIND

The literature on single-sided ventilation driven by both wind and thermal buoyancy is scarce, but W. De Gids and H. Phaff made some full-scale experiments in 1982 which will be described here, /De Gids et al. 82/.

One of the difficulties in the combination of wind and thermal buoyancy is to find the shape of the velocity profile in the opening since this will change depending on which of the two parameters that dominates. An example of different flow patterns is found in /De Gids et al. 82/ and depicted in Figure 2.9.

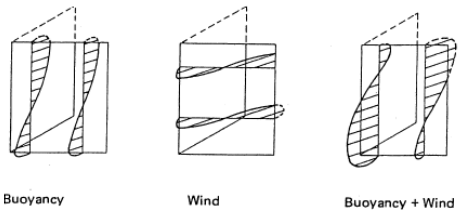

Figure 2.9. *Flow patterns through open windows in single-sided ventilation /De Gids et al. 82/.*

The experiments in their work were carried out at three different locations on buildings in urban environment with surrounding buildings up to four floors high. All measurements were made on the first floor of the building. Different window types with different height/width ratios were tested. The window types were vertically pivoted casement windows, horizontally pivoted vent lights and sash windows, but any large difference between these could not be found.

The experiments consisted of measurements of external velocities, window and room air velocities, air change rates and temperature. The total number of measurements was 33.

From the experiments the following expression was found:

$$U_m = \sqrt{(C_1 \cdot U_{10}{}^2 + C_2 \cdot h \cdot \Delta T + C_3)} \tag{2.19}$$

where C_1 is a nondimensional coefficient depending on the wind effect, C_2 is a buoyancy constant and C_3 is a turbulence constant. From fitting the constants to the measurements the values in (2.20) are found.

$$U_m = \sqrt{(0.001 \cdot U_{10}{}^2 + 0.0035 h \Delta T + 0.01)} \tag{2.20}$$

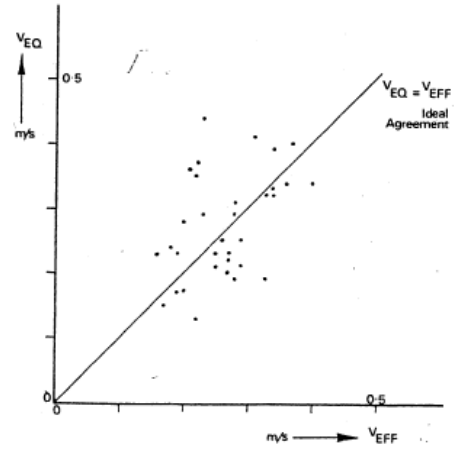

Figure 2.10. *Comparison of the measured velocity (u_{eff}) and the calculated velocity (u_{eq}) found from expression (2.20). /De Gids et al. 82/.*

A comparison of the measured velocity and the one calculated from expression (2.20) is made in Figure 2.10.

To find the volume flow rate expression (2.21) is used.

$$Q_v = A_{eff} \cdot U_m = ½ \cdot A \cdot U_m \tag{2.21}$$

Contrary to most other expressions, this work does not consider the use of a C_D-value. Instead, the value of ½ is added to find the volume flow rate, which comes from the fact that only half of the window area is used as inlet.

2.3 General design methods for single-sided and cross-ventilation

As another way to design natural ventilation, this work by D. Etheridge with nondimensional parameters will be presented. The ideas are not used in the work made in connection to this Ph.D. thesis, but still the ideas are good and are therefore added to this review of earlier work.

In his work, Etheridge /Etheridge 02/ works with different nondimensional graphs to make the design process in natural ventilation easier. The aim of his work is to decide the airflow through the envelope, since, as he points out, the airflow inside the building can always be modelled by CFD, which is harder to do with the airflow through the envelope, since the boundary conditions in this case are much harder to model.

He suggests how the size and position of the opening(s) and the envelope airflow can be found from nondimensional sizes.

The airflow is made nondimensionally by the following expression:

$$Q' = \frac{Q_v}{C_D \cdot A \cdot U_{ref}} \tag{2.22}$$

where

$$C_D = \frac{Q_v}{A}\sqrt{\frac{\rho}{2 \cdot \Delta P}} \tag{2.23}$$

By using the discharge coefficient (C_D), the opening area and a reference velocity, the effects of the opening geometry and wind velocity are included in Q'. It is mentioned that the C_D-value in single-sided ventilation is close to half the size of the situation when two or more openings occur. This is due to the fact that the same opening works as both inlet and outlet.

The reference velocity used in (2.22) is either the wind velocity or a velocity caused by buoyancy in the case with airflow driven by temperature differences. The buoyancy velocity is defined as

$$U_b = \sqrt{\frac{\Delta T \cdot g \cdot h}{T}} \tag{2.24}$$

The area of the opening is made nondimensionally by:

$$A' = \frac{A \cdot U_{ref}}{Q} \tag{2.25}$$

To illustrate how to use the nondimensional number, the following example are made:

Example: Single-sided ventilation through an open window driven by buoyancy

The volume flow is found by

$$Q = C_D \cdot A \cdot U_b \tag{2.26}$$

where C_D is 0.23 and U_b is defined in (2.24).

The area needed for a specified airflow is then found to be

$$A = \frac{Q}{0.23 \cdot U_b} \tag{2.27}$$

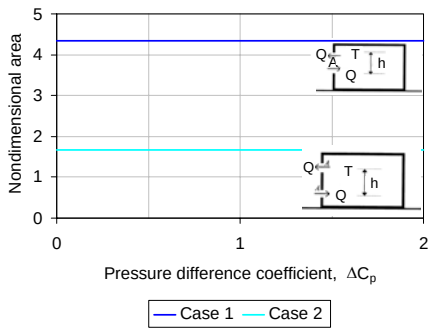

Figure 2.11. *The nondimensional area in the case with buoyancy driven ventilation through one opening (case 1) and two openings (case 2).*

This is inserted into (2.25) which gives

$$A' = \frac{Q \cdot U_b}{0.23 \cdot U_b \cdot Q} = 4.348 \tag{2.28}$$

The same can be done with other combinations. Figure 2.10 shows the example above together with single-sided ventilation through two openings at different heights. The case with single-sided ventilation driven by wind gives a nondimensional area between 20 and 100 and is therefore not depicted in the graph.

The effect of temperature difference and heights in connected spaces is also considered and made into a nondimensional design graph.

Furthermore, the paper considers the effect of unsteady flows. Here the following nondimensional parameter is considered:

$$\frac{W}{\sigma_{\Delta Cp}} \tag{2.29}$$

where

$\sigma_{\Delta Cp}$ is the standard deviation of the instantaneous difference in C_p-values.

and

$$W \equiv Ar_H \cdot \left(\frac{z_2}{H} - \frac{z_1}{H} \right) + \left(\frac{C_{p1} - C_{p2}}{2} \right) \tag{2.30}$$

and

$$Ar_H = \frac{\Delta \rho g H}{\rho \cdot U_{ref}^2} \tag{2.31}$$

Expression (2.29) describes the relative sizes of the steady pressure difference caused by temperate difference and wind (W) and the fluctuating component of the pressure difference caused by wind ($\sigma_{\Delta Cp}$). This means that large values of (2.29) are equal to a small effect from unsteadiness and visa versa.

Finally, the nondimensional design graphs can be used in experimental work in wind tunnels with scale models. The model is then used for direct measurement of the ventilation rates, and with the nondimensional graph the measurements can easily be used for design of full-scale models.

2.4 AIM OF THIS WORK

From the earlier work presented in this chapter, different problems with calculations of airflows in natural ventilation are pointed out. When the airflow is calculated an amount of parameters needs to be taken into consideration. These are

- Wind velocity
- Temperature difference
- Wind direction
- Opening area
- Geometry of the opening
- Position of the opening
- Shape of the building
- Surroundings of the building
- Turbulence in the wind
- Fluctuations in pressure at the opening
- Distribution of wind pressure and air velocity in the opening

It is the combination of these parameters that gives the expected airflow through an opening in the building.

In the description of calculation for *cross-ventilation* a problem with determination of C_p and C_D is described, since these parameters depend on the shape of the building and the surroundings or the shape of the opening, respectively, and it is not always possible to calculate them from current experiments. Another problem mentioned is whether the flow through the opening fulfils the assumptions regarding constant pressure and velocity distribution in the opening made when expression (2.2) was derived from the Bernoulli equation.

In the work with *single-sided ventilation* some effort has been put into the effect on the airflow through the opening coming from the turbulence in the wind and fluctuations in pressure near the opening. A simple expression including only wind velocity and opening area is made by Warren and Parkins, /Warren et al. 85/, who also describe the nondimensional flow number where the actual airflow through the opening is compared to the measured velocity and opening area. In the work of Warren & Parkins it is also investigated whether the air change rate depends on the incidence angle of the wind, but this is not included in any expressions. Instead of the variation with angle, a minimum value for the ratio between U_L and U_R is used in their final expression.

The pulsating flow through the opening has also been modelled by Cockroft and Robertson /Cockroft et al. 76/ who among other things state that the airflow through an opening depends on the internal volume of the room. Also, Crommelin and Vrins look at the unsteady flow near the opening and their suggestion for an expression is defined through some empirical coefficient.

Common concerns for the two types of ventilation are to include the temperature difference together with the wind forces. Often the temperature difference is ignored saying that the wind is much more dominating. In the thesis by M.P. Straw /Straw 00/ it is said that the thermal effect can be ignored when the wind velocity is higher than 1.8 m/s and Warren and Parkins /Warren et al. 85/ recommend calculating the effect from both and then use the higher of the two rates. In the expression made for *single-sided ventilation* by De Gids and Phaff /De Gids et al. 82/ both the wind velocity and the temperature difference are included, but no conditions or limitations of the expression are given.

From the considerations mentioned above, the experiments in this thesis will be carried out. The main part of the experiments will be made as wind tunnel experiments on a full-scale building at the Japanese Building Research Institute. Here both single-sided ventilation and cross-ventilation will be tested. Later on, outdoor experiments with single-sided ventilation will be made to check the results obtained during the wind tunnel experiments. To do this comparison between wind created by mechanical fans and natural wind, at first the differences between these are analysed in *chapter 3*.

The technical specifications regarding the experiments are described in *chapter 4* together with a discussion of the methods used for the calculation of airflows during the experiments. The analyses and comparisons of the results are made in *chapter 5.* In the work with cross-

ventilation the main emphasis is laid on the problems with a constant pressure difference across the opening and how C_D shall be calculated. In the work with single-sided ventilation, the effect from different incidence angles will be investigated since earlier work has indicated a dependence on the airflow through the opening from the direction of the wind. The results from the experiments will be compared to the expressions by Warren & Parkins and by De Gids & Phaff. The expression by Warren and Parkins is only dependent on the wind velocity, but in their work it is stated that the effect from temperature can be left out as long as the wind is dominating. The truth in this will be investigated through the current work. The expression from De Gids and Phaff includes both temperature difference and wind and it will be interesting to see the difference between this expression and the one by Warren and Parkins. Furthermore, the effect on the airflow from changing the internal volume as discussed by Cockroft and Robertson will be investigated.

The result of the experiments and the analysis is hopefully a new design expression for single-sided ventilation which also includes the incidence angle of the wind.

CHAPTER 3

Theoretical analysis of natural and mechanical wind characteristics

This chapter describes the differences between wind measurements made outdoors (natural wind) and measurements made in the laboratory (mechanical wind). At first a decision of the necessary frequency for the measurements is made and afterwards the difference between the two types of wind is analysed through spectral analysis and lagged scatterplots.

3. THEORETICAL ANALYSIS OF NATURAL AND MECHANICAL WIND CHARACTERISTICS

The experiments with natural ventilation have been made both in a wind tunnel and outdoors. In the measurements of wind speed, an important factor is the frequency of the measurements. Too high frequency might result in an enormous amount of unnecessary data, which would have given the same result with a lower frequency. In the opposite case, too low a frequency would result in a wrong reproduction of the wind data. The search for an optimal frequency is described in section 3.1.

To compare the results from the two different setups, it is necessary to know the different characteristics for natural and mechanical wind. The analyses will be made with spectral analyses and lagged scatterplots, which are described in sections 3.2 and 3.3. Earlier works within these topics are described in section 3.4.

In section 3.5 the analyses are made on the measurements from the wind tunnel and outdoors to compare these two types of wind and later on use the results in the design of a new expression for single-sided natural ventilation.

3.1 NECESSARY FREQUENCY OF THE MEASUREMENTS

When working with measurements of wind velocity and wind direction it is important to realize how fast these parameters can change with time. These changes give rise to a discussion of the frequency used for the measurements, since it is necessary to decide which level of details are needed for the work.

As an example, a nine hour period of outdoor wind direction and wind speed measurements is chosen. Data from the period are plotted in Figure 3.1 and Figure 3.2, respectively. The measurements are made with a frequency of 100 Hz. The values of one minute averages are also shown in the figure. The mean value of the entire period is 2.30 m/s.

If the mean value and standard deviation are investigated as a function of the time interval over which they are averaged, the graph in Figure 3.3 is found. Here it is seen that the mean value never gets constant even though it is averaged over a long period of time, but keeps changing during the period, which lies in the nature of the wind. An approximate value is reached after 200 minutes. The standard deviation is more constant with time.

If the nine hour period is instead divided into nine periods of one hour and the same plot is made, Figure 3.4 is found. Here the mean value is reached after approximately 20 minutes, although this requires a reasonably constant period in the wind conditions, see Figure 3.2. If the wind speed is changing to a completely different level even the 20 minutes of measurements would not be enough.

Through this example the problem of choosing the correct length for the measurements is illustrated. In this work a 20 minute measurement period will be used. Furthermore, the results will be held up against

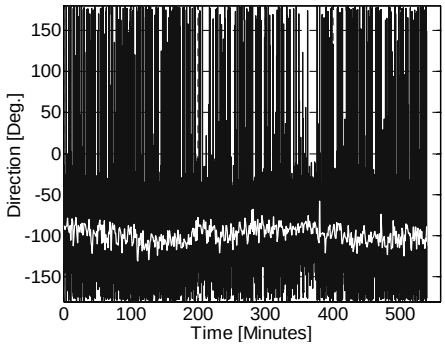

Figure 3.1. *Wind direction measurements in the selected nine hour period. The white line shows one minute averages.*

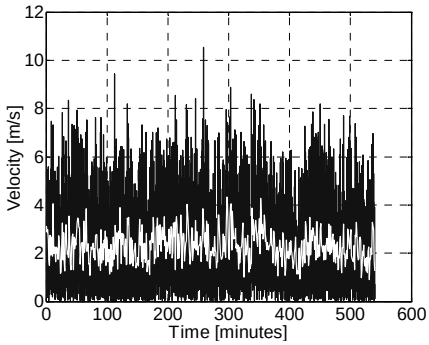

Figure 3.2. *Wind speed measurements in the selected nine hour period. The white line shows one minute averages.*

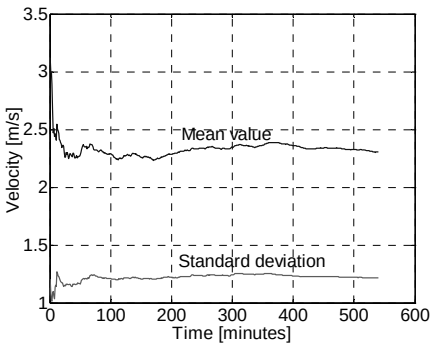

Figure 3.3. *Mean value and standard deviation of the wind speed as a function of the time period over which the values are averaged. Total length of the period is nine hours.*

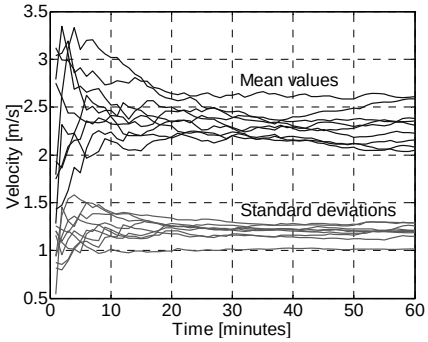

Figure 3.4. *Mean value and standard deviation of the wind speed as a function of the time period over which the values are averaged. Nine periods with a length of one hour.*

Test frequency [Hz]	Mean [%]	Max [%]	Min [%]
50	0.001	0.72	0
25	0.003	3.9	0
20	0.01	3.4	0
10	0.03	11.8	0
5	0.07	12.7	0
1	0.50	31.8	10.5
0.5	1.12	31.8	60.9
0.2	1.82	35.1	95.5

Table 3.1. Maximum difference in % between measurements with 100 Hz and the mentioned test frequency.

measurements for a longer period to make sure that the wind speed is not changing dramatically through the period.

The next thing to be decided is the frequency of the measurements. The frequency needs to be precise enough to hold the main details in the wind, but it is also important not to collect any unnecessary data since the amount of collected data then may, very fast, grow over your head.

A small program is made in the mathematical program Matlab for comparison of measurements made with different frequencies. The idea of the program is to pick out data from the measurements made with 100 Hz and put them into a new set of data. If for instance data measured with 100 Hz are compared with 20 Hz, every fifth measurement is picked out of the 100 Hz data-set and used as a new data-set. Then the mean value is calculated for both data-sets and the maximum and minimum value of both sets are found and compared. The program uses all nine test periods in the nine hour measurements from Figure 3.2. The test periods are divided into sections of 1200 sec, which gives 27 test intervals. The result of the program is the largest difference found between mean, maximum and minimum values in all periods (only one value). The results are shown in Table 3.1.

From the results in Table 3.1 it can be concluded that the greatest loss in data, when using a lower frequency, is for the maximum value. The deviation for this parameter grows fast when the frequency is reduced. From the table it is found that measurements can be made with 5Hz without any great losses in data. In Figure 3.5 measurements made with 100 Hz are compared with three test frequencies.

In this work a deviation of approximately 10% is accepted and, therefore, a frequency of 10 Hz will be used in the experiments.

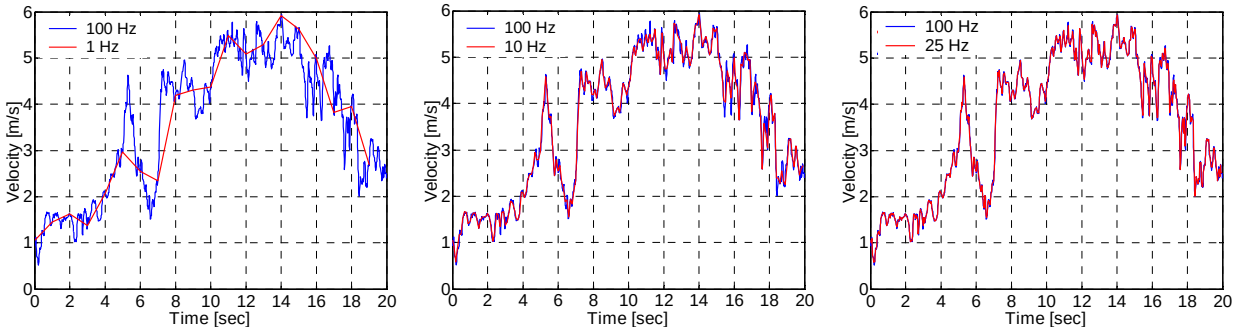

Figure 3.5. *Comparison of wind measurements made with 100 Hz and the specified test frequency.*

3.2 SPECTRAL ANALYSIS

Turbulent wind consists of eddies in different sizes varying from mm to km in length scale. The maximum size of the eddies depends on the surroundings and the accessible volume, which is different from the

laboratory to outdoors. Because of this difference it is assumed that the ventilation rate will vary according to the maximum size of eddies.

With turbulent wind described as a super position of vortices with various sizes, a parallel can be drawn to spectral analysis, where Fourier Transforms are used to find the dominating frequencies in time series.

3.2.1 BASIC KNOWLEDGE OF FOURIER TRANSFORMS

When Fourier first presented his theory with the Fourier transform in 1807, it was made for a sum of sinusoids to represent temperature distributions, but he claimed that any continuous periodic signal could be represented this way. It took him 15 years to convince the researchers of that time, but after that, the transforms have been widely used by mathematicians and scientists all over the world. /Smith97/

The idea of Fourier transforms is to transform a signal that is difficult (or nearly impossible) to describe into a new signal described by a sum of well-known sinusoids.

The input signal can either be continuous or discrete and also either periodic or aperiodic, which results in four different types of signals. To use the Fourier Transform the signal needs to be periodic since the sine and cosine waves are defined from minus infinity to plus infinity. To handle this problem the signal is just copied and put into an infinite row of the same signal. Since the wind measurements in this case are discrete, the Fourier transform used in this work will be the Discrete Fourier Transform (DFT).

3.2.2 DISCRETE FOURIER TRANSFORM (DFT)

The discrete Fourier transform can be made both with input and output as real numbers and with input and output as complex numbers. Common for both methods is that a time signal is transferred into a frequency signal, which is a sum of sine and cosine waves. The real numbered method will here be shortly presented to increase the understanding of the Fourier Transform before the complex method is described.

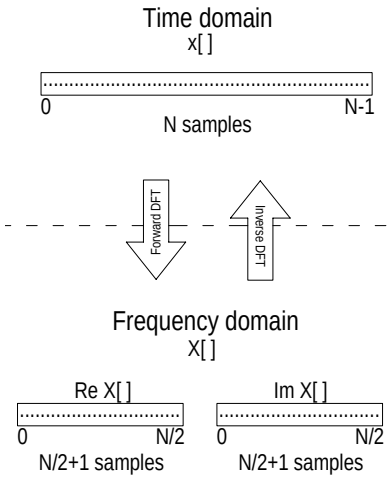

Figure 3.6. *Connection between time domain and frequency domain in a discrete Fourier transform made with real numbers.*

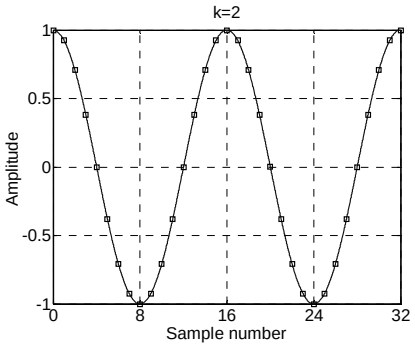

Figure 3.7. *Basis cosine wave for k=2 (2 full cycles) at a 32 point DFT.*

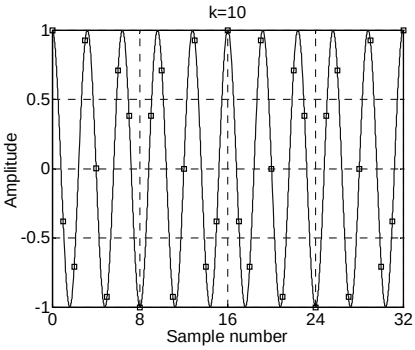

Figure 3.8. *Basis cosine wave for k=10 (10 full cycles) at a 32 point DFT.*

REAL NUMBERED DFT

When you do a DFT on a signal you transfer it from the time domain into a frequency domain. In the time domain your signal has N samples, but after the DFT the signal is divided into a real part and an imaginary part both consisting of N/2+1 samples. This is illustrated at Figure 3.6.

Except for a scaling factor, the real part in the frequency domain consists of the amplitudes for the cosine waves and the imaginary part consists of the amplitudes for the sine waves. In this work the notation x[ ] is used for the samples in the time domain and X[ ] for the samples in the frequency domain.

From the above connection the expression for calculation of the real numbered *inverse* DFT can be written as equation (3.1). /Smith97/

$$x[t] = \sum_{k=0}^{N/2} Re\,\overline{X}[k]\cos(2\pi kt/N) + \sum_{k=0}^{N/2} Im\,\overline{X}[k]\sin(2\pi kt/N) \qquad (3.1)$$

where *t* runs from 0 to N-1

From (3.1) it is seen, that the time signal, x[t], is a sum of N/2+1 sine and cosine functions. These sine and cosine functions can be seen as basis functions for the DFT. This means that for each value of k (running from from 0 to N/2), a sine and a cosine wave with k full cycles over the N points interval exist.

As an example, take a 32 point time series. In the frequency domain this will consist of 17 different sine waves and 17 different cosine waves varying from 0 to 16 full cycles divided on 32 points. This is illustrated in Figure 3.7 and Figure 3.8, where the basis cosine wave is plotted for k=2 and k=10. It is only in the case where k=2 that the N points follow the curve. In the case with k=10 it can be difficult to spot the cosine curve without the plot of the solid line.

As mentioned earlier, the real and imaginary parts in the frequency domain need a scaling factor to give equation (3.1). These scaling factors are shown in (3.2).

$$Re\,\overline{X}[k] = \frac{Re\,X[k]}{N/2}; \quad Im\,\overline{X}[k] = -\frac{Im\,X[k]}{N/2}$$

except for (3.2)

$$Re\,\overline{X}[0] = \frac{Re\,X[0]}{N}; \quad Re\,\overline{X}[N/2] = \frac{Re\,X[N/2]}{N}$$

The reason for using these scaling factors is that the frequency domain (ReX[ ] and ImX[ ]) is defined as a spectral density. The spectral density

gives the amount of amplitude ($\mathrm{Re}\,\bar{X}[k]$ and $\mathrm{Im}\,\bar{X}[k]$) per length of the bandwidth which results in expression (3.2), when the bandwidth is calculated as 2/N. An exception for this is the endpoints where the bandwidth is 1/N (half width). This explains the calculations of $\mathrm{Re}\,\bar{X}[0]$ and $\mathrm{Re}\,\bar{X}[N/2]$ in the lower part of (3.2).

If the frequency domain needs to be calculated from the time domain, the expression in (3.3) is used. This expression calculates the real numbered *forward* DFT. /Smith97/

$$\begin{aligned} Re\,X[k] &= \sum_{t=0}^{N-1} x[t]\cos(2\pi kt/N) \\ Im\,X[k] &= -\sum_{t=0}^{N-1} x[t]\sin(2\pi kt/N) \end{aligned} \qquad (3.3)$$

where *k* is a factor that runs from 0 to N/2

The *forward* DFT needs to be calculated by a *Fast Fourier Transform* (FFT), which will be explained further in the next chapter with the complex numbered DFT.

COMPLEX NUMBERED DFT

After explaining the real numbered DFT, the complex numbered DFT is now considered. Since the mathematics in complex numbers are much more difficult to understand and work with, there must exist a very good reason for using this method. This will be explained later, but firstly the main difference between the real and the complex numbered case is explained.

As in the real numbered case, the complex case transfers values from a time domain into a frequency domain. This is illustrated in Figure 3.9. In the complex case the time domain consists of a real part and an imaginary part both containing N samples. The frequency domain also consists of a real part and an imaginary part and, contrary to the real numbered case, these both contain N samples.

Even though the complex numbered DFT requires a complex numbered time signal, it can easily be used with a real numbered signal since the imaginary part is then just filled with zeros.

To calculate the forward discrete Fourier transform, expression (3.4) is used. To inverse the transform and get back to the time domain, expression (3.5) is used. /Smith97/

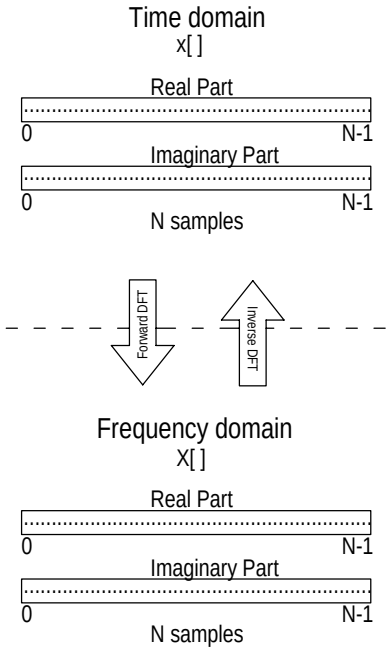

Figure 3.9. *Connection between time domain and frequency domain in a discrete Fourier transform made with complex numbers.*

$$X[k] = \frac{1}{N}\sum_{t=0}^{N-1} x[t] \cdot e^{-i\frac{2\pi}{N}kt} \tag{3.4}$$

$$x[t] = \sum_{k=0}^{N-1} X[k] \cdot e^{i\frac{2\pi}{N}tk} \tag{3.5}$$

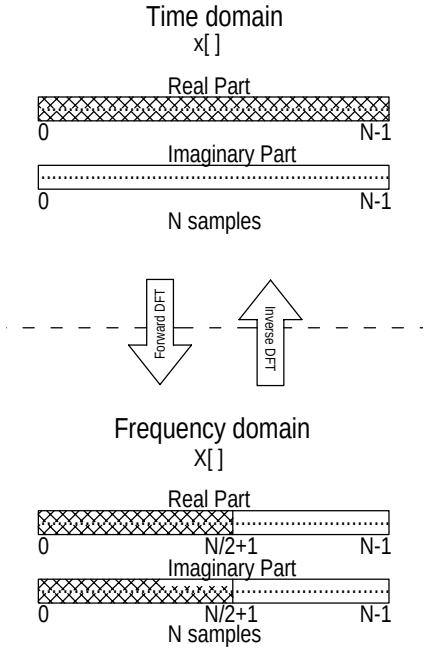

Figure 3.10. *Common values in the real and complex version of the discrete Fourier transform.*

In Figure 3.10 the common values from the real DFT and the complex DFT are marked. The reason why the frequency domain consists of N elements in the complex DFT and only N/2+1 in the real DFT is that the complex DFT also includes the negative frequencies in the frequency domain. The advantages in this are that you avoid the scaling factors from (3.2) and especially the two special cases with ReX[0] and ReX[N/2]. In the complex DFT you also have a scaling factor, but this factor can just be included directly in the expression and it does not matter whether it is added in the forward or the inverse expression. In this way you remove a step in the calculation procedure when you use the complex DFT.

As with the real DFT the complex DFT also needs to be calculated through a Fast Fourier Transform (FFT). The FFT is used to decrease the time of calculation, since the DFT results in an enormous amount of equations that need to be solved. The main idea of the FFT is that it breaks down the N point time signal into N time signals with only 1 point. Then the frequency spectrum for these N time signals is calculated and afterward, these frequencies are composed back into a frequency signal with N elements. Since the FFT always decomposes in pairs of two (e.g. 8 becomes 2X4 that afterwards becomes 2x2 + 2x2) the most effective calculation will be obtained by having an input that is a product of the from 2^n. If the input signal is not in this form, zeros can be added to the signal without disturbing the resulting frequency signal. The will be described further in the next section.

ZERO-PADDING

To obtain a length of the time signal that is a product of 2^n, zeros can be added to the signal. A gain in this zero-padding is that the resolution of the frequency signal is increased. When adding zeroes to a time signal, you are making the sampling period longer and thereby also increasing the number of samples in the frequency signal that is still distributed on the same amount of space. An example is shown in Figure 3.11.

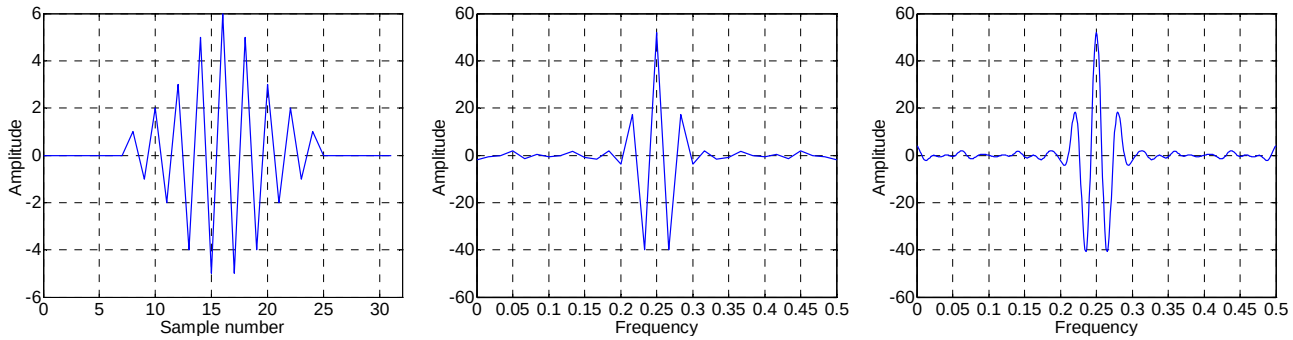

(1) (2) (3)

Figure 3.11. *Example on zero-padding.(1) is the time signal measured over 32 samples. (2) is the DFT of the time signal with 32 samples. (3) is the DFT of the zero-padded time signal with 32 samples added with 480 zeroes so that this time signal (not shown) in total contains 512 samples. The result of the zero-padding is a higher resolution of the DFT.*

NOTATION AND UNITS OF AXES

The horizontal axes on a plot in the frequency domain can be labelled in four different ways. This can easily be different from source to source so it is convenient to be able to calculate from one notation to another. Common for all notations is that they always consist of N/2+1 points, which were the number of samples when the time domain was transferred into the frequency domain.

The first method is simply using the *number of the samples (k)* in the frequency signal. The second method uses a fraction of the sampling rate, which means that the frequency varies between 0 and half the sampling rate. The unit in this case is frequency and the connection between the first method and the second method is that f=k/N. Thereby the *frequency will run from 0 to 0.5*. In the third method the units from the second method is just *multiplied by 2*π. The index in this method is ω, where $\omega=2\pi k/N$, and *runs from 0 to* π. The fourth method uses the units of the sampling rate. The axis will in this case run from *0 to half the frequency of the sampling rate* with the unit in Hertz. Figure 3.12 gives an outline of the different units. /Smith97/

Units in the frequency domain:
1: Sample number in frequency signal, (k)
Runs from 0-N
2: Fraction of sampling rate, frequency (f)
Runs from 0-0.5
3: Natural frequency, radians (ω)
Runs from 0-π
4: Half of sampling rate, frequency (Hz)
Runs from 0-(sampling rate/2)

Figure 3.12. *Outline of possible units in the frequency domain. In this work #4 is chosen.*

Since the DFT in this work will be used for analysis of wind measurements the preferred unit in this work will be Hertz.

DOING THE SPECTRAL ANALYSIS

From the DFT a spectral analysis can be made to investigate whether some frequencies are dominating in natural wind and others in mechanical wind. The results from the spectral analysis will be used in the work with a new design expression for single-sided natural ventilation.

To find the energy in different frequencies, the *power spectrum estimation* is calculated. The expression in (3.6) is used. /Stoica97/

$$S_X = \frac{1}{N} X \cdot X^* \tag{3.6}$$

where X^* is the complex conjugated of X.

The results of the calculations are shown together with the analysis of the measurements in section 3.5.

3.3 LAGGED SCATTERPLOTS

Lagged scatterplots are used to look for coherence in time in the measurements. The idea is to compare the fluctuations in the measurements with a lagged version of itself to find a correlation, if any. Of course the highest correlation is with a zero seconds lag, but other time lags can also reveal whether the measurements are repeating over time. The principle in lagged scatterplots is illustrated in Figure 3.13.

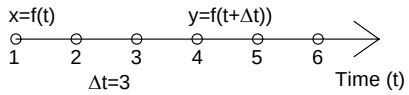

Figure 3.13. *Decision of points for the lagged scatterplot with a time lag of 3. The x-value is given as f(t) and the y-value is obtained from the value in f(t+Δt).*

If the correlation with a certain time lag is high, the points in the lagged scatterplot will be close to the line x=y. The dispersion away from this line will increase with decreasing correlation. Often this dispersion grows with increasing time lag.

The lagged scatterplot can be characterized by a nondimensional width, δ, introduced by /Zhu et al. 03/. This is described further in the next section. The expression for calculation of δ is written in (3.7).

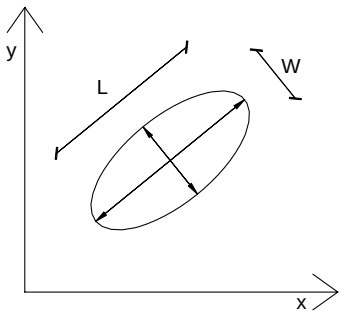

Figure 3.14. *Parameters for calculation of δ in a lagged scatterplot.*

$$\delta = \frac{W}{L} \tag{3.7}$$

The parameters in (3.7) are illustrated in Figure 3.14, where it can be seen that a small δ corresponds to a large correlation.

3.4 LITERATURE REVIEW

In the introduction to this chapter it was mentioned, that the airflow in natural (and actually also mechanical) wind can be seen as a super position of eddies with different fluctuant cycles and frequencies. Even though this sounds very simple and straightforward it is a very complex area where one answer often just results in ten new questions.

Some research in the topic has been done at Tsinghua University in China, where they have tried to classify whether the wind is natural or mechanical and from this classification have tried to find the differences in the two types of wind. The work at Tsinghua University is made with regard to indoor thermal comfort, but the main principles are the same and can therefore also be used as inspiration in this work.

The common opinion of the comfort in a naturally ventilated room compared to a mechanically ventilated room is that it is more comfortable to be in the naturally ventilated room. It can be discussed whether this difference comes from a mental point of view, where the natural air seems more clean and healthy than the air from the diffuser in a mechanically ventilated room. Another aspect can be a physical one where it can be discussed whether there is any difference in the way that the air moves around in the room. The natural air is often more fluctuant in its behaviour with different velocities and frequencies.

In /Zhu et al. 03/ four suggestions for different analyses of mechanical and natural wind are made. One of these suggestions is that the negative slope in a *logarithmic power spectrum* can be used as an indicator of the type of wind, where a slope (β) > 1.1 indicates that the wind is natural and β < 1.1 that it is mechanical, see Figure 3.15. These values indicate that mechanical wind contains a wide range of frequencies compared to natural wind where the slope is steeper and thereby also has a more concentrated variety of frequencies. The analyses are made with frequencies ranging from 0.03 Hz to 1 Hz. This interval is chosen from results of earlier experiments with comfort in different airflows made by others.

Furthermore, Zhu discusses whether β depends on the surroundings and examples are given on a value from open landscape of 1.6 and a near-building value of 1.4. This discussion will be continued in the next section with the results of this present work.

Zhu also introduces a *phase space reconstruction* which corresponds to the lagged scatterplot explained in section 3.3. In connection to this she uses a nondimensional width (δ=W/L, see expression (3.7)) to describe the shape of the lagged scatterplot. From her experiments the shapes in Figure 3.16 and Figure 3.17 are dominating for natural and mechanical wind, respectively.

/Ouyang et al. 03/ describe the analysis of β-values in indoor and outdoor experiments. The experiments are made across an open space, through the opening and into a room. The conclusion is that all points of measurements have a β-value above 1.1, which follows the theory of Zhu, who says that natural wind will always have a value above 1.1. So from this work it is shown, that the theory is also valid inside a room.

A conclusion of the work described above is that natural wind will always have a β-value above 1.1 whether it is inside a room or outside. In other words, this means that the natural wind contains larger eddies than the mechanical wind and that the mechanical wind contains a more evenly

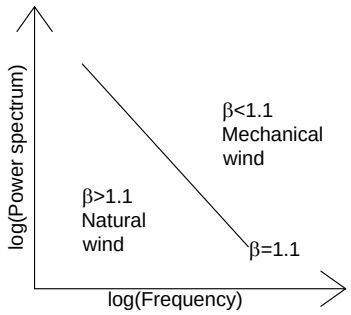

Figure 3.15. *Typical slopes in a logarithmic power spectrum for natural and mechanical wind. /Zhu et al. 03/*

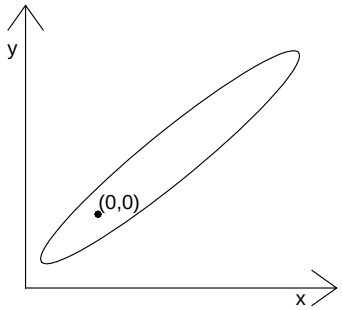

Figure 3.16. *Typical shape of a lagged scatterplot for natural wind according to /Zhu et al. 03/.*

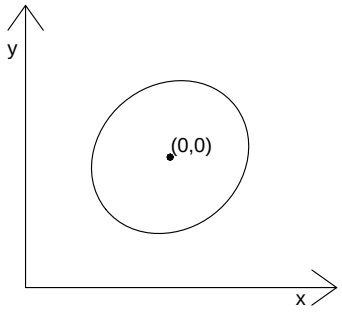

Figure 3.17. *Typical shape of a lagged scatterplot for mechanical wind according to /Zhu et al. 03/.*

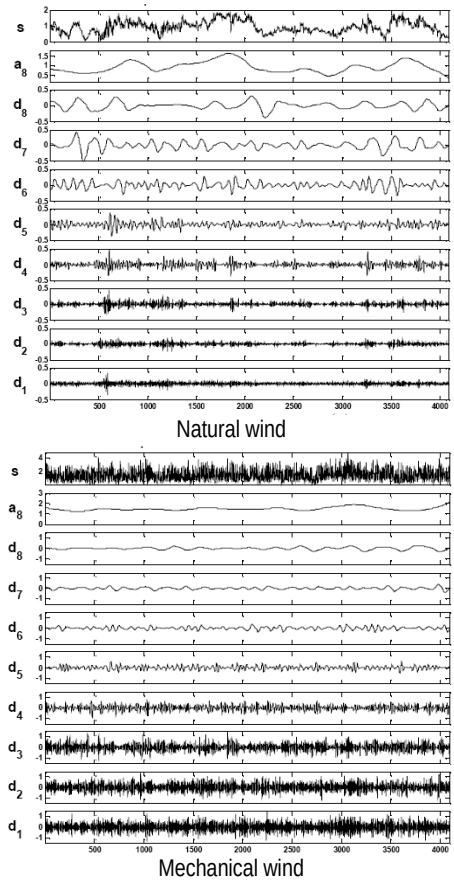

Figure 3.18. *8-level wavelet transform. The first line (s) in each part contains the measured velocity signal /Li et al. 05/.*

distributed spectrum of different eddy sizes. The natural wind is also lacking of small eddies.

A slightly different problem is discussed in /Dai et al. 03/ and /Hara et al. 97/, which both works with the idea of translating mechanical wind into natural wind. To do this they are analysing the natural wind through power spectral analysis and lagged scatterplot to find the characteristics in the natural wind. Dai concludes that the mechanical jet eventually transforms into a natural jet when you get far enough away from the inlet. In his paper a distance of 5 m is enough. Hara uses the analysis to make a program for an electric fan that reproduces the natural wind. He finds that the wind has 1/f characteristics, which means that the slope of the logarithmic power spectrum is 1/f. This is mentioned as an important factor for people's comfort, but still the effect of this 1/f property is quite unknown.

Some of the latest work on the area with classification of wind characteristics is the introduction of wavelet analysis. This type of analysis is similar to the spectral analysis, but in the wavelet analysis it is possible to add an extra dimension beyond the frequency. The dimension can either be time or space, so in analysing the velocity measurements it is possible to analyse the frequency in the measurements, but also how the frequency varies with time. An example of the wavelet analysis is made by Li et al. /Li et al. 05/. In this work velocity measurements from mechanical and natural wind are analysed and compared. An 8-level discrete wavelet transform is carried out on the signal. This means that the data are filtered eight times. In each filtering the dataset is divided into an "approximation"-part and a "detail"-part. The "detail"-part from each filtering is used as the result for this filtering and the approximation-part is filtered again into two new parts. The results are shown in Figure 3.18, where the frequency is changing from low frequencies at d_8 to high frequencies at d_1. Here it is seen how the mechanical wind contains much more energy in the high frequencies than natural wind. In contrast the natural wind contains most energy in the low frequencies.

The results found in the wavelet transform by /Li et al. 05/ are very similar to the results found with spectral analysis even though the time dimension is added to this type of analysis. The wavelet transform is just a more detailed type of analysis, but at the bottom line you get the same results.

3.5 COMPARISON OF MECHANICAL AND NATURAL WIND

In order to find a new design expression for single-sided natural ventilation it is necessary to know the characteristics of the two different types of wind that occur during the measurements. In the wind tunnel the wind is generated by mechanical fans and can be seen as a more or less unidirectional flow. In the outdoor experiments the wind comes from all directions and also often changes direction during the 20 minute period that the measurements last. The impact of this change to the ventilation rate is unknown, but during use of spectral analysis and lagged scatterplots, a wider knowledge of the area will hopefully appear. All data used in the analysis are taken from measurements made in connection with this Ph.D works and further description of the measurements and the conditions during these can be found in chapter 4 and 5.

3.5.1 DESCRIPTION OF CASES USED IN THE ANALYSIS

Some cases in the datasets are picked out for the analysis. The cases are found from the following demands:

- There must exist data from both wind tunnel and outdoor experiments that represents nearly the same situations
- The outdoor cases need to be steady (which means that the wind direction just outside the window cannot change during a 20 minute measurement period)

REPRESENTATION OF FREE WIND

To represent the free wind in the outdoor experiments, case 53 is used. The velocity is measured at the roof of the building used for outdoor experiments. The average velocity in this case is 3.01 m/s and a plot of the measurements is shown in Figure 3.19.

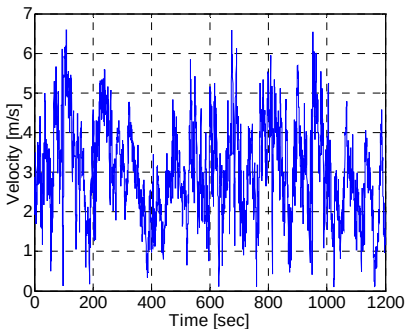

Figure 3.19. *Wind velocity measured at the roof of the office building in case 53 in the outdoor experiments.*

Measurements in the free wind in the wind tunnel are made at four points around the building. The points are shown in Figure 3.20. The points are all 2.78 m away from the building and at each point the velocities are measured at h=1m, h=2m, h=3m, h=4m and h=5 m. The wind velocity just after the inlet was in this case 3 m/s and the building was sealed off during the measurements. The measured velocity at point 15 (3 m above ground) is shown in Figure 3.21.

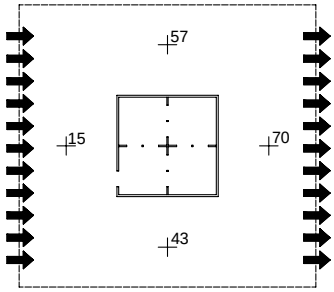

Figure 3.20. *Measurement points for "free wind" in the wind tunnel. All points are 2.78 m away from the building.*

It is seen that the outdoor wind measurements fluctuate more than the one measured in the wind tunnel. Further comparison will be made in the following sections.

CASES USED FOR ANALYSIS OF FLOW IN THE OPENINGS

From the outdoor experiments, the following cases are used in the analysis of flow in the openings:

Case 20: Wind dominated velocity profile
Wind speed = 3.9 m/s, Δt=3.3°C, Incidence angle 341°

Case 62: Wind dominated velocity profile
Wind speed = 2.2 m/s, Δt=4.4°C, Incidence angle 0°

Case 89: Temperature dominated velocity profile
Wind speed = 3.1 m/s, Δt=6.4°C, Incidence angle 342°

Further details about the velocity profiles can be found in chapter 5.

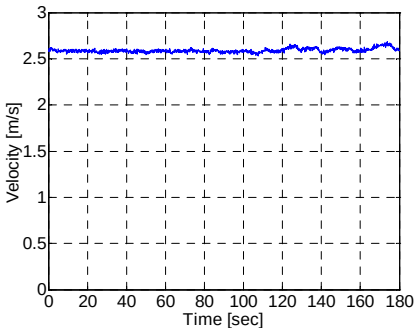

Figure 3.21. *Wind velocity measured 3 m above ground at point 15 in the wind tunnel experiments.*

In the wind tunnel experiments the following cases are used:

Case 0V3000: Wind dominated velocity profile
Wind speed = 3m/s, Δt=0°C, Incidence angle 0°

Case 0V5000: Wind dominated velocity profile
Wind speed = 5m/s, Δt=0°C, Incidence angle 0°

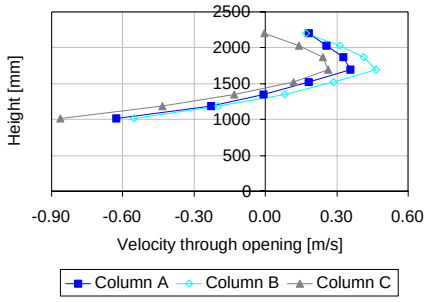

Figure 3.22. *Velocity profiles measured in wind tunnel for wind speed = 3m/s, Δt=0°C, incidence angle 0°. Positive values indicate ingoing flow.*

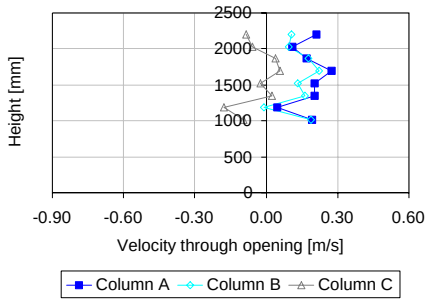

Figure 3.23. *Velocity profiles measured in wind tunnel for wind speed = 3m/s, ⊿t=0°C, incidence angle 330°. Positive values indicate ingoing flow.*

Case 0V3330: Wind dominated velocity profile
Wind speed = 3m/s, Δt=0°C, Incidence angle 330°

Case 0V5330: Wind dominated velocity profile
Wind speed = 5m/s, Δt=0°C, Incidence angle 330°

Case 5V3000: Combined wind and temperature dominated velocity profile
Wind speed = 3m/s, Δt=5°C, Incidence angle 0°

Figure 3.22 and Figure 3.23 shows the velocity profiles for an incidence angle of 0° and 330° respectively. As seen in the figures the profiles are very different from each other. Both cases are dominated by wind but the pressure distribution gives the case with 0° much stronger profiles and makes the flow in Figure 3.23 seem like a fluctuating flow.

3.5.2 SPECTRAL ANALYSIS

The spectral analysis and plots of the power spectrum estimation are divided into two parts. One part describes the flow outside the building (free wind) and the other part describes the flow in the opening, since these flows act differently form each other. To avoid confusion with earlier work made by Zhu /Zhu et al. 03/, where all beta-values are given as positive values even though they are negative, signs will be used here to give the right slope of the line. This means that values below -1.1 indicate natural wind and values above -1.1 indicate mechanical wind. The slope will be calculated for frequencies between 0.03 Hz and 1 Hz to be able to compare the results with the work studied in the literature review.

MEASUREMENTS OUTSIDE THE BUILDING

In the calculations of the power spectrum estimation (PSE) in the "free wind" in the wind tunnel, the results at the three lowest points (h=1m, h=2m, h=3m) in front of the building differ from the points on the sides and behind the building.

An example of the PSE and log(PSE) from h=2 m at point 15 (in front of the building) is shown in Figure 3.24. In this case the frequencies below 0.3 have much more energy than the rest of the frequencies. In this case there is not this even distribution of energy at the frequencies that that you often find in mechanical wind.

This type of energy distribution, found at the three lowest points in position 15 (all in front of the building below building height), looks like natural wind. The β-value is calculated to be -1.02, which corresponds to mechanical wind according to Zhu. In this case the β-value is close to the limit that divides the two types of wind and in h=1m and h=3m the values are -1.75 and -1.37 respectively, so here they correspond to natural wind. At the rest of the points in the wind tunnel this is not the case. Here all points have mechanical characteristics.

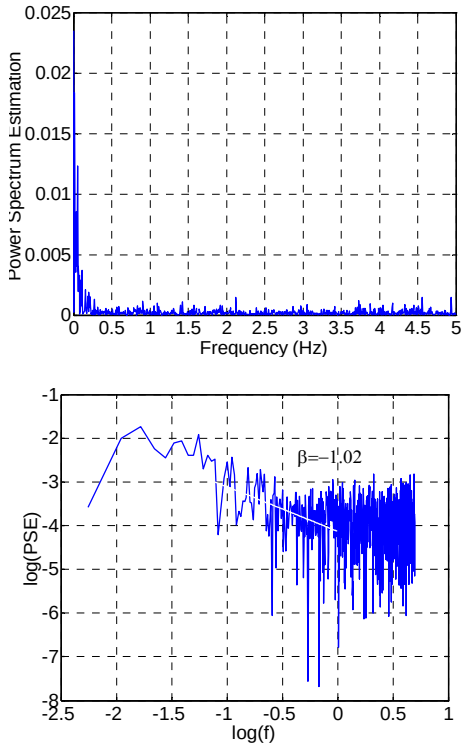

Figure 3.24. *PSE of measurements from point 15, h=2 m.*

In Figure 3.25 the PSE made from measurements at h=2m at point 43 (right side of the building) shows that the energy at the low frequencies is increased and also distributed out on a wider spectrum of frequencies than the points in front of the building.

This change in energy distribution also shows in the beta-value. Here it is calculated to be -0.37 and thereby without any doubt shows that the wind is mechanical.

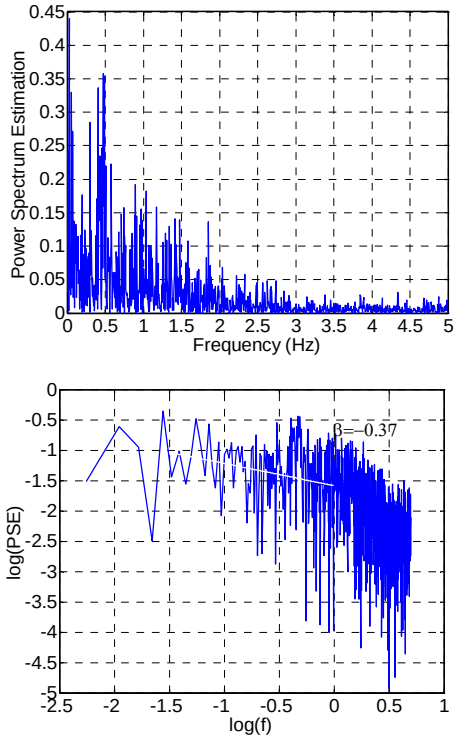

Figure 3.25. *PSE of measurements from point 43, h=2 m.*

To compare the results from the four positions in the wind tunnel (15: in front, 43: right side, 57: left side, 70: behind) all the β-values are shown in Figure 3.26. Here the deviations at the points below building height at point 15 are easily seen. From h=4m the characteristics are similar to the other points. The results from points 43, 57 and 70 look rather similar with β-values ranging from -0.12 to -0.87 and thereby the have very clear mechanical characteristics. They also all have slightly higher β-values at h=5 where the disturbance from the building must be small.

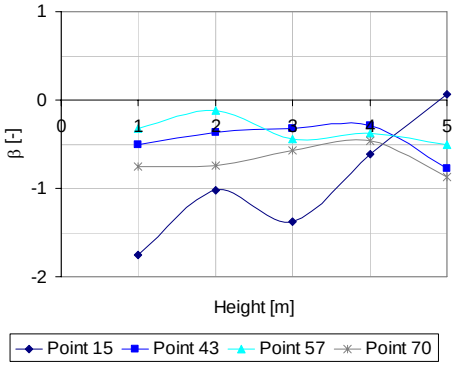

Figure 3.26. *β-values found from the free wind in the wind tunnel. Positions of numbers are shown in* Figure 3.20.

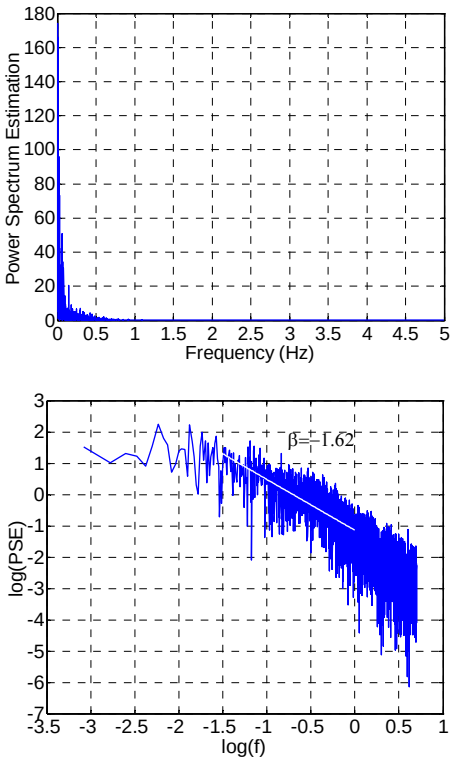

Figure 3.27. *PSE of measurements from the roof in the outdoor measurements.*

The PSE and log(PSE) for the outdoor experiments are shown in Figure 3.27. In this case the β-value is found to be -1.62 which corresponds very clearly to natural characteristics in the wind.

In the PSE in Figure 3.27 the typical distribution for natural wind is also seen. Here the main part of the energy is at the low frequencies.

MEASUREMENTS IN THE OPENINGS

In the wind tunnel experiments five points in the opening were picked out for analysis. These points are A6, A7, B5, C6 and C7. In the outdoor experiments only the results from points L4 and R4 are used, since the direction of the velocity is not measured at the points in the middle of the opening. The points in both openings are shown in Figure 3.28. The exact position of the measurements can be found in chapter 4.

As mentioned before, two different incidence angles were chosen for the analysis to be able to compare the wind tunnel results with the outdoor measurements. The result of the PSE when the wind has an incidence angle of 0° is shown in Figure 3.29. The results show that the wind in the opening has mechanical characteristics in the wind tunnel experiments even though the analysis showed that the wind outside the building had the characteristics of natural wind. The energy in the opening is distributed across a wide spectrum of frequencies and the β-value is -0.61. To the right in Figure 3.29 the velocity measured at point C6 is shown.

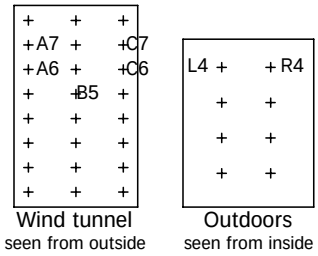

Figure 3.28. *The points in the wind tunnel opening where the PSE has been calculated.*

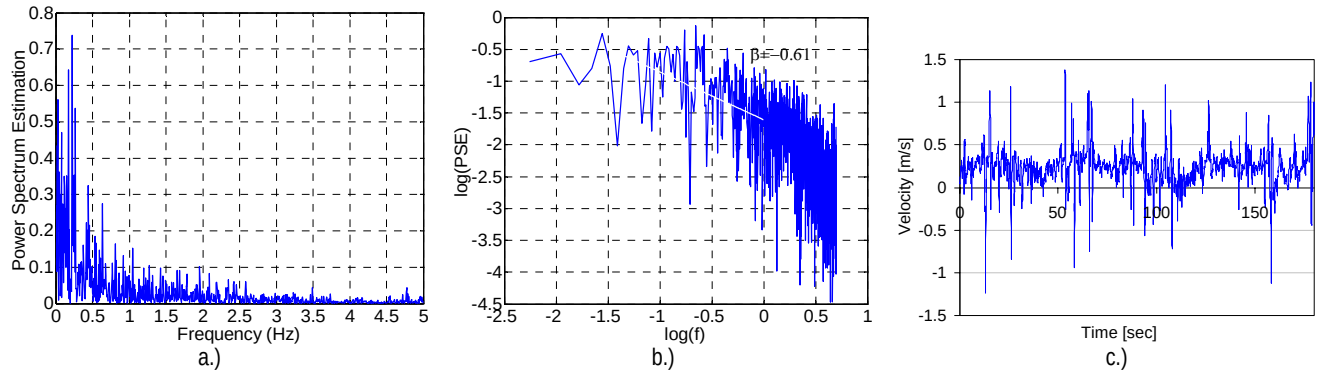

Figure 3.29. *a.) PSE at point C6 with an incidence angle of 0° and a wind velocity of 3 m/s (case 0V3000). b.) log(PSE). c.) The velocity at point C6.*

In Figure 3.30 the PSE at point C6 is made for an incidence angle of 330°. In this calculation the energy distribution differs a lot from the other calculations of PSE, since some frequencies have a peek in the plot. The peaks appear at approximately 1.8 Hz, 3.5 Hz and 5 Hz.

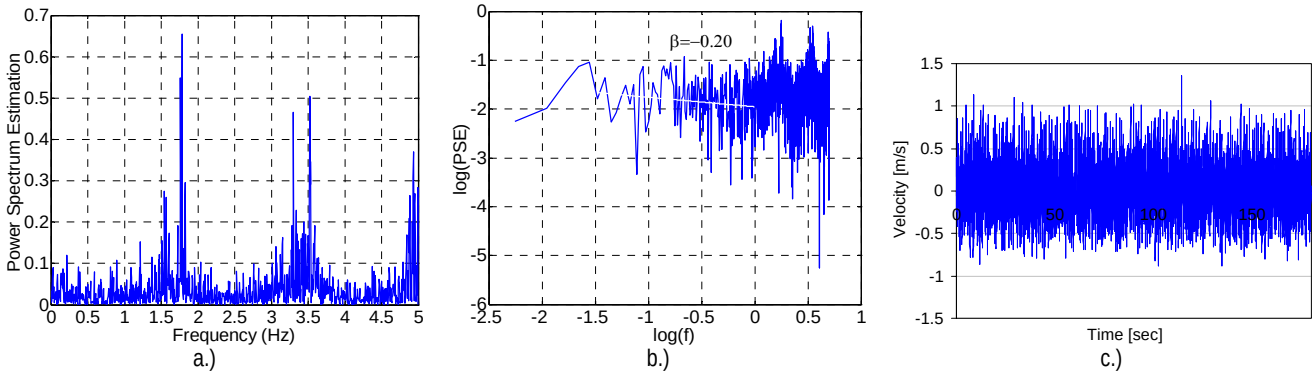

Figure 3.30. *a.) PSE at point C6 with an incidence angle of 330° and a wind velocity of 3 m/s (case 0V3330). b.) log(PSE). c.) The velocity at point C6.*

The plot of the velocity distribution at point C6 (graph c. in Figure 3.30) shows that the direction of the wind fluctuates a lot. An enlargement of the first 20 seconds of the velocity measurements is shown in Figure 3.31. Here it is seen that the velocity constantly changes from ingoing to outgoing.

The reason for the oscillation can be found in the design of the opening, which is around 10 cm deep, or in the way the wind enters the room. To come closer to a solution for this problem, the PSE for point A6 in the same experiment is examined. The results from this point are shown in Figure 3.32. Here the same peaks in the PSE are not found.

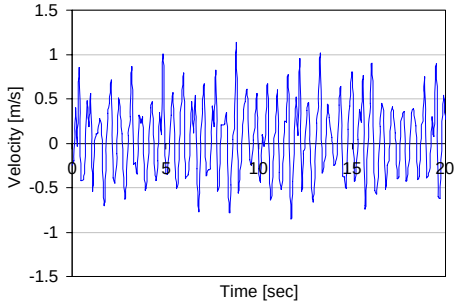

Figure 3.31. *The first 20 seconds of the velocity measurements at point C6, case 0V3330.*

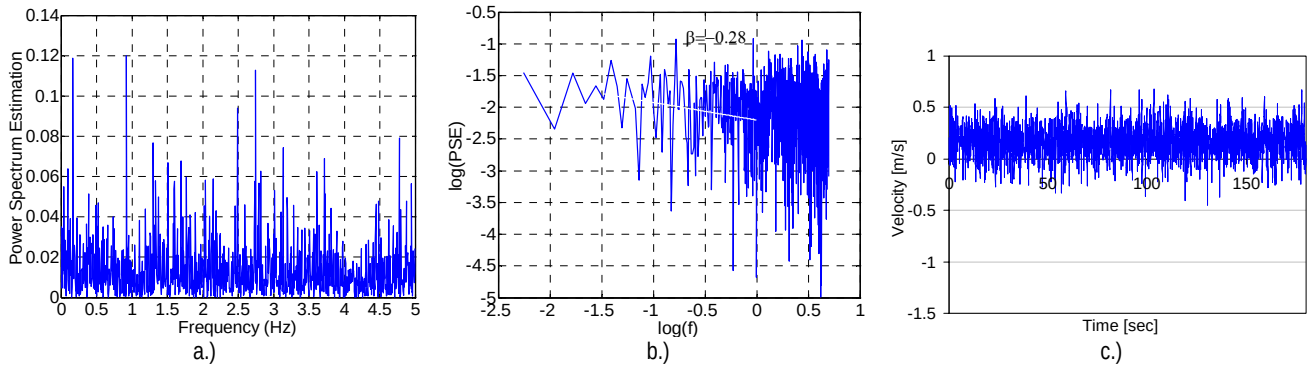

Figure 3.32. *a.) PSE at point A6 with an incidence angle of 330° and a wind velocity of 3 m/s (case 0V3330). b.) log(PSE). c.) The velocity at point A6.*

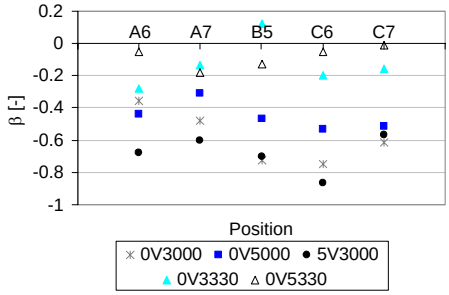

Figure 3.33. *β-values found in the opening during the wind tunnel experiments.*

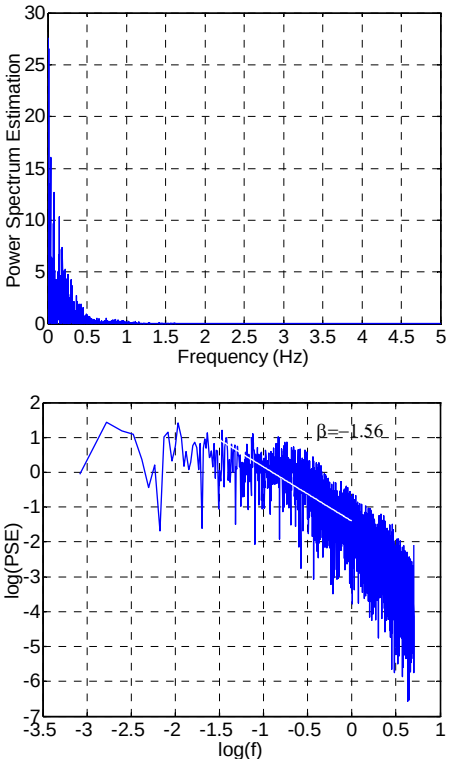

Figure 3.34. *PSE from point L4 in case 20 in the outdoor measurements.*

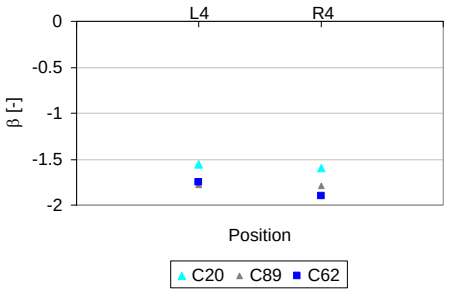

Figure 3.35. *β-values found in the opening during the outdoor experiments.*

If the velocity measurements at point A6 are examined it is seen that the main part of the velocities is positive which indicates an ingoing flow. If the design of the opening was the reason for the oscillations, the same pattern ought to be at this point. So instead the reason for the oscillations probably lies in the room combined with the incidence angle of 330° which results in a pulsating flow into the room in the right side of the opening. The average velocities measured for all the points in the opening is shown in the velocity profiles in Figure 3.23 . Here it is also seen that the average value for point C6 is close to 0 m/s.

The β-values for all points in the five test cases are shown in Figure 3.33. Here it is seen that all the β-values found in the opening in the wind tunnel experiments are below the limit of -1.1 and, therefore, the wind can be classified as wind with mechanical characteristics.

To compare the results from the opening used in the wind tunnel three cases from the outdoor experiments are analysed. In these experiments the PSE and log(PSE) in the opening give very similar results. An example from position L4 in case 20 is shown in Figure 3.34.

In the outdoor cases the PSE in the opening shows that the main part of the energy is concentrated at the low frequencies. This is typical for wind with natural characteristics.

The β-values for all the PSEs made in the outdoor opening are shown in Figure 3.35. Here it is seen that the values are close to each other and that the wind in the outdoor opening has natural characteristics.

MAIN RESULTS FROM SPECTRAL ANALYSIS

Through the analysis of the wind in the wind tunnel it was found that the main part of the wind outside the building has mechanical characteristics. An exception is three points in front of the building where h=1m and h=3m show natural characteristics and h=2m has mechanical characteristics but is very close to the limit of -1.1 that separates mechanical and natural wind.

In the opening in the wind tunnel the wind has mechanical characteristics even though the wind outside the opening showed natural tendencies.

In the outdoor experiments, the wind measured on the roof had natural characteristics with a β-value of -1.62. Compared to the results from Zhu /Zhu et al. 03/, this should correspond to open landscape which is not the case, since it is measured in a rural area. An explanation can be that Zhu has made measurements on the ground and the measurements in this project are made on the roof of the building where there is less disturbance from the buildings.

The PSE made in the outdoor opening also shows that the wind has natural characteristics.

3.5.3 LAGGED SCATTERPLOTS

Another way to compare the measurements from the wind tunnel and the test office outdoors is to create lagged scatterplots for the measurements.

The lagged scatterplots are both made with measurements in the free wind outside the buildings and measurements in the openings. The plots are made with different time lags to see how the δ-value varies with the length of the time lag.

MEASUREMENTS OUTSIDE THE BUILDINGS

The lagged scatterplots are made for the same four points in the wind tunnel as in the spectral analysis. The positions of the points are shown in Figure 3.20. In the outdoor measurements, the results from the roof measurements are used to form the lagged scatterplot.

From the results of the lagged scatterplots in the wind tunnel it is found that the measurements in front of the building have lower δ-values than the rest of the points in the wind tunnel. An example from point 15, h=3m is seen in Figure 3.36.

The lagged scatterplot found in the outdoor measurements with the same time lag is shown in Figure 3.37. When the two plots are compared it is important to notice that the scales on the axes are very different from each other. This shows that the outdoor wind measurements are much more fluctuating than the ones in the wind tunnel. This is also seen on the plots of the velocity in Figure 3.19 and Figure 3.21.

Even though the scales in the two lagged scatterplots are different you can still analyse the shape of the plot to search for different characteristics in the mechanical and natural wind. The δ-values of this comparison are shown in Figure 3.38. Here it is seen that the lowest δ-values for all time lags are found in the outdoor measurements. Point 15 (in front of the building) in the wind tunnel has lower δ-values than the other points from a time lag of Δt= 0.5 sec, but at very low Δt the values are the same for all wind tunnel measurements.

The results of this comparison show that point 15 in front of the building also has some natural characteristics, but they are not clearly natural. The same was found at this point during the spectral analysis.

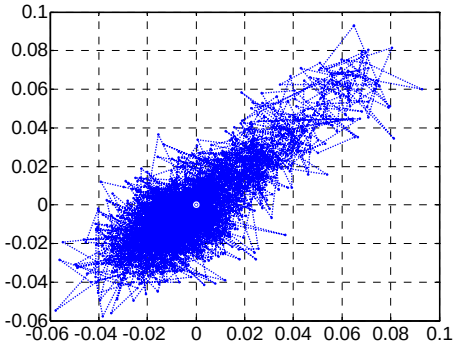

Figure 3.36. *Lagged scatterplot for Δt=0.2 second in point 15, h=3m, in wind tunnel.*

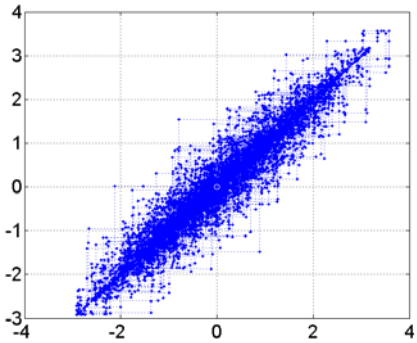

Figure 3.37. *Lagged scatterplot for Δt=0.2 second measured at the roof in the outdoor experiments.*

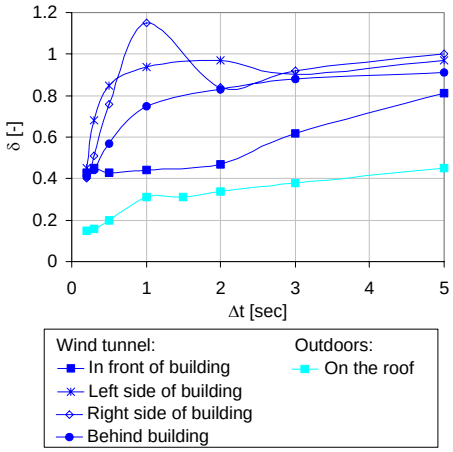

Figure 3.38. *δ-values from the lagged scatterplots made outside the buildings. In the wind tunnel h=3m is used.*

MEASUREMENTS IN THE OPENINGS

In this comparison of natural and mechanical wind, the lagged scatterplots are made for three points in the wind tunnel opening and two points in the outdoor opening. An example of the lagged scatterplots found in the two cases is shown in Figure 3.39.

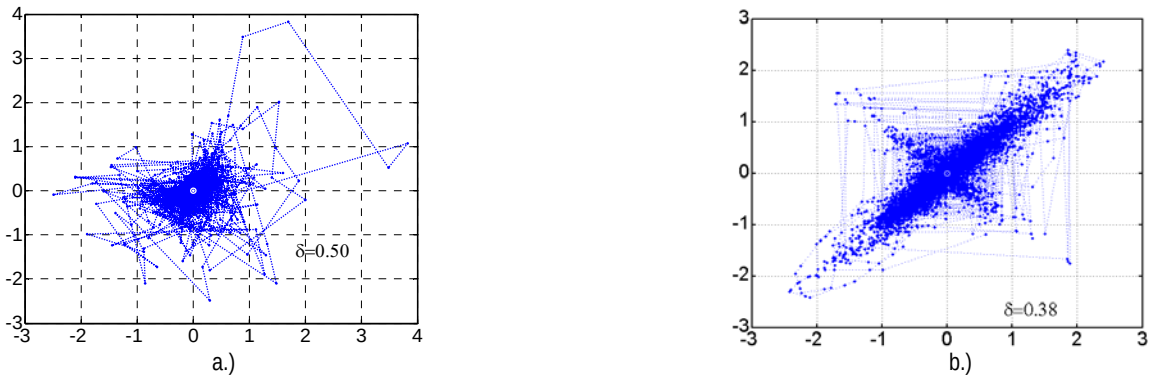

Figure 3.39. *Lagged scatterplots from the openings with Δt=0.2 sec. a.) Point C6 in wind tunnel b.) Point R4 from outdoor measurements.*

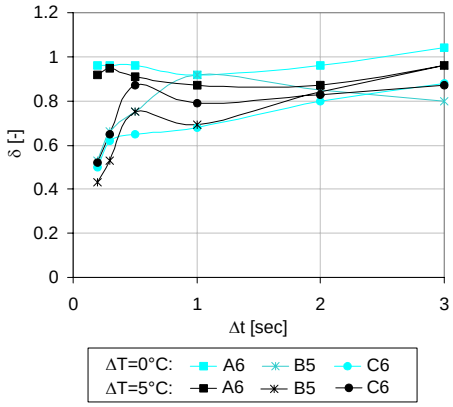

Figure 3.40. *δ-values from the lagged scatterplots made for the wind tunnel opening.*

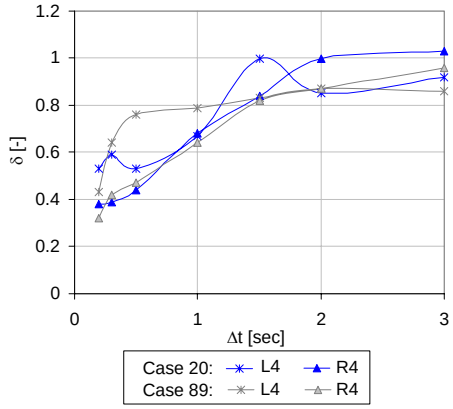

Figure 3.41. *δ-values from the lagged scatterplots made for the outdoor opening.*

In the lagged scatterplots made for the openings, the characteristic shape of the plots mentioned in the literature review is easily seen. A small exception is the "wings" found on the plot from the outdoor opening. These increase the width of the plot and thereby also the δ-value a little. All the δ-values found in the outdoor and wind tunnel experiments are shown in Figure 3.40 and Figure 3.41. Here it is seen that the scattering of the values is small even though the results are from different cases. This indicates that it is the type of wind that defines the δ-value.

When comparing the lagged scatterplot from the two types of experiments, the general level of the δ-value is found to be lower in the outdoor experiments when the time lags are small (up to 1 sec). After this the coherence has disappeared and the same values are found in the two cases.

MAIN RESULTS FROM LAGGED SCATTERPLOTS

The results from the lagged scatterplots are very similar to the results from the spectral analysis. The method with lagged scatterplots are much easier and faster to use, but the level of details fades away with the time you save on using this method. Further discussion of the results will be made in the next section.

3.6 CONCLUSION OF THE ANALYSIS OF WIND CHARACTERISTICS

The aim of this theoretical analysis of the characteristics in mechanical and natural wind was to find major differences in these two types of wind. These differences will later on be included in the considerations when a new design expression for single-sided natural ventilation is set up.

During the analyses with spectral analysis and lagged scatterplots it was found that the wind in front of the building in the wind tunnel experiments (WTE) has some similarities with natural wind. Two of the three points below building height show natural characteristics and the last point is very close to the limit of -1.1 that separates wind with mechanical characteristics from wind with natural characteristics. The points on the sides and behind the building in the WTE all have mechanical characteristics.

In the opening there is a clear separation between wind with natural characteristics (from the outdoor experiments) and mechanical characteristics (from the WTE), especially in the spectral analysis. Some uncertainties are connected to the comparison in the openings since different equipment was used in the WTE and the outdoor experiments (OE). 3D anemometers were used in WTE and 2D in OE. The 2D anemometers were shielded from wind at the top of the anemometer (see Figure 3.42) and the effect of this is unknown.

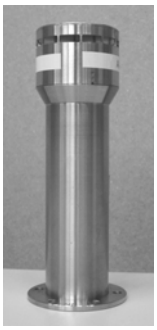

Figure 3.42. *The 2D anemometer used in the outdoor experiments.*

Through this analysis it has been found that small frequencies are more dominating in natural wind. This means that larger eddies than in the wind tunnel are expected when you are measuring outdoors. One of the most obvious reasons for this is the available space for the eddies to be created on. In the wind tunnel the flow is very unidirectional and the possibilities to have different scales of eddies in the flow are limited. Outdoors there are possibilities for different directions and also very large scales since the limitations here are the surroundings of the building.

As a final conclusion to this analysis it can be said that mechanical and natural wind do not have the same theoretical characteristics when analysed. It is therefore not possible just to conclude that results found in the wind tunnel and outdoors can be directly compared. On the other hand, it has not been proved that they cannot be compared and as long as it is borne in mind that natural wind has larger eddies, the work with creating a design expression from a combination of the WTE and the OE should be possible.

CHAPTER 4

Full-Scale Experiments

In this chapter all the preliminary conditions during the wind tunnel and outdoor experiments are described. This includes a description of the equipment, the rooms and also a discussion of the different methods that are used in the experimental work such as use of tracer gas methods for air-change measurements and calculation of air-change rates from velocity measurements in the opening.

4. FULL-SCALE EXPERIMENTS

During this work two different kinds of full-scale experiments have been made to measure the air-change rate as a function of incidence angle, temperature difference and wind velocity. The first experiments were made as wind tunnel experiments in a full-scale building at the Japanese Building Research Institute (BRI), Tsukuba, Japan. These experiments were carried out during the 2nd part of 2002 and are described in section 4.1.

The other part of the experiments was full-scale experiments made outdoors during the summer of 2005 in an office at Aalborg University (AAU). These experiments are described in section 4.2.

The assumptions and calculations made in connection with the performance of the full-scale experiments are described in this chapter together with a description of the test set-ups. Besides this, a discussion of the methods for measuring the air-change rates is made in section 4.3. Here the assumptions in both tracer gas methods and evaluation of velocity profiles for measurements of airflow through the opening are described.

The results of the experiments are described in chapter 5.

4.1 MEASUREMENTS IN A FULL-SCALE BUILDING AT BRI (WIND TUNNEL)

The experiments were carried out in the wind tunnel at BRI shown in Figure 4.1. The wind speed in the tunnel could be varied between 1-5 m/s with a turbulence intensity less than 5%. The wind speed profile created in the wind tunnel was almost uniform. The blocking ratio in the wind tunnel working section was 12% and compared to the outlet the blocking ratio was 34%. The principle and the dimensions of the wind tunnel can be seen in Figure 4.2. The test building was made as a full-scale model sized 5.56 x 5.56 x 3 m, see Figure 4.3, which means that scale effects were avoided. The internal room height was 2.4 m and the thickness of the walls was 0.1 m. The room volume used in the calculations is 68.95 m^3.

The experiments were carried out to investigate how the air change rate depends on the pressure difference measured across the openings, the wind velocity, the turbulence intensity, the wind direction and the temperature difference between inside and outside of the building. Both single-sided ventilation and cross-ventilation were considered.

4.1.1 THE TEST SET-UPS

The set-ups used in the experiments are shown in Figure 4.4 and Figure 4.5. With single-sided ventilation, an internal wall was used to investigate whether changing the volume will decrease the volume flow through the opening.

Figure 4.1. *The building in the wind tunnel at BRI.*

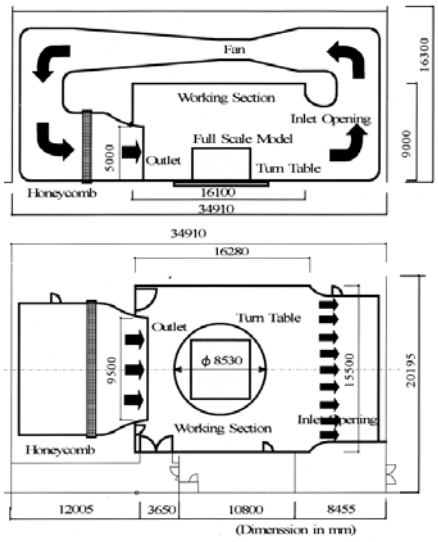

Figure 4.2. *The wind tunnel at BRI.*

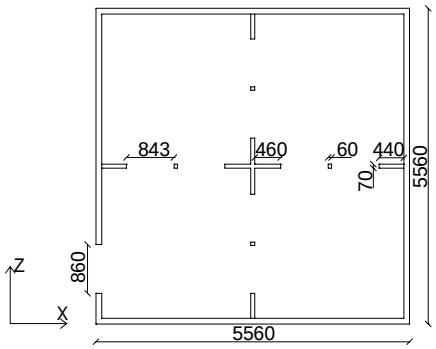

Figure 4.3. *The test building. Dimensions in mm.*

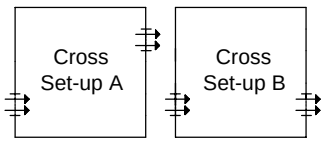

Figure 4.4. *Test set-ups for cross-ventilation.*

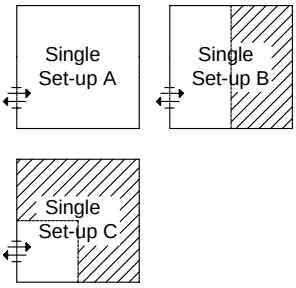

Figure 4.5. *Test set-ups for single-sided ventilation.*

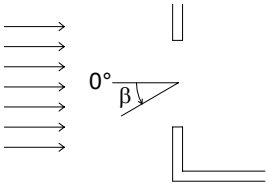

Figure 4.6. *Definition of the incidence angle of the wind*

During the measurements with cross-ventilation, air change rates were measured with airflow crossing the room (Set-up A) and with direct airflow (Set-up B), see Figure 4.4.

In the measurements with single-sided ventilation the volume flow-rate through a single opening in the building was measured and the dependence of the air change rate and the volume of the room were investigated by inserting internal walls and thereby changing the volume (set-up B and C). The experiments were made with an opening in the right side of the outer wall and the main parts of the experiments were made with set-up A. The experiments were made under the same velocity and temperature conditions as cross-ventilation. During the experiments, the model was rotated between 0° and 345° with either a 15° or a 30° increase to get measurements for different angles of the wind.

DEFINITION OF INCIDENCE ANGLES

The direction of the wind coming towards the opening is described by the incidence angle, which is measured counter clockwise. The definition is illustrated in Figure 4.6.

A small "do-it-yourself" building model is made in Appendix 2. By constructing this model you will have en good overview of the incidence angles in the wind tunnel.

4.1.2 CALCULATION OF OPENING SIZES

The following calculations show how the opening areas were calculated. In cross-ventilation the opening size was dictated by the necessary space for the anemometers. In single-sided ventilation a maximum air-change rate around $10h^{-1}$ was wanted. In both cases the width was set to 0.86 m because of the construction of the building in the wind tunnel.

The calculations are based on the expressions from earlier work with cross and single-sided ventilation, which all are described in chapters 1 and 2.

CROSS-VENTILATION

The volume flow through the openings in cross-ventilation is found from the orifice equation in (4.1). /Etheridge et al. 96/

$$Q_V = \pm C_D \cdot A \cdot \sqrt{\frac{2 \cdot |\Delta P|}{\rho}} \qquad (4.1)$$

Since the model has only two openings (one at windward and one at leeward side), the pressure difference can be described from expression (4.2) /Heiselberg05/

$$\Delta P = \Delta C_p \cdot ½ \cdot \rho \cdot U_{ref}^2 \quad (4.2)$$

With C_D = 0.6 as suggested in /Etheridge et al. 96/, C_p = 0.6 at the windward side and –0.2 at leeward side, an opening of 0.15 x 0.86 m, which corresponds to 0.129 m^2, and a reference velocity of 5 m/s will result in an air change rate around 18 h^{-1}.

SINGLE-SIDED VENTILATION

The air change rates in single-sided ventilation in the isothermal case were calculated from (4.3) /Warren et al. 85/

$$Q_V = 0.025 \cdot A \cdot U_R \quad (4.3)$$

If the situation was thermal, the expressions in (4.4) and (4.5) were used. /De Gids et al. 82/

$$U_m = \sqrt{(0.001 \cdot U_R{}^2 + 0.0035 h \Delta T + 0.01)} \quad (4.4)$$

$$Q_V = A_{eff} \cdot U_m = C_D \cdot A \cdot U_m \quad (4.5)$$

An area sized 0.86 x 1.4 m will result in an air change rate of 8.5 h^{-1} in the thermal case with a temperature difference of 10°C. This opening will, according to the calculations, result in an air change rate of 6.1 h^{-1} in the isothermal case with 5 m/s.

POSITION OF THE OPENINGS IN THE BUILDING FAÇADE

The positions of the openings are shown in Figure 4.7 and Figure 4.8.

4.1.3 MEASUREMENTS AND EQUIPMENT

The experiments were made under the following conditions (see further details on the test-plans in appendix 3).

- With test set-ups as in Cross set-up A and B and Single set-up A, B and C
- Wind velocities of 1, 3 and 5 m/s
- Isothermal experiments and experiments with a temperature difference of 5°C and 10°C

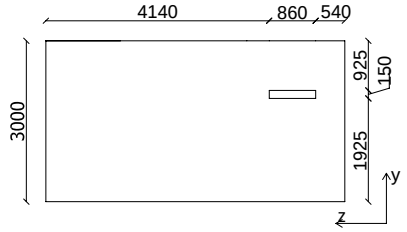

Figure 4.7. *Positions and sizes of the openings in cross-ventilation. Dimensions in mm.*

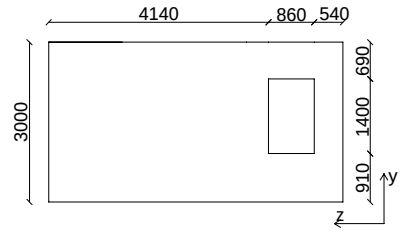

Figure 4.8. *Positions and sizes of the opening in single-sided ventilation. Dimensions in mm.*

- Rotation of the model divided into intervals of 15° or 30°. In single-sided ventilation a full rotation of the building was necessary. In cross-ventilation the building was only rotated between 270° and 75° because of symmetry. In set-up B the symmetry is 0°=180°, 30°=120°, 60°=150°, 210°=300°, 240°=330°. 90° and 270° are not identical in this case, but it was chosen to use only 270°, since this case has the front opening at the same position as set-up 2A.

For all these conditions, measurements of pressure, velocity, temperature and air change rate were made.

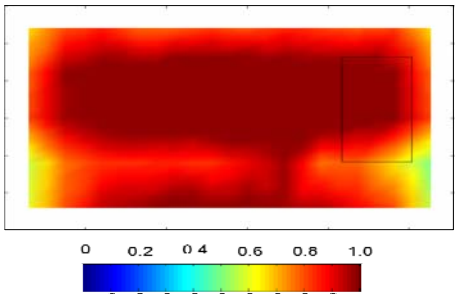

Figure 4.9. *C_p-values measured at the front wall on the closed building with an incidence angle of 0°. The position of the window during the experiments with single-sided ventilation is marked on the building.*

PRESSURE

Measurements of the static pressure *on the building without any openings* had already been made at BRI and were therefore not measured. An example of the pressure distribution on the front wall with an incidence angle of 0° is shown in Figure 4.9. The position of the opening in the later experiments with single-sided ventilation is indicated. Pressure distributions for other angles can be found on the CD in the document Cp-plots.pdf.

The static pressure *on the building with opening(s)* was measured at a frequency of 10 Hz. The internal pressure was measured in two points at the floor. The positions of the pressure measurements are shown in Figure 4.10.

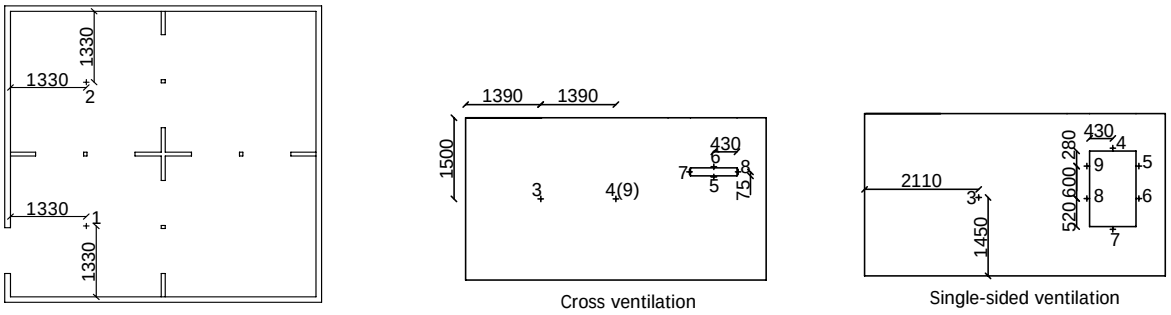

Figure 4.10. *Positions of pressure measurement at the floor and front wall. Numbers in () show the numbers at the back. Points around the openings are app. 50 mm from the edge. Dimensions in mm.*

The exact positions of the pressure points close to the openings are shown in Table 4.1.

The results from the pressure measurements are a pressure difference across the opening depending on the wind velocity and also a picture showing how the pressure on the envelope changes when an opening is added.

The pressure measurements were made with 9 tubes connected to a Baratron Type 220C instrument from MKS. The full span of this instrument is 133 Pa and the accuracy of the measurements is ±1/9800 Pa. The measurements were collected by a TEAC digital recorder and afterwards converted into a text file by a TEAC data processing program.

Point	Cross-ventilation	Single-sided ventilation
4	-	50
5	54	57
6	48	57
7	50	50
8	57	50
9	-	50

Table 4.1. *Distance in mm between the edge and the pressure point. Numbers according to Figure 4.10.*

VELOCITY

The velocity *in the opening* was measured at a frequency of 10 Hz to be able to investigate the effect of fluctuations. During the experiments with cross-ventilation, all velocity measurements (10 points) were made at the same time. To obtain a realistic picture of the velocities in the opening in single-sided ventilation, three separate measurements were necessary. This was due to the fact that only 10 anemometers were available for these measurements and 24 points were necessary. The positions of the measuring points are shown in Figure 4.11.

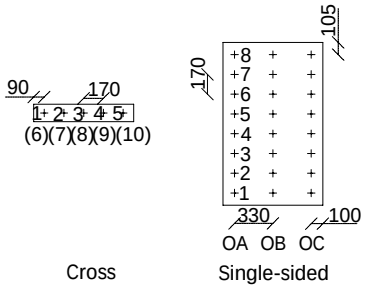

Figure 4.11. *Measurements of velocity in the openings (seen from outside). Numbers in () show the numbers at the back. Dimensions in mm*

The velocity distribution *upstream the building* was already available at BRI.

From the velocity measurements in the opening, a velocity distribution can be made through plots of the velocity profiles. From these measurements it is also possible to estimate the volume airflow from the measured velocity multiplied by the matching area.

The velocity measurements were ultrasonic anemometers produced by Kaijo, type WA-390 and DA-600-3, see Figure 4.12. The measurements were collected by the same TEAC digital recorder as the pressure measurements and also converted into a text file. The local axes of the anemometers are shown in Figure 4.13.

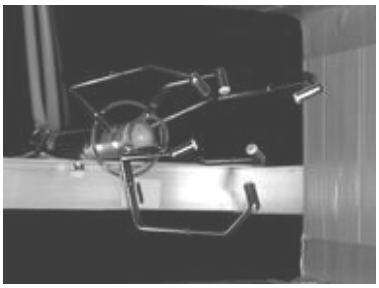

Figure 4.12. *Ultrasonic anemometer.*

The accuracy of the anemometers is ±2% of full span, which in this case was set to 5 m/s. This results in an accuracy of ±0.1 m/s.

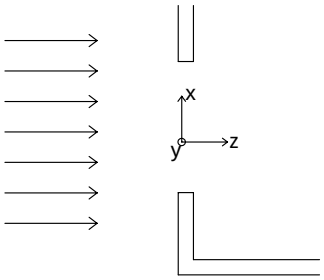

Figure 4.13. *Local axes of the anemometers. Y is upwards directed.*

TEMPERATURE

The temperatures were measured both outside the building (2 points), in the opening(s) (8 points) and at 16 positions inside the building. This was necessary to find the temperature difference driving the air through the openings. The measurements were made at a frequency of 1/15 Hz. The distribution of the temperature measurements is shown in Figure 4.14. The points in the openings are positioned 5 cm behind the opening in cross-ventilation and 17 cm in single-sided ventilation.

From the temperature measurements the vertical temperature gradient in the room (if any) is found. The degree of mixing in the room is also checked from these measurements by looking at internal temperature differences.

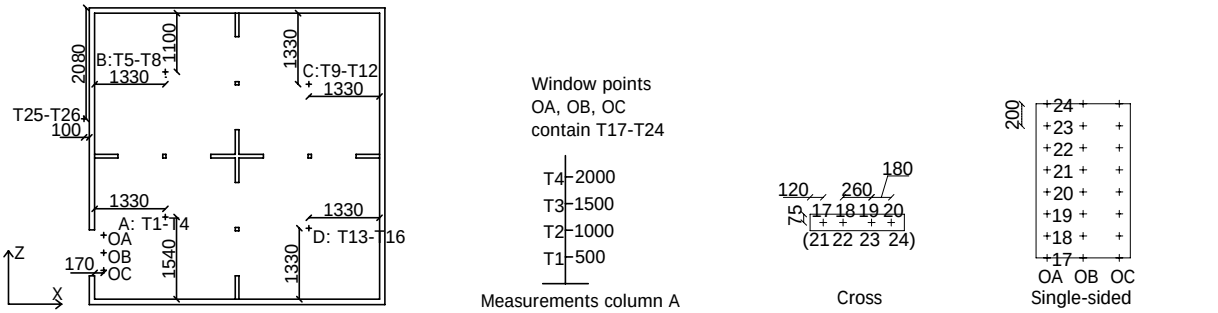

Figure 4.14. *Measurements of temperature outside and inside the building. Marks indoors show the positions on the columns (A-D), where the lowest number is positioned nearest the floor. The measurements of temperature in the openings are seen from the outside. Numbers in () show the numbers at the back side. Dimensions in mm.*

The temperature was measured with thermocouples of copper and constantan connected to an ice point reference. The temperature was collected by a Thermodac logger produced by Eto Denki.

The error is found to be around ±0.15°C by measurements in a homogeneous environment.

CREATION OF TEMPERATURE DIFFERENCES

Heat was added to the room by four electric heaters positioned in each quarter of the building. Each heater (1000 W) was controlled by at thermostat to keep the desired temperature difference of 5°C or 10°C.

AIR CHANGE RATES

The measurements of air change rates in the wind tunnel experiments were made with tracer gas (SF6) at a frequency of 1/15 Hz. The problem in measuring air change rates with gas is that the method requires full mixing in the building during the experiments, which is hard to get in this model – especially in the cases with single-sided ventilation. The only way to mix the air inside the room is to use small fans, but the effect of this is

unknown. A discussion of the possible errors in using this method is made in section 4.3.

During the experiments gas was added inside the building (all openings closed). Small fans inside the room were turned on until full mixing was accomplished, then the fans were turned off and the experiment was started. A problem with this method in the BRI wind tunnel was that no fresh air was added, see Figure 4.2, and the concentration in the wind tunnel, therefore, increased after each experiment and lead to a small concentration of gas in the "fresh air" coming through the tunnel. This problem was solved by subtracting the concentration in the tunnel (measured before the experiment starts (C_0)) from the measured concentration inside the test building and by this calculate the mean airflow from expression (4.6). /Etheridge et al. 96/

$$\overline{Q_v} = V \frac{ln \frac{C(t_1) - C_0}{C(t_2) - C_0}}{(t_2 - t_1)} \qquad (4.6)$$

The expression above is a straight line in a single logarithmic graph, which is illustrated in Figure 4.15 with an air-change rate of 10 h^{-1} and C_0 = 0 m^3/m^3.

From the figure it is also seen that the expression can be written as

$$\overline{Q_v} = V \cdot slope \qquad (4.7)$$

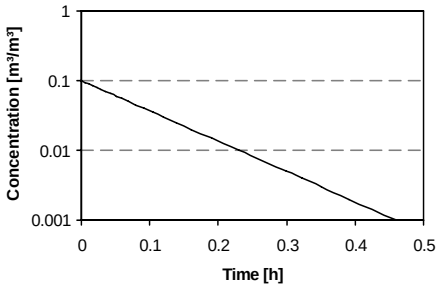

Figure 4.15. *Concentration vs. time with n = 10 h^{-1}.*

The concentration used in the experiments was around 100-150 ppm since the Innova Gas Analyser used at BRI had an accuracy of 1 ppm.

The measurements were made with eight tubes connected to a small container which was connected by a single tube to the gas analyzer, see Figure 4.16. Due to these eight tubes a mean value of the gas concentration was found which was more accurate than just measuring at one point.

Figure 4.16. *Tube system for tracer gas measurements.*

The tubes were placed at the columns used for temperature measurements at heights of 1 and 2 m.

To check the level of mixing in the room, the doors were closed in some of the first experiments, the air was fully mixed by fans and the concentration was measured again.

The concentration in the wind tunnel was measured just before every experiment by a separate tube.

The concentration of SF6 used in the experiments was measured by an Innova 3429A fast response Triple-gas Monitor.

MEASUREMENTS DURING A TEST SESSION

The following measurements were made during every test session:

1. The heaters (if used in the experiments) were turned on the night before the experiment to ensure steady state conditions in the room. The temperature was kept fixed by thermostatic controllers on the heaters. All openings were closed.
2. The wind tunnel was turned on.
3. The gas concentration in the wind tunnel was measured.
4. Small fans were turned on and tracer gas was added with the gas analyser running.
5. The door(s) in front of the openings were removed.
6. Temperature measurements were started.
7. The experiments ran until the curve of the gas analyser was long and constant enough to give a reasonable picture of the air change. Three minutes before this, velocity and pressure measurements were started. In single-sided ventilation two further measurements of velocity and pressure were made after the gas measurements were stopped because the anemometers had to be moved to other positions.

4.2 MEASUREMENTS IN AN OFFICE AT AAU (OUTDOORS)

The outdoor experiments were made in an office building at Aalborg University, Sohngaardsholmsvej 57. The area is shown in Figure 4.17.

The experiments were made in an office at the second floor in building B, see Figure 4.18. The size of the room was 6.15 x 3.45 m. Only single-sided ventilation was investigated.

In the experiments it was investigated how the air change rate depends on the pressure difference measured across the openings, the mean velocity of the wind, the turbulence intensity, the direction of the wind and the temperature difference between inside and outside of the building.

Figure 4.17. *The area around the office building*

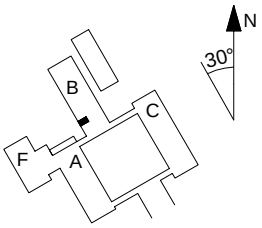

Figure 4.18. *Position and direction of the test office in building B.*

4.2.1 DESCRIPTION OF THE TEST OFFICE

As mentioned, the room was 6.15 x 3.45 m with a room height varying from 2.65 m to 3.0 m. This gives a total room volume of 59.9 m^3. The plan of the test office is shown in Figure 4.19.

The opening towards the outdoors was a hinged part of the window, which was kept open during the experiments. The size of the opening was 91 x 116.5 cm. The position of the opening in the wall is shown in Figure 4.20.

During the experiments the closed window area was shaded from the sun to avoid uncontrollable solar heat gains.

4.2.2 MEASUREMENTS AND EQUIPMENT

The experiments were made under the following conditions:

- Fully opened window.
- Wind velocity and direction were measured both 4m above the roof of the building and 1m away from the façade near the opening. Since the measurements were made outdoors, the conditions could not be preset.
- Temperature difference was measured as the difference between an average in the room and the temperature just outside the room.

Pressure, velocity, temperature and air change rate were measured during all experiments.

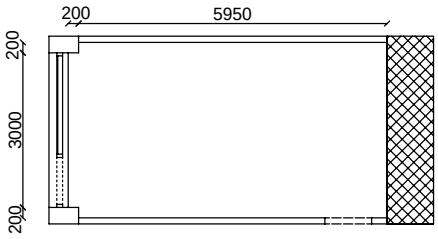

Figure 4.19. *Plan of the test office. Dimensions in mm.*

Figure 4.20. *Position of the opening in the wall.*

PRESSURE

To know the pressure difference across the opening (inside – outside) and in the opening itself, pressure measurements were made at six different points. The pressure was measured at two points in the façade, two points at the floor inside the room and two points at the edge of the window. All points were connected to a metal container to have the same reference pressure. The container is constructed with a very small opening at the bottom to avoid a fluctuating reference pressure. The positions of the measuring points are shown in Figure 4.21.

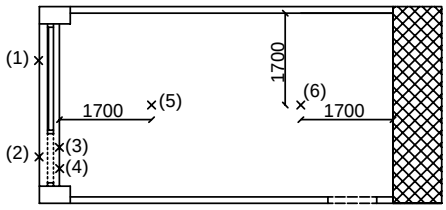

Figure 4.21. *Position of pressure measurements. Dimensions in mm.*

To calculate the C_p-value during the experiment, the pressure in the reference container is measured by a Mensor digital pressure gauge. The accuracy of the manometer is +/-1 Pa. Calculations of the C_p-value are made as shown in (4.8) - (4.10).

$$\begin{aligned} \Delta P_{wall} &= P_{wall} - P_{ref} \\ &\Updownarrow \\ P_{wall} &= \Delta P_{wall} + P_{ref} \end{aligned} \tag{4.8}$$

where ΔP_{wall} is measured by the pressure transducers and P_{ref} is measured by the precision manometer.

$$P_{wall} = C_p \cdot \tfrac{1}{2} \rho U_{roof}^2 + P_{atm} \tag{4.9}$$

where P_{atm} is measured by the precision manometer. This value is added because P_{wall} is the total pressure.

If (4.8) and (4.9) are set equal, C_p can be calculated, see (4.10).

$$\Delta P_{wall} + P_{ref} = C_p \cdot \tfrac{1}{2}\rho U_{roof}^2 + P_{atm}$$
$$\Updownarrow$$
$$C_p = \frac{\Delta P_{wall} + P_{ref} - P_{atm}}{\tfrac{1}{2}\rho U_{roof}^2} \qquad (4.10)$$

The pressure measurements were made by six differential pressure transducers from Furness Controls Limited, type FCO44. The full spans vary between 20, 100 and 500 Pa (two transducers for each interval) and the accuracy of the transducers is +/- 0.2% of the full span. The measurements were collected by a HBM data logger 334 measuring at a frequency of 10 Hz.

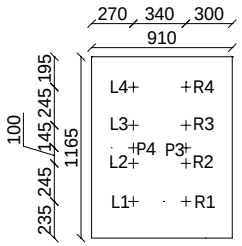

Figure 4.22. *Position of velocity measurements in the opening (seen from inside). Dimensions in mm.*

Figure 4.23. *The hot-sphere and the 2D ultrasonic anemometers used in the experiments.*

VELOCITY

Compared to the wind tunnel case the outdoor case gets more complicated regarding the velocity in the opening. In the outdoor case it is not possible to move the anemometers during a test case, since the wind suddenly can change and thereby change the conditions in the opening radically. The velocity in the opening was measured by 8 anemometers uniformly distributed in two columns across the opening. The positions of the anemometers are shown in Figure 4.22.

Since it was important to know the direction of the velocity, four 2D ultrasonic anemometers were used in the corners of the opening. These were used together with four hot-sphere anemometers.

The measurements were made with a frequency of 10 Hz.

The 2D ultrasonic anemometers were type FT702 from FT Technologies Ltd. The range for the anemometer was from 0 to 30 m/s with a resolution of 0.1 m/s. The accuracy was +/- 4% of the reading. The accuracy of the wind direction measurement was +/- 3° and the resolution was 1°.

The hot sphere anemometers (illustrated in Figure 4.23) were a IFS system from Dantec with 8 channels. The accuracy was +/- 0.05m/s.

TEMPERATURE

To find the temperature distribution in the test office, the temperature was measured at 16 points inside the room. The measurements were distributed on four columns with four points on each. The measuring points are shown in Figure 4.24.

The thermocouples used for the measurements were of type K. The measurements were made at a frequency of 10 Hz. The accuracy of the measurements was +/- 0.15°C.

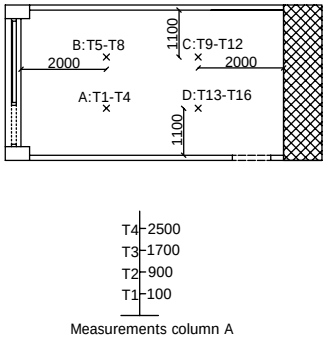

Figure 4.24. *Position of temperature measurements inside the test office. Dimensions in mm.*

CREATION OF TEMPERATURE DIFFERENCES

As in the wind tunnel experiments, heat was added to the room by 3 electric heaters positioned farthest away from the openings and also out of reach of the thermocouples. Each heater (750W) was controlled by a thermostat to keep the desired temperature difference of 5°C or 10°C.

AIR CHANGE RATES

Because of problems with remote control of the opening it was decided to leave the opening open at all times. The air change rates were then measured by the constant injection method, where a constant volume of tracer gas was added to the room at four different points. The flow rate can be found from expression (4.11). /Etheridge et al. 96/

$$Q_v = \frac{\dot{m}}{C_i(t_1) - C_o} - \frac{V}{t_2 - t_1} \cdot ln \frac{C(t_2) - C_o}{C(t_1) - C_o} \qquad (4.11)$$

N_2O was used as tracer gas and the constant flow rate was found from an estimated air change rate of $10h^{-1}$ and a concentration level around 35 ppm. The calculation is made for at steady condition and is shown in (4.12).

$$Q_v = \frac{\dot{m}}{C} \Rightarrow$$

$$\dot{m} = (10h^{-1} \cdot 59.9m^3) \cdot 35 \cdot 10^{-6} m^3/m^3 \cdot \frac{1000l/m^3}{60 min/h} = 0.35 l/min \qquad (4.12)$$

The measurements were made at a frequency of approximately 1/90 Hz. To increase the accuracy of the measurements, gas samples were taken at 8 points and then mixed in a small container which was connected to the gas analyser. The measurement points were positioned on the four temperature columns (see Figure 4.24) in the room in 1m and 2m's height.

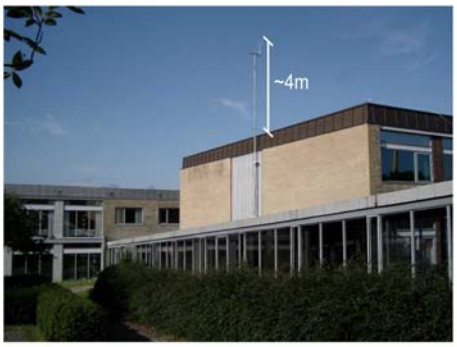

Figure 4.25. *Position of the anemometer measuring the outdoor wind speed.*

WIND SPEED AND OUTDOOR TEMPERATURE

The wind speed and outdoor temperature were measured simultaneously with the measurements inside the test office to make sure that the outside conditions are known at all times.

The wind speed was measured at the south end of the roof on building B with a 3D ultrasonic anemometer R3 at a frequency of 10 Hz. The position of the anemometer is shown in Figure 4.25. The outdoor temperature was measured outside the window in the test office.

4.2.3 CONTROL OF AIRTIGHTNESS IN THE TEST OFFICE

During the experiments it was important that the room was kept very tight and that the only air exchange happened through the window. Since the door into the room and the mechanical ventilation opening near the ceiling are sources for leakage, these were sealed off. Before the experiments started a test was made in the room to ensure that the room was tight enough. The test was made with equal pressure inside and outside and also with an overpressure created by the inlet diffuser normally working in the office. The outlet was sealed off in both tests.

In the case with approximately equal pressure the air change rate was measured to $0.4h^{-1}$. In the case where the overpressure was created the air change rate was measured to $1.4h^{-1}$. Unfortunately the pressure measurements between the room and the adjacent room in this case has failed, so only the pressure difference between the test office and outside is known. This pressure difference is 3.8 Pa, but this value does not tell anything since nearly the same is measured in the equal-pressure situation.

4.3 DISCUSSION OF METHODS USED IN THE EXPERIMENTAL WORK

During the measurements of air-change rates in this project some decisions and approximations needed to be taken. This section is written to give some insight into how the decisions were made.

4.3.1 TRACER GAS METHODS FOR CALCULATION OF AIR-CHANGE RATES

In the experiments two different tracer gas methods was used. In the wind tunnel experiments the tracer gas decay method was used and in the outdoor experiments the tracer gas constant-injection method was used. Looking back, the choice with two different methods has not been clever since the fact that there are two different methods also give more sources for errors than if the same method had been used for both kinds of experiments.

The reason for the different methods was a problem with the window opening in the outdoor experiments. It was not possible to open the window from outside the room so instead the window needed to be constantly open during the experiments, which excluded the decay method. Since the wind tunnel measurements were already made at that time it became two different tracer gas methods.

DESCRIPTION OF THE PROBLEM WITH INCOMPLETE MIXING

When tracer gas methods are applied to measure air-change rates an assumption of full mixing in the room is made. During the experiments this is difficult to check.

The sources for incomplete mixing can be divided into three cases. The first problem is that *the airflow does not reach the back of the room,* but only ventilates the area nearest the window and thereby creates *a horizontal gradient in the room*. This problem is illustrated in Figure 4.26. This problem can appear in a wind dominated case where the outdoor temperature is close to the indoor temperature. If this is the case both the decay method and the constant injection method will result in *measurements of lower air changes* than the actual air change.

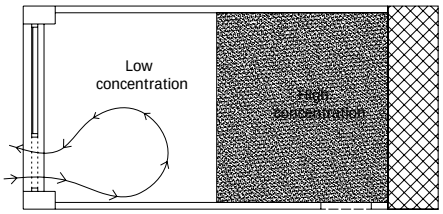

Plan of the room

Figure 4.26. *Problem with incomplete mixing in the room because of a horizontal gradient.*

The second problem is when the temperature difference becomes larger and the stratification of the room air increases. This is illustrated in Figure 4.27. In this case the cold and clean outdoor air will spread out across the floor and slowly rise in the room. Here *vertical stratification in the gas concentration* can also be expected and since the exhaust air will be the warm air near the ceiling with high gas concentration, the air that leaves the room will have a higher concentration than the concentration measured in the room. In this case the *measured air change is higher* than the actual air change.

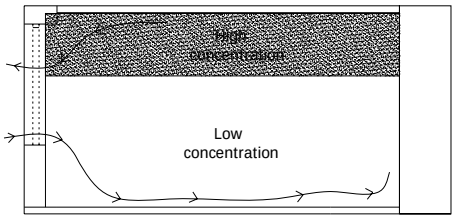

Section of the room

Figure 4.27. *Problem with incomplete mixing in the room because of a vertical gradient.*

The third problem is connected to the constant injection method. If the point with *gas injection is close to the opening/exhaust*, concentrated gas might leave the room again without any mixing with room air. In this case the *measured air change rate will be higher* than the actual air change.

COMPARISON OF THE TWO METHODS

To investigate the differences between the decay method and the constant injection method, Sandberg et al. made some experiments using the two methods in the same building. /Sandberg et al. 85/, /Sandberg et al. 89/ & /Etheridge et al. 96/

The experiments were carried out in a full-scale indoor test house at the National Swedish Institute for Building Research. The house had a floor area of 70.2 m^2 and a total volume of 175.7 m^3 including a living room, bedroom, hall, kitchen and bathroom, see Figure 4.28. The air from the house was mechanically exhausted from the kitchen (app. 68%) and the bathroom (app. 32%). The inlets consisted of two openings in the living room and bedroom ceilings, respectively. These were not mechanically controlled. During the experiments all internal doors in the house were open. All experiments were made both with and without mixing fans running inside the building.

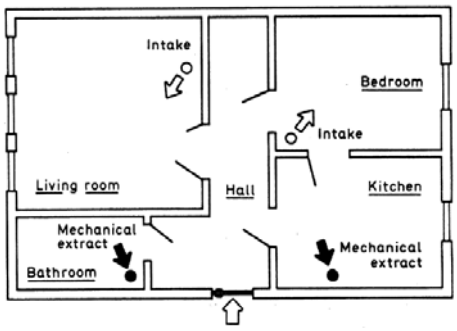

Figure 4.28. *The test house used in the comparisons of different tracer gas methods. /Etheridge et al. 96/*

During the use of both methods it was easily seen that the main importance was to assure complete mixing in the rooms/building. The best mixing was accomplished in the cases where gas was added near the fresh air inlet and the concentration was measured near the exhaust. In fact, this knowledge improved the first results of the decay method considerably. The first experiments showed an error in the estimate of air changes of 11% +/- 6% (described in /Sandberg et al. 85/), but later

experiments with the decay method have shown errors ranging from 0% to 6% (described in /Ehteridge96/). Experiences with the decay method also show that larger airflows result in better mixing of the tracer gas with the room air.

In the experiments with the constant injection method the results differed very much depending on whichever room was used as source room for the tracer gas. If the gas was added and removed as described above, an accuracy within 5% of the nominal flow rate was obtained. If the gas was added close to one of the outlets, errors up to 100% were obtained. The reason for this large error is the removal of concentrated gas from the building. The experiments show that this direct removal results in the greatest errors and therefore also must be considered to be of great importance.

From this comparison of the decay method and the constant injection method it is shown that both methods result in errors around 5%. The main importance in both methods is the degree of mixing between tracer gas and room air. Therefore +/-5% will be used as an estimate of errors in this work with tracer gas measurements as long as the mixing is found to be reasonable.

EXAMPLES OF MEASUREMENTS WITH DECAY AND CONSTANT INJECTION METHOD FROM THIS PH.D WORK

As mentioned before, the air-change rates measured in connection to this Ph.D work have been found both through the decay method and the constant injection method. To give an idea of how steady the airflow was in the experiments, plots from both types of measurements are shown.

In the wind tunnel experiments the decay method was used. The length of the measurements in these experiments varied according to the air change rate because a sufficient length of the decay curve was necessary to make an accurate reading of the slope. An example of a decay curve is shown in Figure 4.29. From the concentration plot it seems like the mixing in the room is good since the deviation of the points from the tendency line is low.

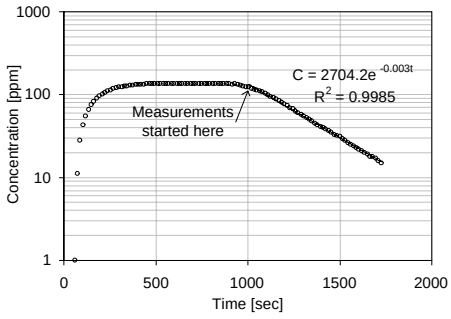

Figure 4.29. *Example of a decay curve measured during the wind tunnel experiments in case 0V5000.*

During the experiments with the constant injection method in the outdoor experiments it was harder to get the same level of mixing in the room judged from the results of the concentration measurements. The concentrations are shown in Figure 4.30. Here it is seen that the measurements fluctuate much more than in the wind tunnel experiments and that the tendency line plotted from the points does not have a horizontal slope. The situation is therefore not completely steady.

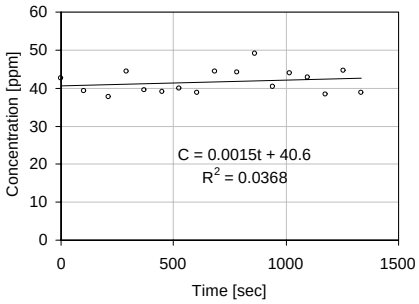

Figure 4.30. *Example of the concentration measured during experiments with the constant injection method in case 70.*

EVALUATION OF MIXING DURING THE ANALYSES

The concentration plots in Figure 4.29 and Figure 4.30 indicate that the mixing between tracer gas and room air is best in the wind tunnel experiments. Further studies of this will be made during the analyses in chapter 5, where the level of mixing in the experiments will be evaluated from temperature gradients measured in the rooms.

4.3.2 VELOCITY MEASUREMENTS FOR CALCULATION OF AIR-CHANGE RATES

In the analysis of the experiments in the wind tunnel, the air-change rates are calculated from measurements with tracer gas methods and from measurements of velocities across the opening.

The velocities are measured at 5 points across the opening in the cross-ventilation experiments and at 24 points across the opening in the single-sided ventilation experiments. A detailed description of the positions is shown in Figure 4.11.

To calculate the air-flow rate from the measured velocities, the velocity needs to be multiplied by a corresponding area, but before this area can be defined a discussion of the shape of the velocity profiles needs to be taken. In laminar flow the velocity profile is pointed compared to the flat velocity profiles obtained in turbulent flows. The different shapes are illustrated in Figure 4.31.

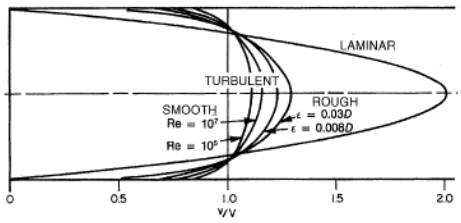

Figure 4.31. *The shape of turbulent and laminar velocity profiles in a pipe flow. /ASHRAE01/*

In the wind tunnel experiments with cross-ventilation the flow is turbulent which also reflects in the shape of the horizontal velocity profiles recorded during the measurements. An example from set-up A with an incidence angle of 0° is shown in Figure 4.32. Here the very flat turbulent profile is recorded. The outer points in the profile are 9 cm away from the edge of the opening, where the velocity is equal to 0 m/s. The velocity distributions on the last 9 cm to the vertical edge and also above and below these measurements are unknown, but to calculate the air-flow rate it is necessary to decide a velocity distribution in this area. Three suggestions for the flow in the horizontal direction are made in Figure 4.33.

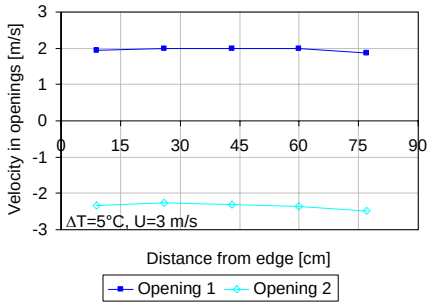

Figure 4.32. *Horizontal velocity profiles from cross set-up A at 0° with a temperature difference of 5°C and a velocity of 3 m/s.*

In the suggested velocity profiles near the edge profile A uses the velocity measured at point 1 (9 cm away from the edge) all the way to the edge even though the velocity is always 0 m/s at the edge. This profile will result in an overestimate of the air-change rate. Profile B uses a linear profile from the value at point 1 and down to 0 m/s at the edge. This profile will probably result in an underestimate of the air-change rate because the profiles will be flatter than this (see Figure 4.31). Profile C suggests that the velocity at a distance of 2 cm all around the edge is equal to 0 m/s. In the vertical direction in the opening this corresponds to 25% of the height and in the horizontal direction it corresponds to 5%. This profile is physically incorrect, but for the calculations it can be used as an estimate. As an illustration of the idea in profile C, the "0 m/s edge" is added to the flat velocity profile from Figure 4.31. Then the approximate error of this assumption is shown. This is done in Figure 4.34 where it is seen that the approximation seems reasonable.

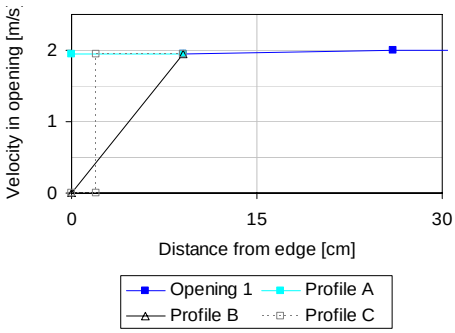

Figure 4.33. *Three suggestions for velocity profiles in the area between the vertical edge and the measurement 9 cm away.*

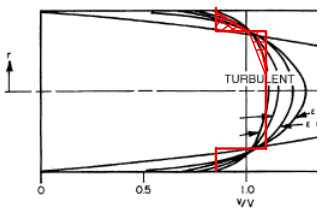

Figure 4.34. *Illustration of the assumption made in cross-ventilation with profile C in the vertical direction in the opening.*

In the calculations used for comparison of air-change rates measured with tracer gas and velocity measurement in the opening, profile C will be used.

For the calculations of air-change rates in the openings in single-sided ventilation the entire area is used. In these cases the flow is bidirectional and the shape of the profiles is more unclear.

CHAPTER 5

Results and Analysis of Experiments

In this chapter the results from wind tunnel experiments and outdoor experiments will be described. The wind tunnel experiments are both made with cross-ventilation and single-sided ventilation. The outdoor experiments are made with single-sided ventilation only. The chapter will go through all the results, but since the main aim in this work is to find a new design expression for single-sided ventilation the emphasis will be on this work.

5. RESULTS AND ANALYSIS OF EXPERIMENTS

To find the different characteristics in cross-ventilation and single-sided ventilation, all the results from the experiments will be described in this chapter. During this, the results will be compared with earlier work made in this field and finally, a new design expression for single-sided ventilation will be set up.

In section 5.1 the results of cross-ventilation made in the BRI wind tunnel will be described and compared to already known expressions for calculating airflows through the openings. In section 5.2 the experiments with single-sided ventilation in the wind tunnel are described and analysed with the aim of finding a new design expression for single-sided natural ventilation depending on wind velocity, temperature differences and the incidence angle of the wind. In section 5.3 analyses are made for the outdoor experiments with the purpose of comparing the results with the wind tunnel experiments. The comparison is made in section 5.4 where the results from the spectral analysis and lagged scatterplots made in chapter 3 are also discussed in order to find the differences between the mechanical wind in the wind tunnel and the natural wind in the outdoor experiments. As a conclusion of this comparison, a new design expression for single-sided natural ventilation is set up.

5.1 CROSS-VENTILATION IN WIND TUNNEL

During the experiments with cross-ventilation two different setups were used. These are shown in Figure 5.1. The idea of the two set-ups is to see how the position of the openings influences the air-change rate.

Measurements were made at angles between 270° and 75° since further angles were not necessary because of symmetry. In the experiments with setup B all measurements were made with 30° intervals contrary to setup A where some cases were made with 15° intervals. To ease the reading it is recommended to have the small model from appendix 2 nearby.

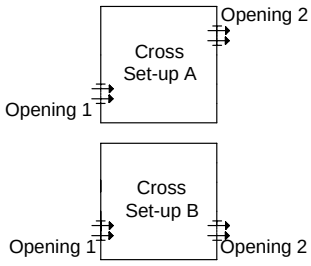

Figure 5.1. *The two set-ups used in experiments with cross-ventilation.*

5.1.1 AIR-CHANGE RATES

In the experiments with cross-ventilation the air-change rate was measured both by the tracer gas decay method and by multiplying the measured velocities in the openings with the corresponding areas.

To use tracer gas for measurements of air-change rates it is assumed that complete mixing between tracer gas and room air is obtained (see discussion in chapter 4). To check the mixing during the cross-ventilation experiments, the temperature gradients in the room are plotted in the experiments with 10°C temperature difference and wind velocity of 1m/s and 5 m/s. The temperature profiles are shown in Figure 5.2 and Figure 5.3 together with the calculated temperature gradients. The positions of the measurement in the room are seen in Figure 4.14.

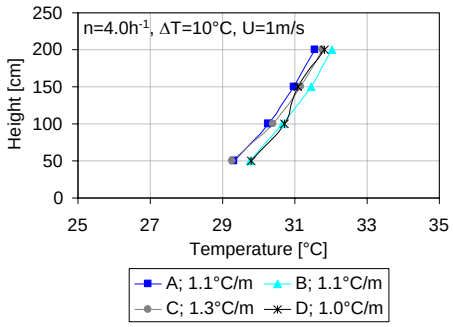

Figure 5.2. *Temperature gradients measured in cross-ventilation with U=1m/s. Incidence angle = 0°.*

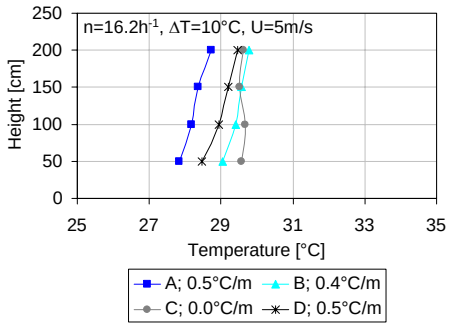

Figure 5.3. *Temperature gradients measured in cross-ventilation with U=5m/s. Incidence angle = 0°.*

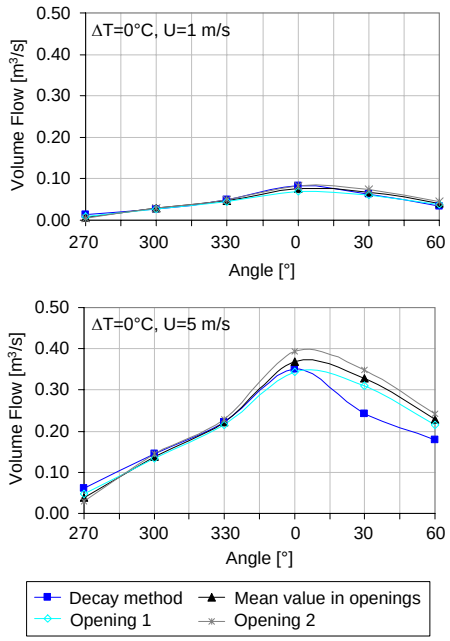

Figure 5.4. *Deviations between the decay method and calculation of flow rate from velocity measurements. Set-up A.*

It is seen from the temperature profiles that the lowest temperature gradients are obtained in the case with high wind velocity. Here the gradients are between 0 and 0.5°C/m. In the case with U=1m/s the gradients are between 1.0 and 1.3°C/m. Therefore, it is assumed that the best mixing is obtained in the cases with high velocities. This is also one of the conclusions in /Sandberg et al. 85/ where measurements with the decay method have been described.

Furthermore, it is assumed that cases with lower temperature gradients will have a better mixing in the room. From the level of the temperature gradients during the experiments with cross-ventilation the mixing in the room is estimated to be quite good.

DETERMINATION OF AIR-CHANGE RATES

In the comparison between air-change rates measured by tracer gas and by velocities in the opening it is seen in Figure 5.4 that the main part of the incidence angles results in nearly the same air-change rates. A deviation is seen with U= 5 m/s at the angles between 0° and 60° (opening nearest the wind direction) where the decay method gives lower air-change rates than that found by use of the velocity measurements. The explanation of the deviations must be the difficulties in deciding the right velocity profile near the edges of the opening. Here it is assumed that the velocity is zero at a distance of 2 cm away from the edge even though this is a very rough estimate which in this case seems to be incorrect. This problem is also discussed in chapter 4.

The examples of deviations for set-up A in Figure 5.4 are very similar to the tendency found for set-up B.

Since the correct volume flow is unknown, it is hard to pick one method from the other. Since the evaluation of the mixing in the room showed good results and there are some uncertainties regarding the velocity near the edges, the decay method will be used as the correct value.

AIR-CHANGE RATE AS A FUNCTION OF TEMPERATURE DIFFERENCE

The air-change rates at different incidence angles of the wind are compared at different temperature differences and fixed wind velocities. Only the results from set-up A are shown in Figure 5.5, but the same results are found in set-up B (see section 5.1.3).

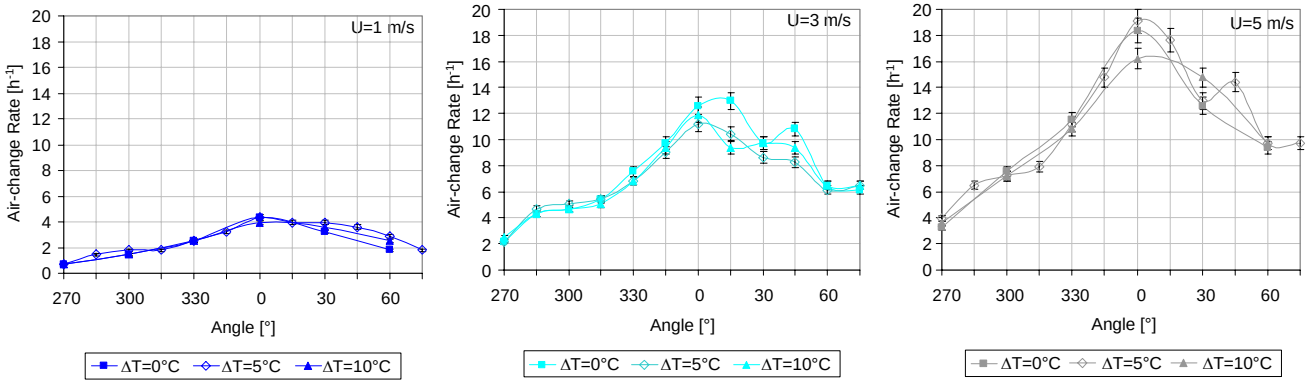

Figure 5.5. *Effect on the air-change rate from changing the temperature difference at different incidence angles and wind velocities.*

As a result of the comparison in Figure 5.5 it is seen that a change in the temperature difference does not seem to increase the air-change rate, since all the curves are nearly similar at the same velocity level. Even at 1 m/s, which must be seen as a low velocity, any major effect of the temperature difference cannot be found. The reason for this is the position of the openings, which are placed at the same height.

In all the cases except one the highest air-change rates are found with an incidence angle of 0°.

In Figure 5.6 all the measured air-change rates are plotted as a function of the temperature and also here it can be found, that an increase in temperature difference does not have any effect on the air-change rate.

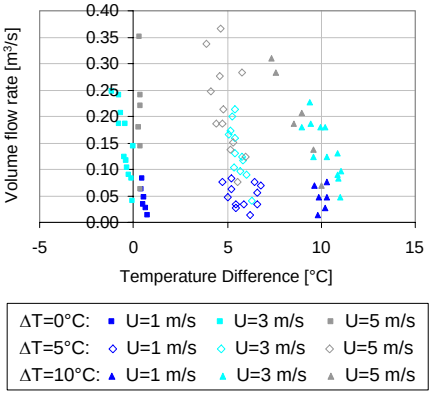

Figure 5.6. *Volume flow rate as a function of the temperature difference (inside-outside).*

AIR-CHANGE RATE AS A FUNCTION OF WIND VELOCITY

In the same manner as in the previous section, a change in the velocity is compared at different temperature differences. The results are shown in Figure 5.7.

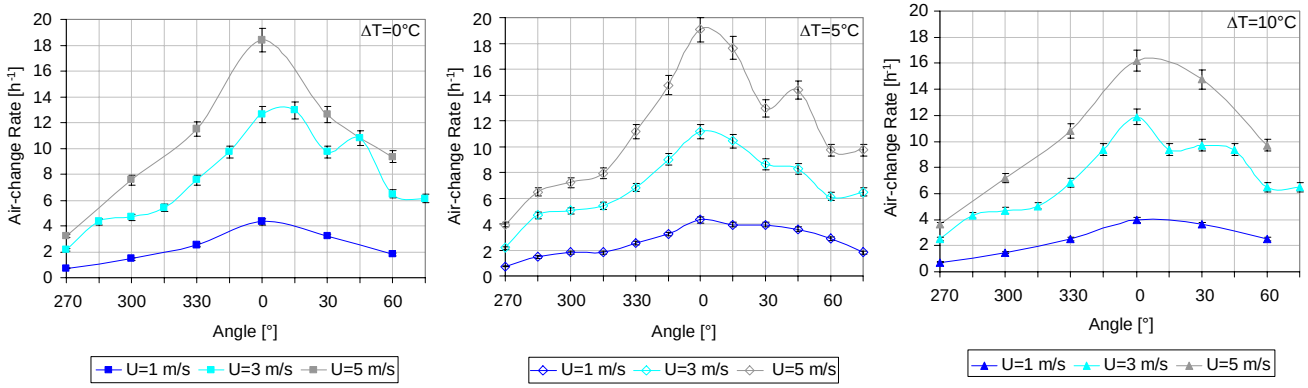

Figure 5.7. *Effect on the air-change rate from changing the wind velocity at different incidence angles and temperature differences.*

Figure 5.7 also shows that the temperature difference does not have any influence on the air-change rate when using cross-ventilation and

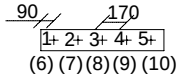

Figure 5.8. *Position of velocity measurements in the opening. Points 1 to 5 are positioned at opening 1 (front wall when β=0°). Dimensions in mm.*

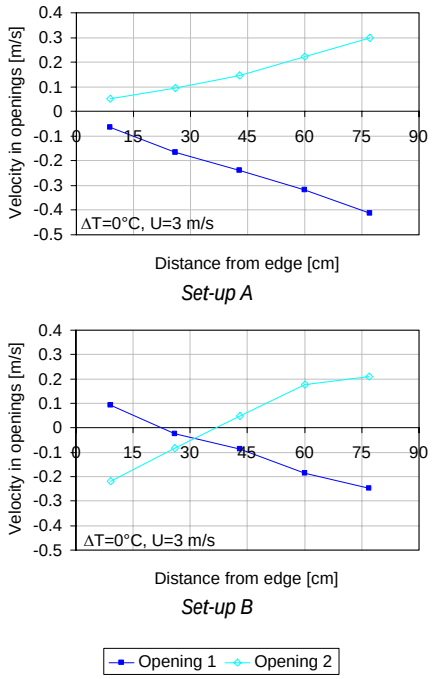

Figure 5.9. *Velocity profiles from cross set-ups A and B at β=270° with a temperature difference of 0°C and a velocity of 3 m/s.*

apparently it looks so if the only way to increase the volume flow is by increasing the wind velocity or changing the angle as long as the openings are at the same height.

5.1.2 VELOCITY PROFILES

The velocity was measured at five points across each of the two openings. The positions are shown in Figure 5.8.

At all angles from 285° to 75° the air enters through opening 1 and leaves through opening 2. At 270°, where the wind is parallel to the openings, this is not the case. At set-up A the air enters through opening 2 for all except one case, and with set-up B each opening is used as both inlet and outlet with air coming in through the openings at the end closest to the origin of the wind since the highest pressure is here.

The reason for this difference in the velocity profiles at β=270° between setup A and B is the different pressure distributions that occur in these cases. With set-up A the highest pressure is at opening 2, but in set-up B the pressure difference between the openings is close to zero which is the reason for the different flows in the openings. Examples of velocity profiles in the two cases are shown in Figure 5.9.

At the angles from 285° to 315° and 30° and 45° the tendency is that most of the air enters at the right side of the opening, where the highest pressure around the opening occurs. An example of these types of velocity profiles is shown in Figure 5.10.

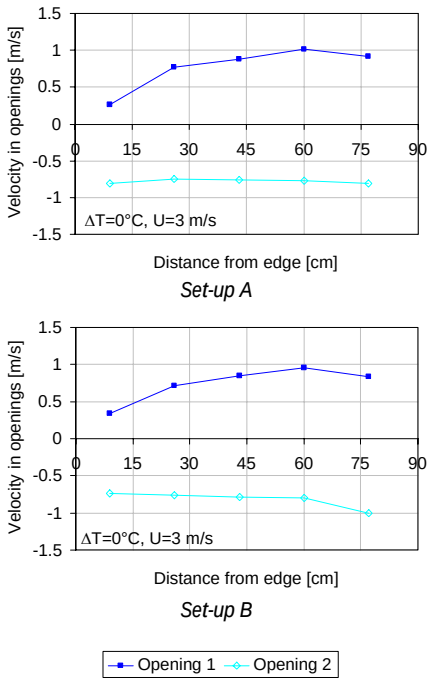

Figure 5.10. *Velocity profiles from cross set-ups A and B at β=300° with a temperature difference of 0℃ and a velocity of 3 m/s.*

At 330° to 15° the air enters equally distributed across the opening as shown in Figure 5.11.

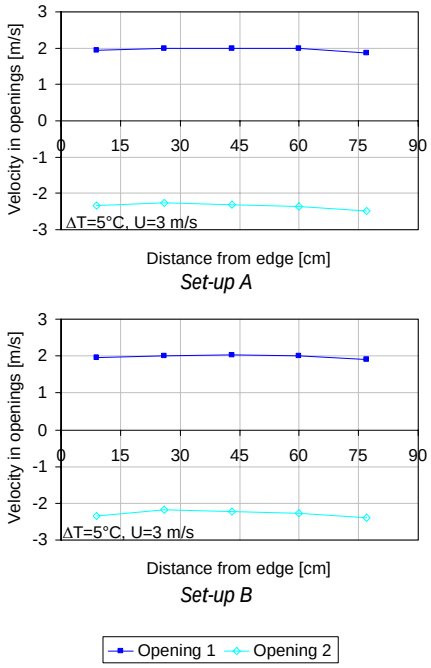

Figure 5.11. *Velocity profiles from cross set-ups A and B at β=0° with a temperature difference of 5℃ and a velocity of 3 m/s.*

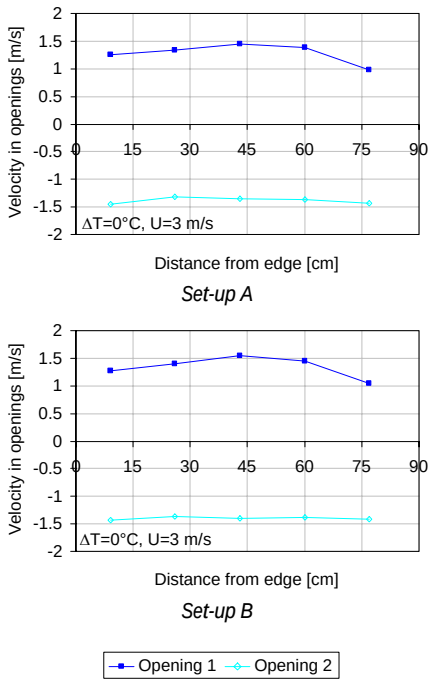

Figure 5.12. *Velocity profiles from cross set-ups A and B at β=60° with a temperature difference of 0°C and a velocity of 3 m/s.*

At 60° most air enters in the middle of the opening and at 75° most air enters in the left side of the opening. An example of a 60° case is shown in Figure 5.12.

In all cases except for 270° the velocity profiles in set-ups A and B are nearly identical for the incoming air, but the profiles of the outgoing air differ in some cases in a way indicating, that the pressure distribution from left to right at the opening varies more in set-up B since these profiles in some cases show different airflows from one side to the other, unlike set-up A.

5.1.3 INFLUENCE FROM THE POSITION OF THE OUTLET OPENING

As discussed in sections 5.1.1 and 5.1.2, the air change rates are very similar in set-up A and set-up B. A comparison of the air change rates obtained in the two set-ups is made in Figure 5.13 and Figure 5.14.

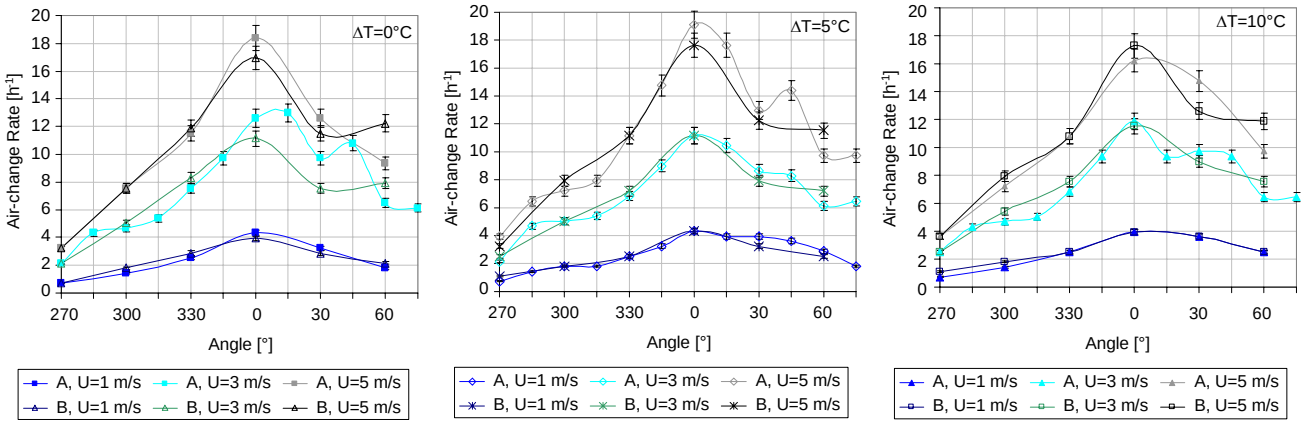

Figure 5.13. *Differences in air-change rates between set-up A and set-up B as a function of different velocities at fixed temperature differences.*

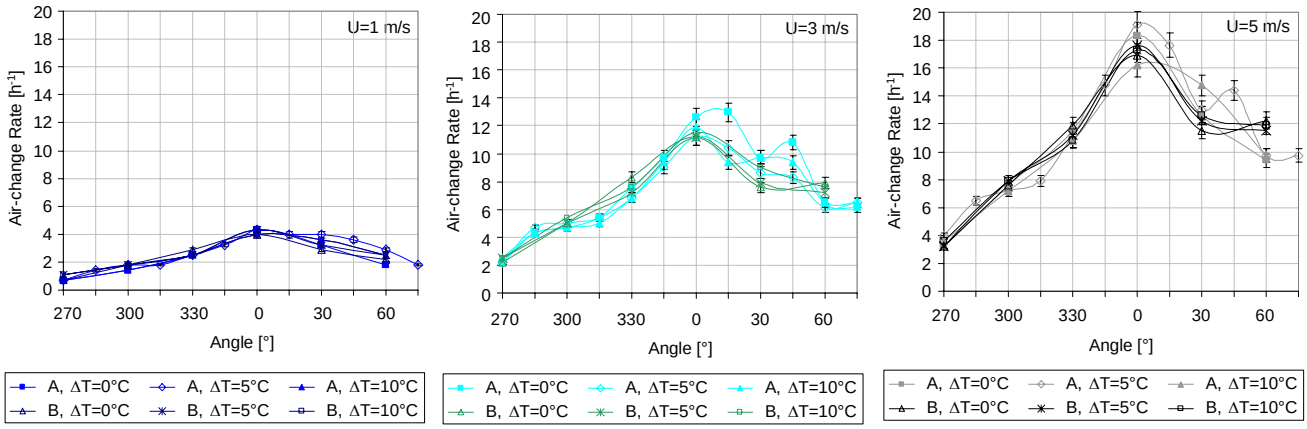

Figure 5.14. *Differences in air-change rates between set-up A and set-up B, here as a function of different temperature differences at fixed velocities.*

From Figure 5.13 and Figure 5.14 it is seen that moving opening 2 from a position where the air is crossing the room (set-up A) to a position where the air goes the direct way through the room (set-up B) does not have any effect on the air-change rate. The graphs show that especially at low wind velocities the air-flow is nearly the same. The larger deviation at higher wind velocities can be caused by poor mixing in set-up B since the way of the air through the room, as mentioned before, is much more direct.

As a result of these measurements one position of the opening cannot be preferred from the other, if the air-change rate is the deciding factor.

5.1.4 PRESSURE DISTRIBUTION ON THE BUILDING

Earlier pressure measurements for the sealed building have been made at BRI (see Figure 4.9). These measurements are compared to the measurements made for the building design used in the experiments with cross-ventilation. In both types of experiments the reference pressure is measured in the free wind at a distance of 0.5 m away from the inlet of the wind tunnel. In all cases the temperature difference is 0°C.

At first the pressures measured in the BRI-experiments at the sealed building were calculated for points corresponding to the points measured in the current experiments. This was done by interpolation between the BRI results. The positions of the points at the open building are shown in Figure 5.15. The exact positions of the pressure points close to the opening can be found in the description of the experiments in table 4.1.

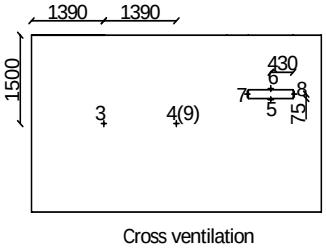

Figure 5.15. *Positions of pressure measurement at the front wall (wall facing the wind when β=0°). Number (9) shows the point at the opposite side. Points around the openings are app. 50 mm away from the edge of the opening. Dimensions in mm.*

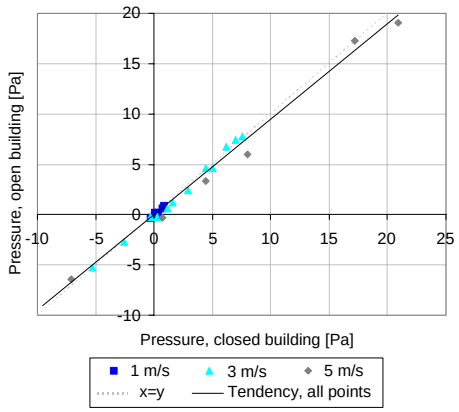

Figure 5.16. *Pressures measured around the opening at the open building compared to those measured on the closed building.*

Point 3	Expression	R^2
No zero point	$P_{open}=0.973 \cdot P_{closed}$	0.9942
Fixed zero point	$P_{open}=0.973 \cdot P_{closed}$	0.9942
Point 4		
No zero point	$P_{open}=0.946 \cdot P_{closed}+0.044$	0.9890
Fixed zero point	$P_{open}=0.949 \cdot P_{closed}$	0.9890
Point 9		
No zero point	$P_{open}=0.897 \cdot P_{closed}-0.181$	0.9774
Fixed zero point	$P_{open}=0.948 \cdot P_{closed}$	0.9710
Opening		
No zero point	$P_{open}=0.956 \cdot P_{closed}-0.121$	0.9897
Fixed zero point	$P_{open}=0.948 \cdot P_{closed}$	0.9893

Table 5.1. *Expressions of tendency lines for pressure calculations at points 3 and 4 (front wall), in point 9 (back wall) and in the opening (front wall) at the open and closed building.*

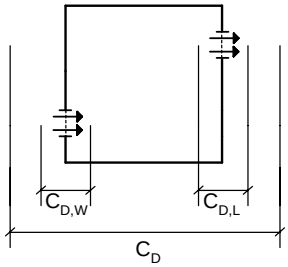

Figure 5.17. *Discharge coefficient for the windward opening ($C_{D,W}$), the leeward opening ($C_{D,L}$) and both openings (C_D).*

The mean value of the four pressure points around the opening are used and compared to a point on the closed building positioned in the middle of the opening (at the open building). The comparison of the pressures is shown in Figure 5.16.

The expressions of the tendency lines for points 3, 4, 9 and opening are calculated in two ways – both with and without a fixed zero point. The fixed zero point is chosen for physical reasons. The expressions are written in Table 5.1.

From the expressions calculated from the measurements it is found, that the pressure differences between the reference point and the points on the walls are reduced by about 5%-10% when measured on the open building compared to the closed building.

5.1.5 CALCULATION OF DISCHARGE COEFFICIENTS (C_D)

The discharge coefficient (C_D) for the openings can be calculated from expression (5.1): /Etheridge et al. 96/

$$Q_V = \pm C_D \cdot A \cdot \sqrt{\frac{2 \cdot |\Delta P|}{\rho}} \tag{5.1}$$

The coefficient will be calculated for the leeward ($C_{D,L}$) and windward ($C_{D,W}$) openings, but also for both openings together (C_D). The three different C_D-values are illustrated in Figure 5.17.

The pressure differences used in the calculations are as follows:

$$\begin{aligned} C_{D,W}&: \quad \Delta P = P_{around\ opening,\ front\ wall} - P_{inside} \\ C_{D,L}&: \quad \Delta P = P_{inside} - P_{back\ wall} \\ C_D&: \quad \Delta P = P_{around\ opening,\ front\ wall} - P_{back\ wall} \end{aligned} \tag{5.2}$$

$P_{around\ opening,\ front\ wall}$ is calculated as an average value of points 5, 6, 7 and 8 in Figure 5.15. P_{inside} is calculated as an average of points 1 and 2. On the leeward side of the building the pressure for $P_{back\ wall}$ is only measured at a single point in the middle of the wall (point 9 on Figure 5.15), since lack of channels in the equipment made it impossible to measure around the opening in this case.

The calculated values of C_D are shown in Figure 5.18.

From the results in Figure 5.18 it can be seen that the C_D coefficients are not constant, but change slightly with the incidence angle of the wind. Since the C_D-value normally is considered as a constant value for a specific opening, another parameter in expression (5.1) is the cause of this variation.

One of the reasons for the variation can be that one of the main assumptions in expression (5.1) is not fulfilled. In the expression which was originally developed for an airflow through a sharp-edged orifice in a tube, it is assumed that constant pressure and velocity distributions in the opening are present. This is not the case during these experiments which can be seen in the velocity profiles shown e.g. in Figure 5.10 where the velocity distribution in the openings changes. Therefore, you get different opening characteristics at different angles. The largest variations are seen in $C_{D,L}$.

Between $C_{D,W}$ and $C_{D,L}$ a difference in levels is observed that also shows that the pressure drop across the openings is neither similar nor constant. The lowest values of $C_{D,W}$ are found between 0° and 60°. This corresponds to having the largest pressure difference between the front opening and inside when the corner of the building with the window is towards the wind direction.

When the discharge coefficient is calculated across both openings (C_D) it is less sensitive to the different incidence angles and, therefore, the variation in these values becomes smaller, see Figure 5.18.

The problem with variation in C_D-values is discussed further in the next section where it will be compared to earlier work.

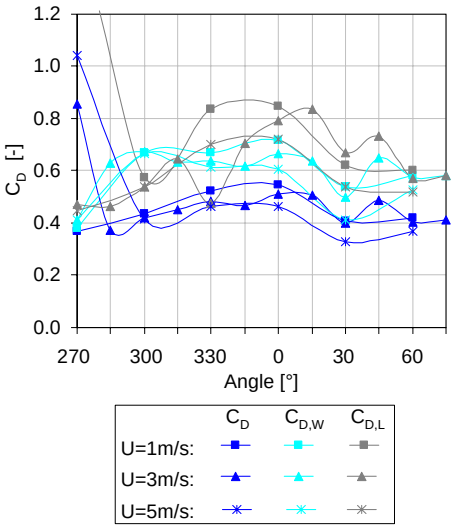

Figure 5.18. *Calculated C_D values. All cases are with 0°C temperature difference.*

5.1.6 COMPARISON WITH EARLIER WORK

In the work with cross-ventilation the calculation expressions are well defined and it might seem easy to predict the airflow in this type of natural ventilation.

In chapter 2 some of the assumptions for expression (5.1) (the orifice equation) were discussed in connection with determination of the C_D-coefficient. Here it was mentioned that constant pressure and velocity across the opening are assumed, but from the calculation of C_D-values in this work it is shown that this assumption is apparently not obtained. The C_D-values calculated in the previous section fluctuate at different angles.

The most obvious reason for these non-constant C_D-values is that the pressure and velocity distributions in the opening are not constant and also that the kinetic energy in the flow affects the velocity in the opening. In the work by Jensen True the porosity of the building is seen as a parameter for indication of the obtained flow pattern in the building. In his work 1% porosity is mentioned as the limit between purely pressure driven flow and flow affected by the kinetic energy in the wind, /True03/ and /Heiselberg et al. 05/. In the present thesis the porosity was calculated to 0.95% with a room height of 2.4 m. This is very close to the limit mentioned in /True03/ and therefore there is reason to believe that the airflow in this work is influenced by the kinetic energy in the flow.

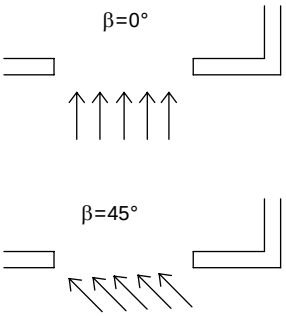

Figure 5.19. *An example of different flow directions through the opening.*

Another reason for the different C_D-values might lie within the shape of the opening. In these experiments the depth of the opening is 10 cm. With this depth the opening might act like a small tube. This way of thinking is illustrated in Figure 5.19. With a deep opening the opening characteristics change with the incidence angle. This means that the C_D-value should actually also change, but normally this is considered a constant, which in this case may be wrong.

5.1.7 CONCLUSION

A general conclusion of the measurements with cross-ventilation is that the temperature difference in this type of ventilation does not influence the air-change rate which apparently is only affected by the angle and velocity of the wind. The reason for this is found in the theory of thermal buoyancy where a difference in height between the openings is necessary to have an airflow driven by temperature difference. Other shaped and larger openings might give other results to this conclusion, since a difference in height in the opening could also increase the airflow caused by thermal buoyancy.

During the work with cross-ventilation it was also investigated how the air change rate depends on the position of the openings. Two sets of opening positions with air either crossing the room or going straight through the room were tested. In this case the results showed that the air change rate is independent of the position, but the result will always depend on the shape of the building through the C_P-values.

To analyse the effect of adding openings to the building, earlier measurements of the pressure distribution on the sealed building were compared to the measurements made on the building with openings. Here it was shown that the openings only have a small effect on the pressure distribution which was 5-10% less than on the sealed building.

Finally the C_D-values were calculated from pressure differences measured during the experiments with different incidence angles. From this it was seen that the assumptions made in connection to the use of the orifice equation concerning constant pressure and velocity distribution across the opening was not obtained in this work since the C_D-values were varying at different incidence angles. Another idea for this variance in C_D-value was also discussed, but not further developed. It was suggested that the C_D-value in deep openings depends on the angle since different incidence angles of the wind will change the characteristics of the opening in this case.

5.2 SINGLE-SIDED VENTILATION IN WIND TUNNEL

The following section describes the results from the experiments with single-sided ventilation made at the BRI wind tunnel. Before the experiments it was already known that the airflow through an opening will be influenced by wind velocity and temperature difference between the inside and the outside of the building. Another factor that may affect the air change is the incidence angle of the wind, which will also be analysed here by rotating the building during the experiments.

In the experiments three different set-ups were used, see Figure 5.20, where the main parts of the experiments were made with set-up A. Set-ups B and C were used for analysing the importance of the room volume. Further details about the set-ups are described in the chapter 4.

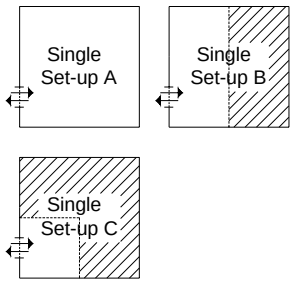

Figure 5.20. *The three different set-ups used for changing the room volume.*

5.2.1 AIR-CHANGE RATES

To find the effect from different wind velocity, temperature difference and incidence angle, the air change rates were measured during all the experiments.

METHOD FOR DETERMINATION OF AIR-CHANGE RATES

As for cross-ventilation, the air change rates were measured by two different methods. The first method was the tracer gas decay method, where an assumption of full mixing in the room was made. This method was compared to calculation of the air change rate from velocity measurements in the opening multiplied by the corresponding area. In single-sided ventilation the entire area is included in these calculations, see discussion of this in chapter 4.

To evaluate the obtained degree of mixing between tracer gas and room air during the experiments, the temperature gradients in the room are controlled in the cases with 10°C temperature difference and wind velocities of 1m/s and 5 m/s. The temperature profiles are shown in Figure 5.21 and Figure 5.22 together with the calculated temperature gradients.

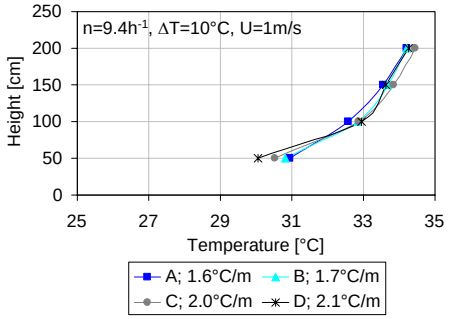

Figure 5.21. *Temperature gradients measured in single-sided ventilation with U=1m/s. Incidence angle = 0°.*

As with cross-ventilation it is seen that the lowest temperature gradients are obtained in the case with high wind velocity. Here the gradients are between 0.9 and 1.5°C/m. In the case with U=1m/s the gradients are between 1.6 and 2.1°C/m. Therefore, the best mixing is obtained in the cases with high velocities. The general level of the temperature gradients is a little higher in the cases with single-sided ventilation compared to cross-ventilation. This shows that the risk of measuring too high air-change rates is higher in these cases, but still the mixing is estimated to be quite good.

In this case the decay method is considered to be more accurate than the velocity measurements. The reason for this assumption is the fluctuations in the opening which are very large especially in single-sided ventilation. This can result in flows that do not affect the air-change rate, but just leave the room again as “clean” air. The mean velocity will be affected by the many fluctuations contrary to the decay method.

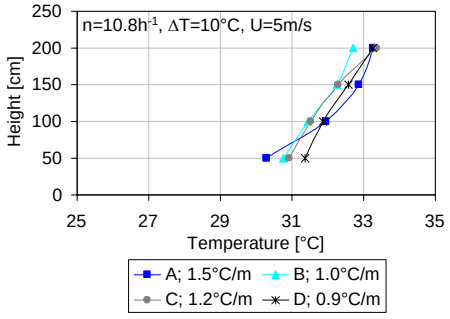

Figure 5.22. *Temperature gradients measured in single-sided ventilation with U=5m/s. Incidence angle = 0°.*

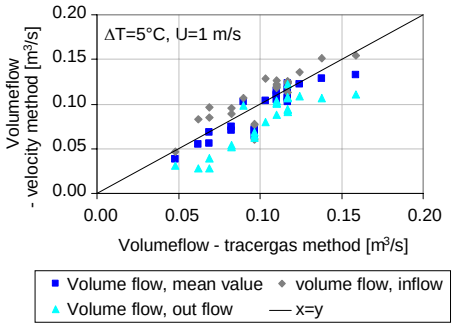

Figure 5.23. *Coherence between volume flows found from the decay method and from calculations of measured velocities in the opening.*

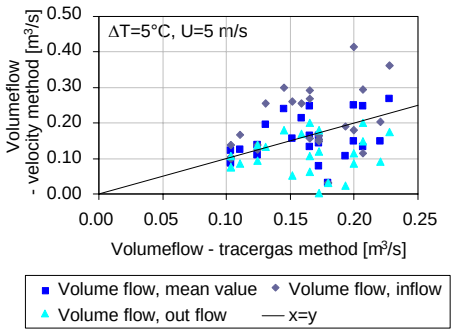

Figure 5.24. *Coherence between volume flows found from the decay method and from calculations of measured velocities in the opening.*

The calculated values of the mean flow, the incoming flow and the outgoing flow are compared with the values found from the decay method. An example of this is shown in Figure 5.23 and Figure 5.24 with a temperature difference of 5°C and a wind velocity of 1 m/s and 5 m/s.

If the two plots in Figure 5.23 and Figure 5.24 are compared it is seen that the method of calculation by velocities is closest to the values found by the decay method, when the wind velocity is low and the mean values of the calculated volume flow are used. In the cases with high wind speeds the dispersion between the points are greater and in this case it is hard to find a pattern although the volume flow found from the incoming air still gives the highest values. The same tendency is found for both 0°C and 10°C temperature difference. A reason for the large deviation from the decay method in the cases with high velocities can be that the velocity profiles in the opening are much more fluctuating in these cases than in the cases with low velocities. Larger fluctuations in the opening will affect the velocity profile, but as mentioned before not necessarily the air-change rate. Another reason can be the overestimate coming from the calculation with velocities where the same velocity is assumed across the entire area near the edges.

From this investigation again it is concluded that the decay method gives the most accurate prediction, and further use of the air-change rates will be from predictions with the decay method.

AIR-CHANGE RATE AS A FUNCTION OF TEMPERATURE DIFFERENCE

To investigate how the temperature difference between the inside and the outside of the building affects the air-change rate at different incidence angles of the wind, the results are compared in the cases with different temperature differences and fixed wind velocity. The results are shown in Figure 5.25.

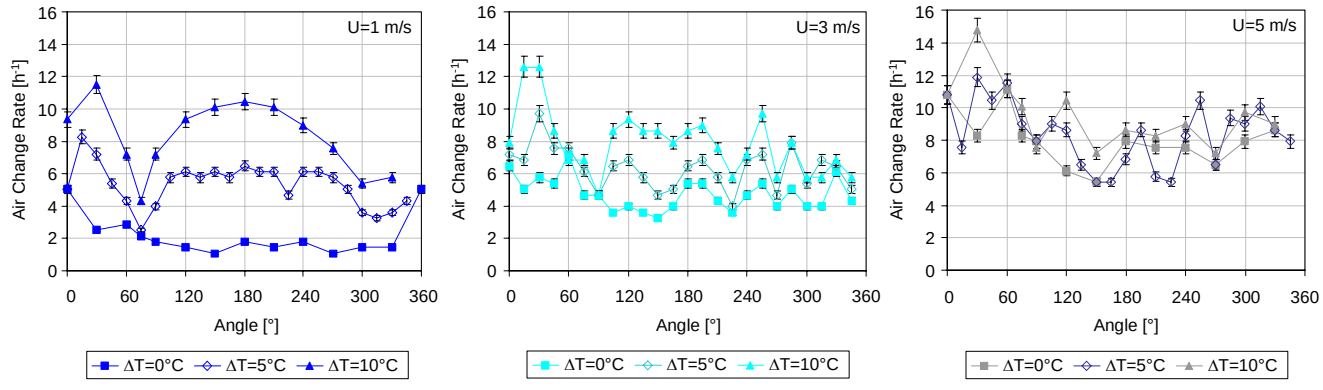

Figure 5.25. *Effect on the air-change rate from changing the temperature difference at different incidence angles and wind velocities.*

From Figure 5.25 it is seen, that changing the temperature difference will have the largest effect at low wind velocities. Especially in the cases where the wind flows parallel or nearly parallel to the opening or the opening is at the leeward side (90° to 270°) the effect of the temperature

difference is large. This indicates that the airflow through the opening in these cases is mainly driven by the temperature difference. As the velocity is increased the curves of the air-change rate are approaching each other, which shows that the effect of the temperature difference is minimized. At a velocity of 3 m/s the effect of the temperature difference is largest at the angles between 105° and 210° and has almost disappeared at angles from 210° to 360°. When the velocity is increased to 5 m/s the effect of the temperature difference becomes hard to see and is close to non-existing. All measurements show that incidence angles between 0° and 60° (wind directly towards the opening) results in a slightly higher air-change than the rest of the measured positions.

The decrease in influence from the temperature difference as the wind velocity rises can also be seen if the air-change rate is plotted only as a function of the temperature. This is done in Figure 5.26. Here the experiments with high velocities (grey points) are all close to the same mean value of the flow rate independently of the temperature difference. In contrast the experiments with low velocities (blue and turquoise points) are lying on a sloped line where the slope depends on the temperature difference.

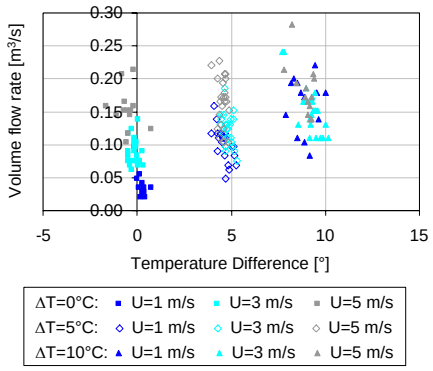

Figure 5.26. *Volume flow rate as a function of the temperature difference (inside-outside).*

AIR-CHANGE RATE AS A FUNCTION OF WIND VELOCITY

In the same manner as in the previous section, a change in the velocity is compared at different temperature differences. The results are shown in Figure 5.27.

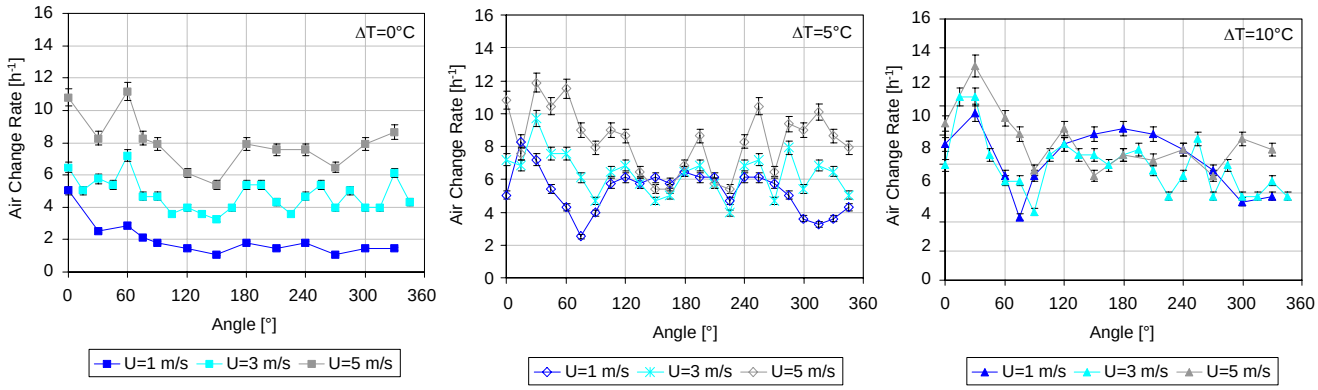

Figure 5.27. *Effect on the air-change rate from changing the wind velocity at different incidence angles and temperature differences.*

In the situation where there is no temperature difference the effect of increasing wind velocity is obvious – higher wind velocity results in higher air-change rates and the curves are close to parallel in this case. When the increase in wind velocity is combined with a temperature difference, the effect fades, especially at angles where the wind does not have any direct influence. In the cases where the temperature difference is 5°C these angles span from 135° to 270°, but when the temperature difference is increased to 10°C the spectre of angles with small or no

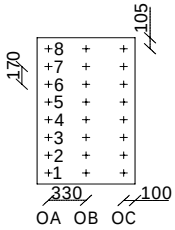

Figure 5.28. *Position of the velocity measurements in opening seen from outside the building. Dimensions in mm.*

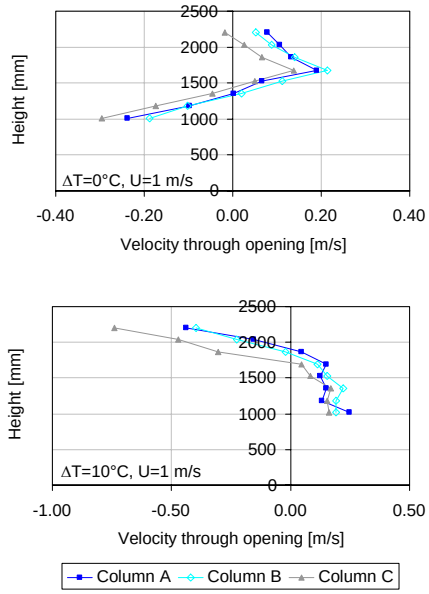

Figure 5.30. *Change in velocity profiles with increase in temperature. Angle = 0 °. Positive values indicate an ingoing flow.*

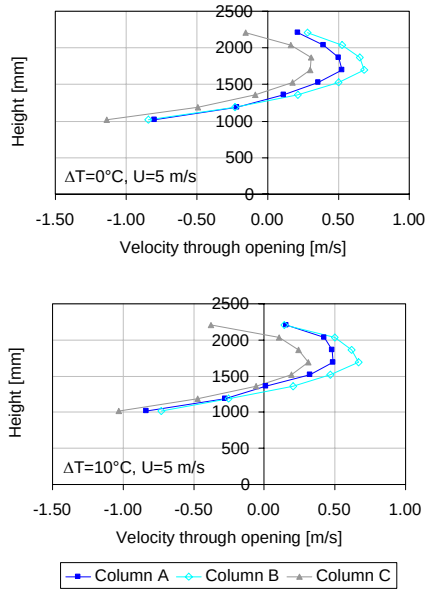

Figure 5.29. *Change in velocity profiles with increase in temperature. β = 0 °. Positive values indicate an ingoing flow.*

influence from increased wind velocity is from 90° to 270°, which indicates a stronger influence from thermal forces.

5.2.2 VELOCITY PROFILES

Another way to look at the connection between temperature difference and wind velocity is to observe the measured velocity profiles. The different shapes of the profiles are discussed in chapter 2 in connection with the work by De Gids & Phaff, who have also worked with single-sided ventilation, /De Gids et al. 82/.

The velocity profiles were measured at three different positions all with eight vertical points. The positions of the measurements are shown in Figure 5.28.

An example of velocity profiles in four different set-ups is shown in Figure 5.30 and Figure 5.29. The two upper graphs show the profiles for 1 m/s. Here it can be seen how the profiles are changing from being influenced mainly by the wind at a 0°C temperature difference to more temperature dominated profiles at a 10°C temperature difference. The same picture cannot be found in the profiles for 5 m/s where both of the profiles are dominated by the strong wind which greatly reduces the effect of the temperature difference.

The velocity profiles for an angle of 270° are plotted in Figure 5.31 and Figure 5.32 to se how a flow parallel to the opening influences the velocity distribution in the opening. In this comparison it is seen, that wind parallel to the opening gives a much more fluctuating picture. Especially at 1 m/s where the difference between 0°C and 10°C becomes very clear. This indicates a very strong temperature driven airflow in this case. When the velocity is increased to 5 m/s it is seen, that the temperature still influences the flow contrary to the situation where the flow is perpendicular to the opening.

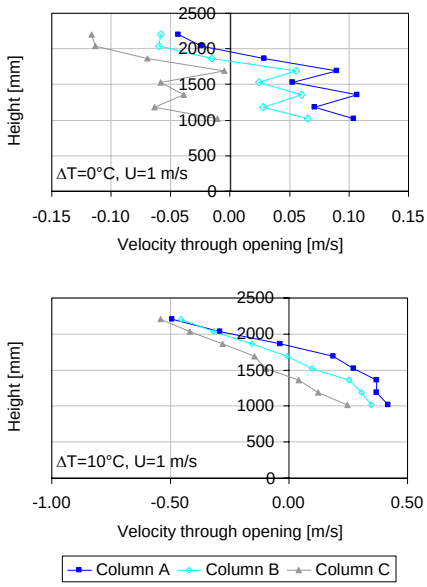

Figure 5.31. *Change in velocity profiles with increase in temperature. β=270°. Positive values indicate an ingoing flow.*

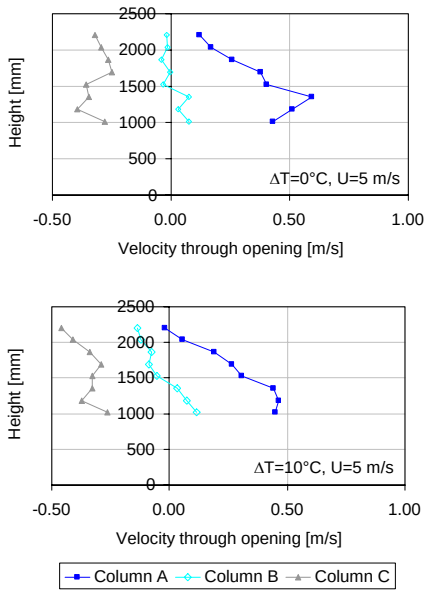

Figure 5.32. *Change in velocity profiles with increase in temperature. β = 270°. Positive values indicate an ingoing flow.*

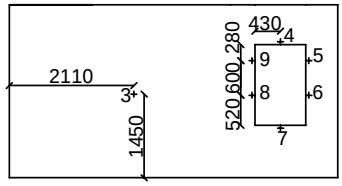

Figure 5.33. *Pressure measurement at the front wall. Points around the openings are app. 50 mm from the edge. Dim. in mm.*

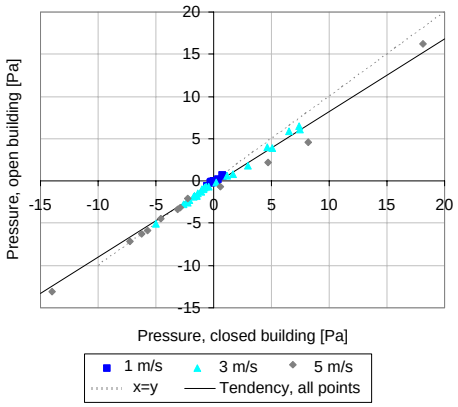

Figure 5.34. *Comparison of pressures measured at the front wall on the open and the sealed building.*

Point 3	Expression	R^2
No zero point	$P_{open}=0.959 \cdot P_{closed}+0.038$	0.9948
Fixed zero point	$P_{open}=0.959 \cdot P_{closed}$	0.9947
Opening		
No zero point	$P_{open}=0.860 \cdot P_{closed}-0.406$	0.9869
Fixed zero point	$P_{open}=0.855 \cdot P_{closed}$	0.9795

Table 5.2. *Expressions of tendency lines for pressure calculations at point 3 and in the opening (averaged) on the open and closed building.*

5.2.3 PRESSURE DISTRIBUTION ON THE BUILDING

As with cross-ventilation, the pressure measurements for the sealed building made at BRI are compared to the results found for the building with the opening used in the current experiments with single-sided ventilation. The positions of the points on the open building are shown in Figure 5.33. The exact positions of the pressure points close to the opening can be found in Table 4.1.

Also this time a mean value of the six pressure points around the opening are used and compared to a point on the closed building positioned exactly in the middle of the opening (on the open building). The comparison of the pressures is shown in Figure 5.34.

The expressions of the tendency lines are outlined in Table 5.2.

From the expressions calculated from the measurements it is found, that the pressure difference between the reference point and the point on the wall is slightly reduced and that the pressure around the opening is reduced by approximately 14% compared to the sealed building.

5.2.4 EFFECT OF CHANGING THE ROOM VOLUME

During the experiments with single sided ventilation the room volume was changed to half and a quarter of the original volume, see Figure 5.20.

The cases B and C, where the room volume is changed, are only made with a wind velocity of 3 m/s and the temperature differences 0°C and 10°C. The results are plotted in Figure 5.35.

The results from the volume changing experiments show that a change in volume does not have a great impact on the flow through the opening. Especially with a temperature difference of 0°C, it is hard to find any change. When the temperature difference is increased to 10°C a slightly smaller volume flow is observed in the experiments with small room volumes. A reason for this can be, that the difference of 10°C was hard to obtain especially in the experiments with the small rooms where a very large amount of heat was necessary to maintain this high difference. To investigate this, the actual temperature differences in the three cases are plotted in Figure 5.36.

When the temperature differences are observed it is found, that the temperature difference in Figure 5.36 and the volume flow in Figure 5.35 are following the same pattern by having high temperature differences and high volume flows in the same cases. But there are some deviations to this pattern since setup C has the highest temperature difference at 90°, but the lowest volume flow, and at 240° the volume flow in the three cases is nearly the same, but the temperature differences deviate. Because of these deviations from the suggested pattern it is hard to give any conclusion to the airflow through openings in rooms with different volume, but the same temperature difference. Apparently it seems that the temperature difference has a slightly larger influence in larger rooms, but this conclusion needs to be investigated further.

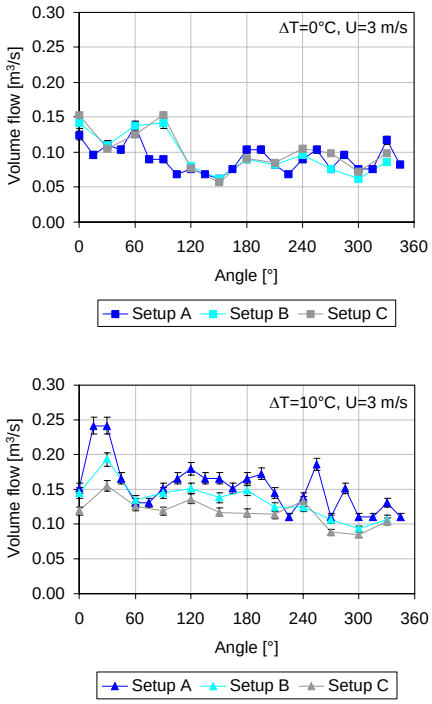

Figure 5.35. *Volume flow rate found with three different room volumes.*

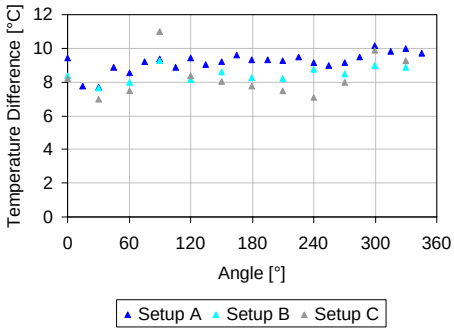

Figure 5.36. *Actual temperature difference in the cases where 10 °C was wanted.*

5.2.5 COMPARISON WITH EARLIER WORK

To see how the results from the measurements correspond to earlier work on the same subject, the results are compared to expressions found by De Gids & Phaff (1982) and Warren & Parkins (1985). The work is described in chapter 2 and, therefore, only the expressions will be shown here.

Expressions (5.3) and (5.4) are found by De Gids and Phaff /De Gids et al. 82/

$$U_m = \sqrt{(0.001 \cdot U_{10}{}^2 + 0.0035 h \Delta T + 0.01)} \qquad (5.3)$$

$$Q_v = A_{eff} \cdot U_m = ½ \cdot A \cdot U_m \qquad (5.4)$$

Warren and Parkins found expression (5.5), which contrary to De Gids and Phaff does not include effects from a temperature difference. /Warren et al. 85/

$$Q_V = 0.025 \cdot A \cdot U_{10} \tag{5.5}$$

The experimental results are compared to the work of De Gids & Phaff and Warren & Parkins in Figure 5.37, Figure 5.38 and Figure 5.39 for temperature differences of 0°C, 5°C and 10°C, respectively.

Since the incidence angle is not included in the expressions by De Gids & Phaff and Warren & Parkins, these predictions are constant and, therefore, only result in an average value of the predicted airflow.

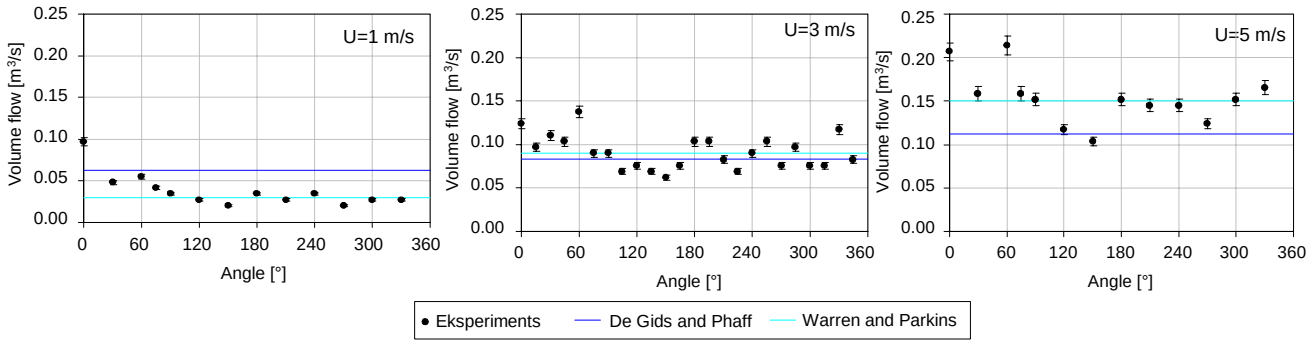

Figure 5.37. *Volume flow found by experiments and earlier expressions. Temperature difference = 0 ℃.*

In the isothermal case seen in Figure 5.37 the expression by Warren and Parkins gives reasonable results for all three velocities, whereas the De Gids and Phaff expression returns values that are too high in the case where the velocity is low and underestimates the volume flow in the case with high velocity. The reason why the calculated values from the De Gids and Phaff expression are not completely constant as expected is that a tiny temperature difference was recorded in some of the experiments.

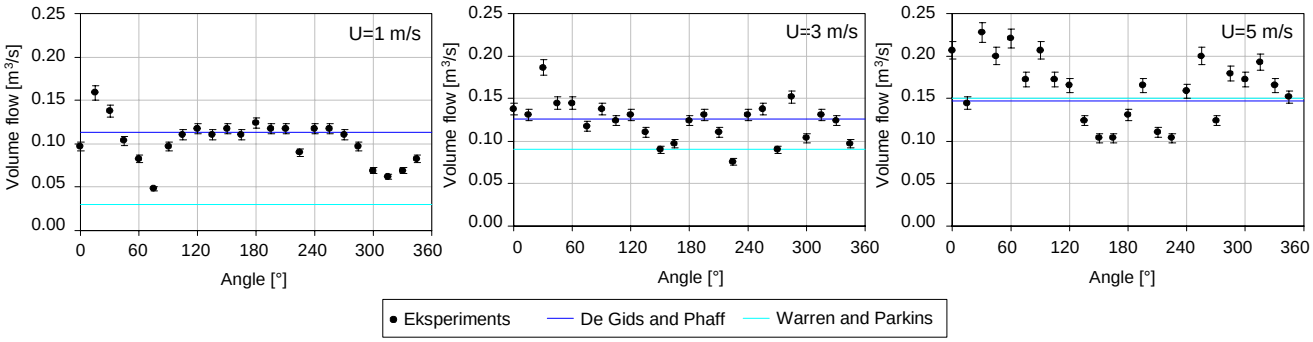

Figure 5.38. *Volume flow found by experiments and earlier expressions. Temperature difference =5 ℃.*

In Figure 5.38 where the temperature difference is 5°C the De Gids and Phaf expression corresponds fairly well to the experiments in all cases. The Warren and Parkins expression gives the best results in the cases with high velocities where the effect from the temperature difference is very low. The same pattern can be found in the cases with a 10°C temperature difference seen in Figure 5.39.

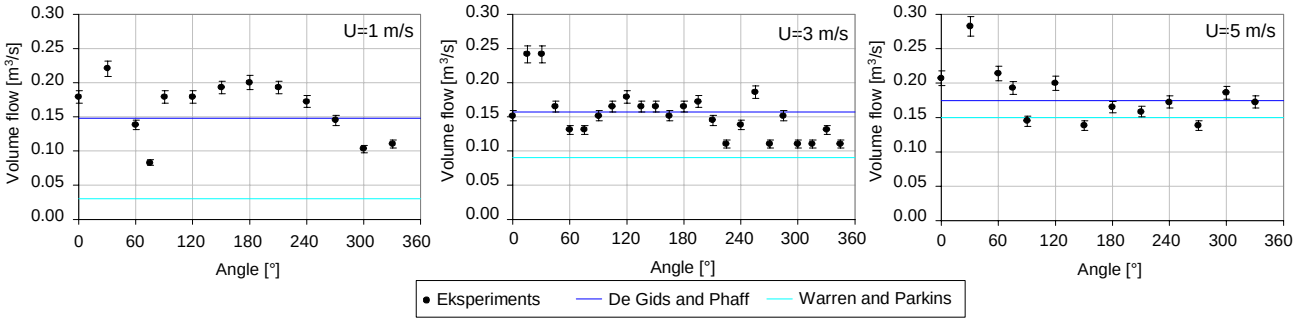

Figure 5.39. *Volume flow found by experiments and earlier expressions. Temperature difference =10 °C.*

In all the comparisons made it is seen how the volume flow depends on the incidence angle of the wind. This is also supported by the work of Warren /Warren77/ and Crommelin & Vrins /Crommelin et al. 88/ who all found the same tendency. Although Warren later on published a design expression for single-sided ventilation, this dependency was not directly included in the expression.

5.2.6 DESIGN EXPRESSION FOUND FROM THE RESULTS IN WIND TUNNEL

From the comparison with earlier design expressions by Warren & Parkins and De Gids & Phaff in the previous section it is seen that the volume flow through the opening in single-sided ventilation depends on the incidence angle of the wind. Furthermore, it is seen that an increase in temperature difference or wind velocity also in some cases will increase the flow. In this case, the increase is dependent on how the wind and temperature difference are combined and which of the two forces is the dominating one.

This tendency is also found in the velocity profiles seen in section 5.2.2, where the profile at a certain angle can change from wind dominated to temperature dominated when the temperature difference increases and visa versa.

From these results it is found that it is necessary to include the incidence angle of the wind in a new design expression for single-sided natural ventilation that also includes the combination of wind pressure and temperature difference to have a more accurate prediction of the airflow through an opening.

Before the work with the expression begins the different parameters that affect the airflow in single-sided natural ventilation will be listed. These are:

- Wind velocity
- Temperature difference
- Wind direction
- Opening area
- Geometry of the opening
- Position of the opening
- Shape of the building
- Surroundings of the building
- Turbulence in the wind
- Fluctuations in pressure at the opening
- Distribution of wind pressure and air velocity in the opening

The wind velocity (U) and temperature difference (ΔT) need to be included directly in the expression since no other parameter indirectly describes these two. The geometry of the opening can be included through the C_D-value. The wind direction (β) and the shape and surroundings of the building can be included through the C_p-value.

As a basis for a new design expression, the orifice equation in (5.6) is used. /Etheridge et al. 96/

$$Q_V = \pm C_D \cdot A_{eff} \cdot \sqrt{\frac{2 \cdot |\Delta P|}{\rho}} \tag{5.6}$$

where A_{eff} refers to the fact that only half of the opening area in single-sided ventilation is used for the ingoing airflow. A_{eff} can therefore be replaced by $\frac{1}{2}A$.

The pressure difference in expression (5.6) consists of contributions from wind, thermal buoyancy and fluctuations. This can be expressed as

$$Q_V = \pm C_D \cdot \tfrac{1}{2} A \cdot \sqrt{\frac{2 \cdot |\Delta P_{wind} + \Delta P_{thermal} + \Delta P_{fluct}|}{\rho}} \tag{5.7}$$

which is the same basic expression as used by De Gids and Phaff, /De Gids et al. 82/.

The idea for the calculation of pressure difference caused by wind is found from the expressions by Warren & Parkins described in chapter 2. Here it is found that

$$Q_V = 0.1 \cdot A \cdot U_L \tag{5.8}$$

$$Q_V = 0.025 \cdot A \cdot U_R \tag{5.9}$$

The connection between U_L and U_R is found by Warren & Parkins as a function of the incidence angle. Most often the incidence angle is included in calculations through the C_p-value which is much more common than the relation found by Warren in /Warren77/. Therefore, a connection between U_L/U_R and C_p is analysed. Here C_p-values from an exposed building with length to width ratio 2:1 is used, which is the same data as used in the outdoor experiments, /AIVC96/.

It is found that the shape of the curve from U_L/U_R can be expressed as a constant depending on the incidence angle (K_β) multiplied by num$(C_p)^{½}$. The shape of num$(C_p)^{½}$ is seen together with U_L/U_R in Figure 5.40. The expression is seen in (5.10).

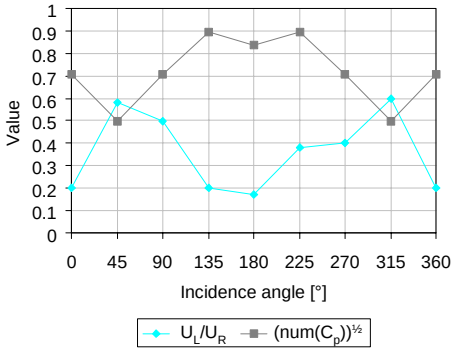

Figure 5.40. *Comparison of U_L/U_R and num$(C_p)^{½}$.*

$$\frac{U_L}{U_R} = K_\beta \cdot (num(C_p))^{½} \tag{5.10}$$

The value of the constant (K_β) is divided into windward, leeward and parallel flow so that three different constants are used. This is done in Figure 5.41 where the different incidence angles are marked with different colours. It is seen that a slight deviation exists at the windward side.

From expression (5.10) an expression for U_L can be found

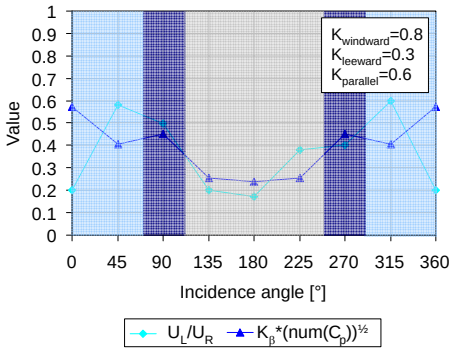

Figure 5.41. *Comparison of U_L/U_R and $K_\beta \cdot num(C_p)^{½}$ where K_β is a constant depending on the incidence angle. The values of K_β are shown at the top of the diagram.*

$$U_L = K_\beta \cdot (num(C_p))^{½} \cdot U_R \tag{5.11}$$

and from this combined with (5.6) an expression for ΔP_{wind} can be found

$$U_L = \sqrt{\frac{2 \cdot \Delta P_{wind}}{\rho}} = K_\beta \cdot (num(C_p))^{½} \cdot U_R$$
$$\Delta P_{wind} = \frac{\rho_e}{2} \cdot K_\beta^2 \cdot (num(C_p)) \cdot U_R^2 \tag{5.12}$$

An expression for the flow rate through a single large opening caused by thermal buoyancy was found in chapter 2. This is seen in (5.13) /Warren et al. 85/.

$$Q_v = \tfrac{1}{3} \cdot C_D \cdot A \cdot \sqrt{\frac{(T_i - T_e) \cdot g \cdot (H_t - H_b)}{\overline{T}}} \tag{5.13}$$

where

$$\sqrt{\frac{(T_i - T_e) \cdot g \cdot (H_t - H_b)}{\overline{T}}} = \sqrt{\frac{2|\Delta P|}{\rho}}$$

To isolate ΔP from the expression, some rewriting needs to be done. Since the difference in height in (5.13) is usually calculated from the bottom or top of the opening to the level of the neutral plane (H_0-H_1), the denomination with (H_t-H_b) has replaced 2(H_0-H_1) in the original expression.

$\Delta P_{thermal}$ is then found to be

$$\Delta P_{thermal} = \frac{(T_i - T_e) \cdot g \cdot (H_t - H_b)}{\overline{T}} \cdot \frac{\rho}{2} \tag{5.14}$$

In chapter 2 it was concluded that one of the main sources for the ventilation in single-sided ventilation is the turbulent movements in the opening. The last pressure difference included in expression (5.7) describes the airflow caused by the turbulence in the wind, the temperature difference and the pressure fluctuations, described by $\Delta C_{p,opening}$ which is the largest deviation between C_p-values in the opening. The parameters will be included in an empirical expression shown in (5.15).

$$\Delta P_{fluct} = \frac{½ \cdot \rho \cdot \Delta C_{p,opening} \cdot (T_i - T_e)}{U_{ref}^2} \tag{5.15}$$

The pressure differences found from expressions (5.12), (5.14) and (5.15) can now be inserted into (5.7).

$$Q_v = \pm C_D \cdot \tfrac{1}{2} A \cdot \sqrt{K_\beta^2 \cdot num(C_p) \cdot U_{R\,i}^2 + \frac{(T_i - T_e) \cdot g \cdot (H_t - H_b)}{\overline{T}} + \frac{\Delta C_{p,opening} \cdot (T_i - T_e)}{U_{ref}^2}} \tag{5.16}$$

The expression will be simplified by adding three constant weight factors which also include the constant or nearly constant parts of the pressure differences.

The determination of the C_D-value also includes some uncertainties and, therefore, this value is included directly as a part of the weight factors, which will make the expression valid only for openings with a C_D-value close to the one valid for this type of opening.

From these assumptions a basic design expression for single-sided ventilation can be set up. This is seen in (5.17).

$$Q_V = A \cdot \sqrt{C_1 \cdot num(C_p) \cdot U_{ref}^2 + C_2 \cdot \Delta T \cdot H + C_3 \cdot \frac{\Delta C_{p,opening} \cdot \Delta T}{U_{ref}^2}} \quad (5.17)$$

CALCULATION OF $\Delta C_{P,OPENING}$

To include the pressure fluctuations in the opening, the largest difference between the C_p-values measured around the edge of the opening is used. This difference is denoted $\Delta C_{p,opening}$. Since this value is difficult to measure or calculate in the daily work with natural ventilation, an expression for $\Delta C_{p,opening}$ expressed as a function of the incidence angle of the wind is made for design purposes. This can only be seen as a rough estimation since the expression will also depend on the position of the window in the building and therefore is only correct for this specific position.

The measured values of $\Delta C_{p,opening}$ are seen in Figure 5.42. The expression for the fitted curve is

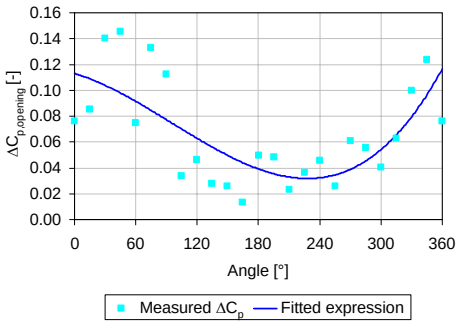

Figure 5.42. *Measured values of $\Delta C_{p,opening}$ as a function of the incidence angle (β) together with the curve for the fitted expression in (5.18).*

$$\Delta C_{p,opening} = 9.1894 \cdot 10^{-9} \cdot \beta^3 - 2.626 \cdot 10^{-6} \cdot \beta^2 - 0.0002354 \cdot \beta + 0.113 \quad (5.18)$$

NEW DESIGN EXPRESSION FOR SINGLE-SIDED VENTILATION

From the experiments it is seen that the wind is most dominating on the windward side of the building and that the temperature difference is most dominating on the leeward side of the building. Furthermore, it was found that that pressure difference caused by wind depends on the incidence angle of the wind. Therefore, it is decided to divide the calculation into the following three parts:

- Windward, β=285°-360°, β=0°-75°
- Leeward, β=105°-255°
- Parallel flow, β=90°, β=270°

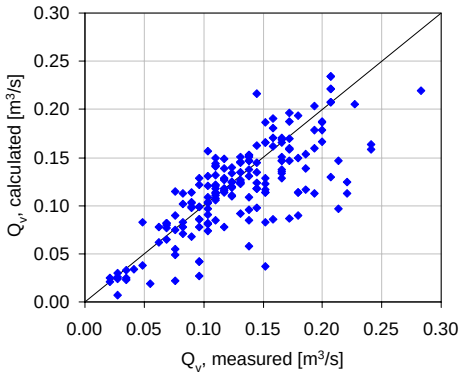

Figure 5.43. *Comparison between measured and calculated volume flows.*

By fitting the three constants C_1, C_2 and C_3 in expression (5.17) with the measurements in the windward, leeward and parallel cases, the following values for the constants are found:

	C_1	C_2	C_3
Windward:	0.0012	0.0006	-0.0006
Leeward:	0.0026	0.0006	0.0273
Parallel:	0.0012	0.0004	0.0097

where exp. (5.18) is used for calculation of $\Delta C_{p,opening}$.

To show the deviations between measured airflows from the experiments and calculated airflows from expression (5.17), the values are shown in Figure 5.43. Here it is seen that most of the points are close to the line x=y which shows a good correspondence between measured and calculated values.

It is also seen that the largest deviations between measured and calculated values are found when the calculated values are smaller than the measured ones. This must be seen as an advantage since the expression gives results on the safe side because the opening most often is easier to close than to extend.

In Figure 5.44, Figure 5.45 and Figure 5.46 the results for each combination of temperature difference and wind velocity are seen. A 5% margin of error is added to the measurements. This error is due to the uncertainties included in tracer gas methods, see the discussion in chapter 4.

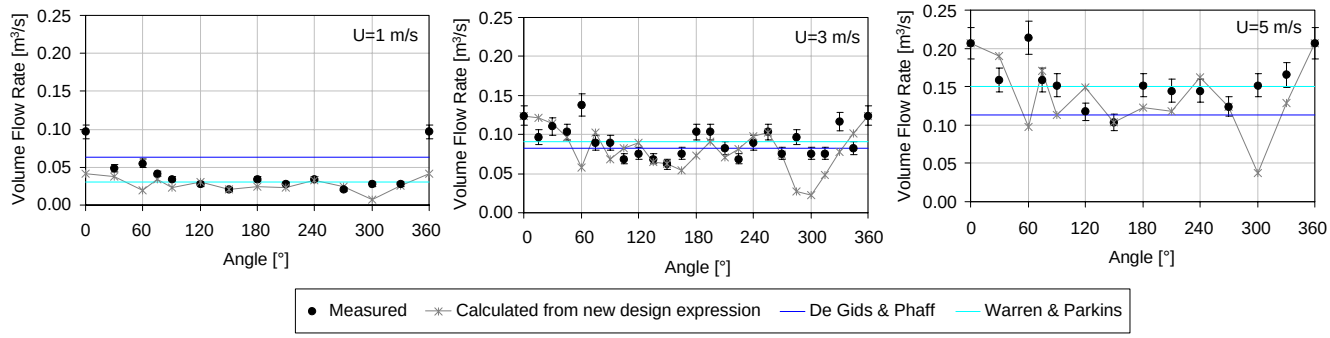

Figure 5.44. *The volume flow found by experiments and the new design expression in (5.17) compared with the expressions from De Gids & Phaff and Warren & Parkins. Temperature difference = 0 ℃.*

The results in Figure 5.44 are from the isothermal cases. It is seen that there are some problems with the calculation of the airflow around 300° when the velocity increases. This seems to be a general problem especially for 5 m/s.

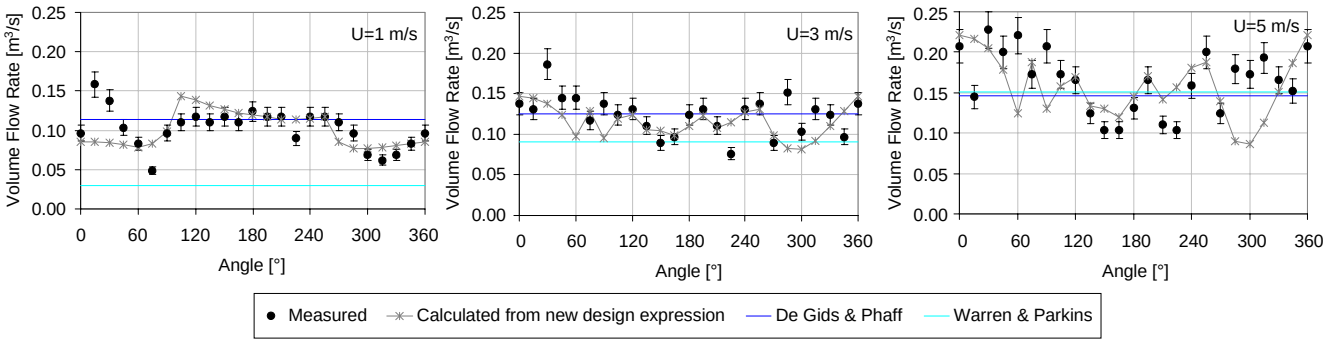

Figure 5.45. *The volume flow found by experiments and the new design expression in (5.17) compared with the expressions from De Gids & Phaff and Warren & Parkins. Temperature difference = 5 ℃.*

In Figure 5.45 the tendencies from the measurements are reasonably depicted in the calculations. A problem with underprediction is found at angles between 0° and 30° in U=1 m/s which is also seen in Figure 5.46. This must be due to the reason that these angles are wind dominated in all other cases and therefore not include the temperature effect very well when this is dominating.

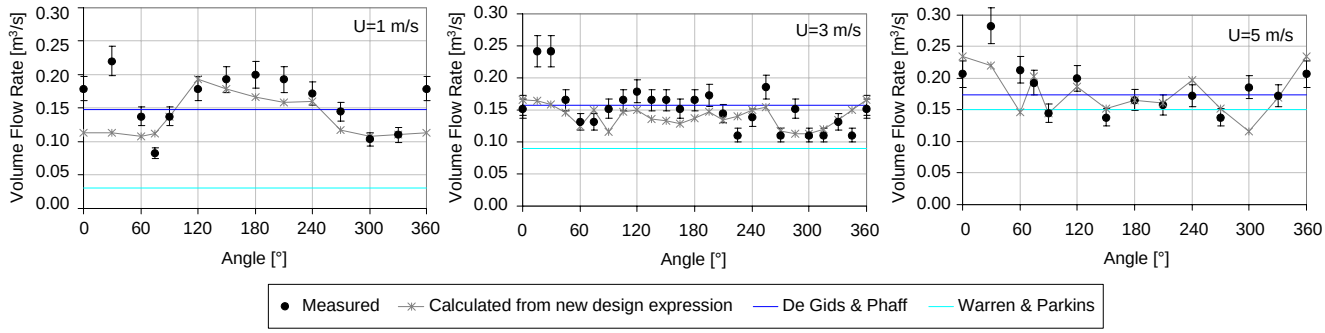

Figure 5.46. *The volume flow found by experiments and the new design expression in (5.17) compared with the expressions from De Gids & Phaff and Warren & Parkins. Temperature difference =10 ℃.*

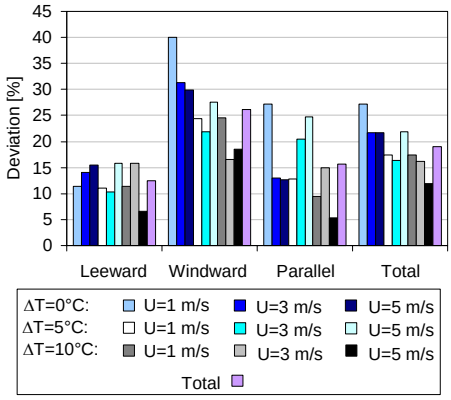

Figure 5.47. *Errors found for each case divided into leeward, windward or parallel.*

UNCERTAINTY IN THE CALCULATIONS

To have an idea of the deviations between the measured values and the calculated values found from the expressions, the deviation in % is found. This is calculated as an average value of the absolute %-values of the deviation, e.g. average of 10% and -10% = 10%.

If the error is estimated from the results of all the calculated values the average deviation is 19%. If the calculations are divided into the three cases mentioned above the following errors are found:

- Windward: 26%
- Leeward: 12%
- Parallel: 16%

The errors for each case are shown in Figure 5.47. It is seen that the largest errors are found at the windward side, which was also the side where the greatest deviation was found in the fitting between U_L/U_R and $num(C_p)^{½}$.

In the earlier expression found by De Gids & Phaff the average error for all cases was found as 29%.

If the results from for the new design expression are compared to the results from De Gids & Phaff an improvement in the predictions is obtained by including the incidence angle in the design expression. To this it must be stated that the new expression is fitted to the actual measurements and the conclusion can therefore not be seen as general. A further discussion of this is made in the conclusion in section 5.4.

5.3 SINGLE-SIDED VENTILATION, FULL-SCALE, OUTDOORS

The outdoor experiments were made in an office at the second floor in an office building at Aalborg University. The idea with the experiments was to check the design expression found from the wind tunnel experiment and maybe also adjust the constants in the expression if the outdoor experiments show a constant deviation from the design expression. The physical frames during the experiments are described in chapter 4.

In contrast to the experiments made in the wind tunnel it was difficult to get steady state conditions in these experiments. The problems with the outdoor conditions will be discussed in the next section. After this the results from the experiments will be described and analysed.

5.3.1 OUTDOOR CONDITIONS

A problem during the outdoor experiments was that it was impossible to control the conditions for wind direction, wind speed and temperature. Often the wind direction just outside the window changed during a measurement period, which lasted for 20 minutes. Another problem in the experiments was the main wind direction measured at the roof which was mainly coming from west during the 1½ month the experiments were running. This problem resulted in many cases being nearly the same. The outdoor conditions will be described in the following.

WIND DIRECTION

As mentioned above, one of the problems during the experiments was to achieve measurements with different wind directions. In Denmark the main wind direction is west and this is also clearly seen in these experiments. The wind directions recorded during all the experiments are shown in Figure 5.48. Here it is seen that eastern wind was only present in six experiments (36-42) all recorded during the same day. Southern wind was recorded in experiments 78-84 and south-eastern wind in experiments 91-94. Also these two directions were only present for one day.

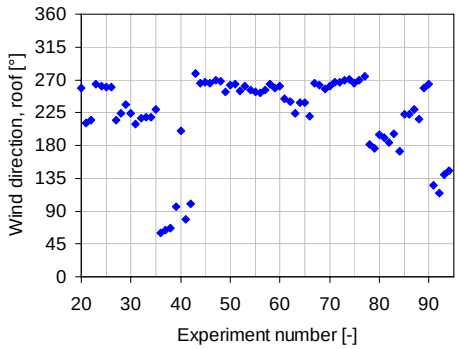

Figure 5.48. *Wind direction measured at the roof. (0°: north, 90°: east etc.)*

Due to the rotation of the building it is easier to transform the wind direction on the roof into an incidence angle at the window. Here the same definition of the incidence angle is used as in the wind tunnel experiments, where 0° corresponds to wind directly towards the window (see Figure 4.6). This can be seen in Figure 5.49. From this figure it is seen that in the main part of the experiments wind was coming directly towards the window and in only six experiments the window was at the leeward side. The small building model from appendix 2 can also be used for better understanding of the angles in these experiments since the same definition is used.

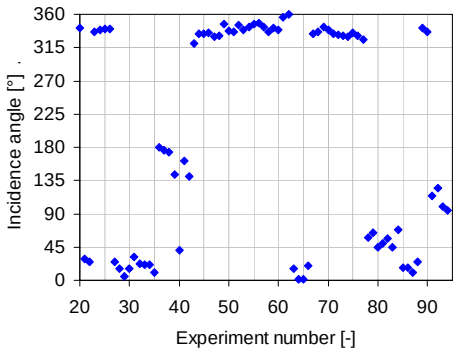

Figure 5.49. *Incidence angle measured according to the window (0°: Directly, 90°: from left side etc.)*

To be able to make a general evaluation of the expression found from the wind tunnel experiments, it is necessary to have many different incidence angles of the wind. This is not the case here, and this fact needs to be taken into consideration when a final comparison is made.

WIND SPEED

In the main part of the 75 experiments the wind speeds recorded were between 1 and 4,5 m/s. The wind tunnel experiments were made with velocities of 1, 3 and 5 m/s so this gives a good agreement later on when the results will be compared.

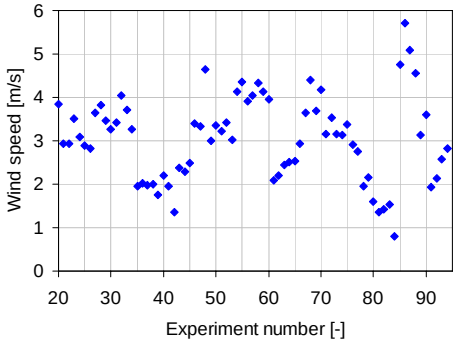

Figure 5.50. *Wind speeds during the outdoor experiments.*

TEMPERATURE DIFFERENCE

The main part of the experiments was made without any additional heating in the test office. The temperature difference in these experiments came from heat stored in the building. From experiment 71, heaters were added inside the room to increase the temperature difference.

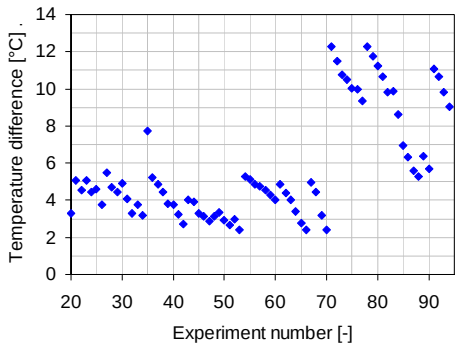

Figure 5.51. *Temperature differences during the outdoor experiments.*

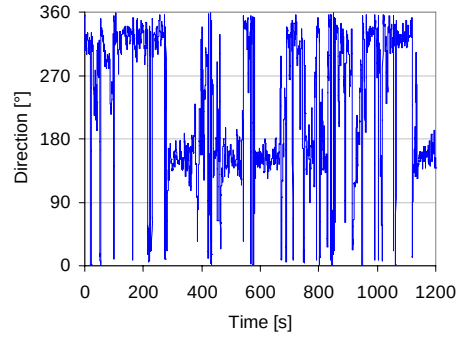

Figure 5.52. *Wind direction just outside the window in experiment 78.*

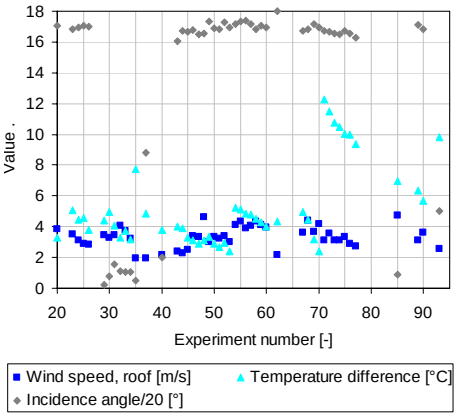

Figure 5.53. *Wind speed, incidence angle and temperature difference in the 48 cases selected for analysis.*

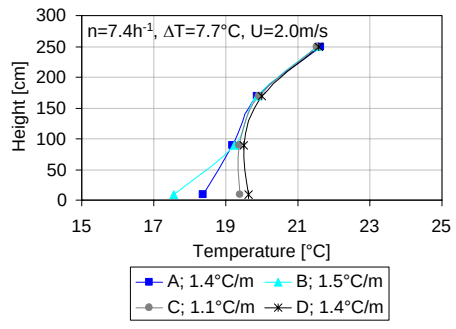

Figure 5.54. *Temperature gradients measured in case 35. Incidence angle = 10°.*

The recorded temperature differences are shown in Figure 5.51. Here it can be seen how the temperature difference drops during a row of experiments. The reason for this is the outside air which cools the room during the day. This also shows that the temperature difference is probably not steady during one experiment (20 minutes), but the change is very small and will therefore be ignored.

In the wind tunnel experiments temperature differences of 0, 5 and 10°C were used so also the temperatures are in good agreement when the results will be compared.

5.3.2 SELECTING CASES FOR ANALYSIS

To be able to compare the results from the outdoor experiments with the wind tunnel experiments, the conditions need to be steady. This concerns temperature difference, wind direction and wind speed at roof level and also wind direction outside the window. Especially the wind direction measured just outside the window has been a problem since the direction in some measurement periods changed 180°. Figure 5.52 shows one of these cases.

Since the effect of this sudden change in direction is unknown it was decided to remove all cases with many changes in direction from the data set. After this the number of experiments was reduced to 48.

The measured wind speed, incidence angles and temperature differences from the 48 cases selected for further analysis is shown in Figure 5.53. Here it is seen that the lowest wind speed was 2 m/s and that the incidence angle only in two cases deviated from wind directly towards the window.

The varieties in wind velocity and temperature differences are maintained even though the total amount of cases is reduced.

5.3.3 AIR-CHANGE RATES

As in the wind tunnel experiments, tracer gas was used to measure the air change rates, but in this case the constant injection method was used. Also in this case the temperature profiles are shown to judge the mixing between tracer gas and room air. To be able to compare the results with the temperature gradients found in the wind tunnel experiments case 35 and case 73 were picked out since these cases also had high temperature differences and low/high wind velocity, respectively. The results are shown in Figure 5.54 and Figure 5.55. The temperature gradients were calculated between 0.5m and 2.5m since this is how it was done in the wind tunnel experiments. Even though the conditions in cases 35 and 73 are different the measured air-changes were nearly the same. The reason for this can be the different incidence angles since an incidence angle of 330° also in the wind tunnel experiments resulted in relatively low air-change rates.

In both cases the temperature gradients was larger than those found in the wind tunnel experiments. Here the temperature gradients varied between 1.1 and 2.4°C/m. This indicates that the mixing between tracer gas and room air during the outdoor cases is less than during the wind tunnel experiments. This will probably result in the measured air-change rates being too high. Another source of error in the constant injection method is the possibility of tracer gas going directly out the window without mixing with the room air. This will also increase the measured air-change rate. In these experiments the tracer gas was added through four points in the room and only one of these points might have this direct access to the window. Therefore this error is estimated to be present but small.

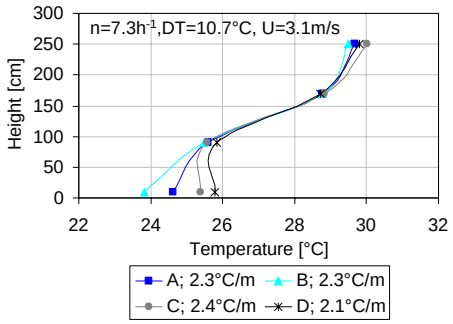

Figure 5.55. *Temperature gradients measured in case 73. Incidence angle = 331°.*

Before trying to divide the cases into smaller groups all data were plotted as a function of wind speed or temperature difference to find the effect of increasing wind speed and increasing temperature difference.

In Figure 5.56 the volume flow is held up against the wind speed measured at the roof. Here it is seen that increasing wind speed also results in increasing volume flow. The same tendency was found in the wind dominated cases from the wind tunnel experiments.

In Figure 5.57 the volume flow is plotted as a function of temperature difference. Here it is not possible to see the effect of increasing volume flow with increasing temperature difference. The reason for this may be that almost all cases must be considered as wind dominated cases because of the narrow interval of incidence angles.

In the following sections a more specific analysis is made on how the air change rate is affected in different situations. In these analyses the measurements are divided into smaller groups. The division is made from the experiences in the wind tunnel experiments which showed a clear difference between wind dominated and temperature dominated cases.

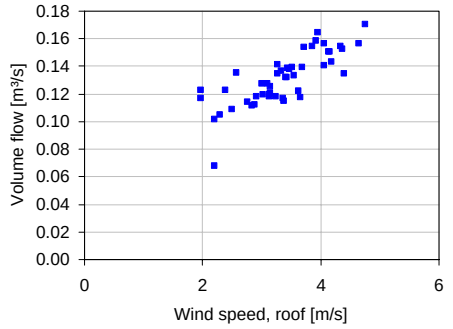

Figure 5.56. *Volume flow as a function of wind speed.*

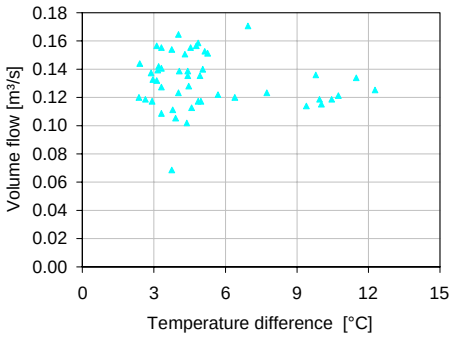

Figure 5.57. *Volume flow as a function of temperature difference.*

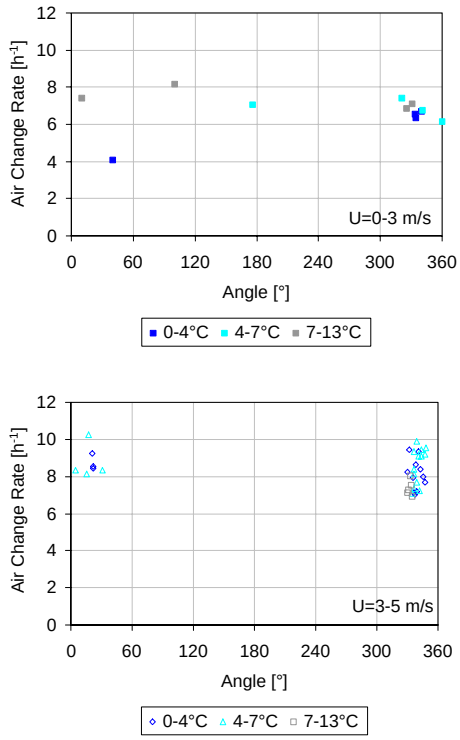

Figure 5.58. *Air change rate as a function of temperature difference at velocities from 0-3 m/s and 3-5 m/s.*

AIR CHANGE RATE AS A FUNCTION OF TEMPERATURE DIFFERENCE

To analyse how the temperature difference affects the air change rate, the measured wind speeds are sorted into two groups ranging from 0-3 m/s and 3-5 m/s. In the “0-3 m/s”-group there are 12 measurements and in the “3-5 m/s”-group there are 36 measurements. Afterwards, each group are divided into three groups of temperature differences ranging from 0-4°C, 4-7°C and 7-13°C.

In Figure 5.58 the result of the plots are shown. In the cases with low velocities (upper part of Figure 5.58) and wind coming directly towards the opening (330°-30°) no effect from the temperature difference can be seen. In the leeward cases a small effect is seen, but since there are only two measurements in this area the basis for conclusions is too small.

In the cases with higher velocities (lower part of Figure 5.58) it is not possible to see any effect at all from the temperature difference.

AIR CHANGE RATE AS A FUNCTION OF WIND SPEED

The same type of analysis is now made to see how the wind speed affects the air change rate at different temperature differences. In this case the measured temperature differences are divided into the same three groups of temperature differences ranging from 0-4°C, 4-7°C and 7-13°C and then afterwards are sorted into two groups ranging from 0-3 m/s and 3-5 m/s. In the "0-4°C"-group there are 18 measurements, in the "4-7°C"-group there are 21 measurements and in the "7-13°C"-group there are 9 measurements.

The results of the plots are shown in Figure 5.59. In the two cases with temperature differences from 0-4°C and 4-7°C (the two upper graphs in Figure 5.59) the cases can all be considered as wind dominated cases since higher wind velocity also results in higher air change rate.

In the cases with temperature differences from 7-13°C (lower graph in Figure 5.59) the effect from higher wind velocities is reduced, but can still be found in the cases with wind directly towards the window. In the case where the window is at the leeward side (angle is 100°) the air change rate has the same level as the other measured air change rates even though the velocity is low in this case. This indicates a temperature dominated case at this angle.

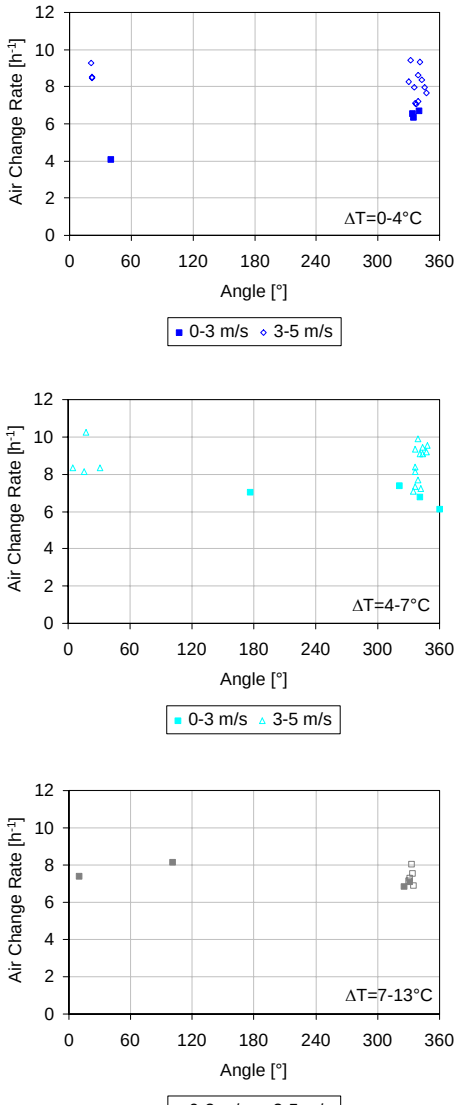

Figure 5.59. *Air change rate as a function of wind velocities at temperature differences from 0-4°C, 4-7°C and 7-13°C.*

5.3.4 VELOCITY PROFILES

To evaluate the shape of the velocity profiles, a wind dominated and a temperature dominated case have been picked out of the data set. The problem in this selection is that only four of the eight points with velocity measurements in the window gives the direction of the wind. These points are located at the corner points. To find a wind dominated case it was assumed that when the top and bottom point in a case were both negative, also the two vertical points between these were negative.

WIND DOMINATED CASE

As an example of the velocity profiles in a wind dominated case, case 20 was picked out.

This case has the following parameters:

Temperature difference:	3.3°C
Wind speed at roof:	3.9 m/s
Incidence angle	341°

The profiles are plotted in Figure 5.60. Here it is seen that the profiles are nearly similar, but the direction is mirrored. The air is going into the room in the left side of the opening (seen from inside). This is illustrated in Figure 5.61.

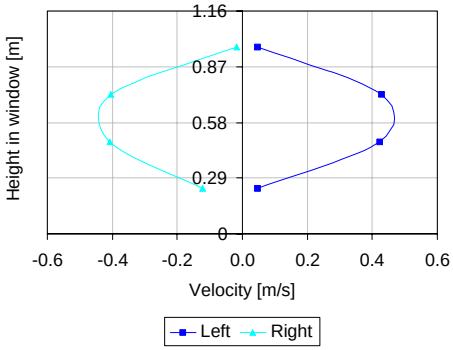

Figure 5.60. *Velocity profiles from case 20 (wind dominated). Positive values correspond to ingoing flow.*

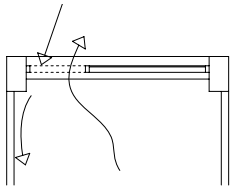

Figure 5.61. *Air streams in the room with an incidence angle of 340°.*

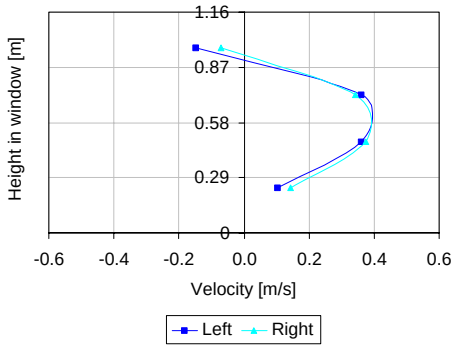

Figure 5.62. *Velocity profiles from case 93 (temperature dominated). Positive values correspond to ingoing flow.*

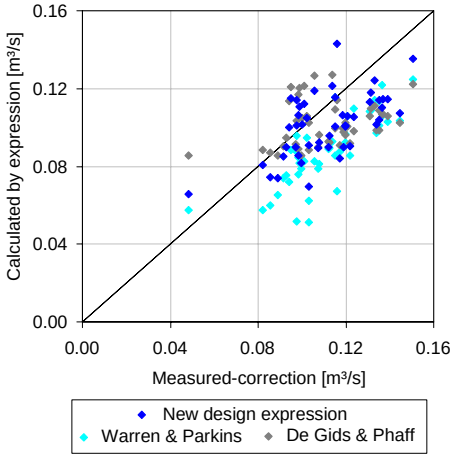

Figure 5.63. *Comparison between the measured values (corrected because of infiltration) and the flow rate calculated by the new design expression in (5.17), Warren and Parkins and De Gids & Phaff.*

The appearance of the profiles at this angle was also found in the wind tunnel experiments.

TEMPERATURE DOMINATED CASE

As an example of the velocity profiles in a temperature dominated case, case 93 was picked out. Contrary to case 20, the wind direction is in this case from south-east which places the window at the leeward side of the building.

This case has the following parameters:

Temperature difference:	9.8°C
Wind speed at roof:	2.6 m/s
Incidence angle	100°

The velocity profiles from case 93 are shown in Figure 5.62. In this temperature dominated case the air is going in through the lower part of the window and leaving the room again through the upper part of the window. Also this type of velocity profile was found in the wind tunnel experiments.

5.3.5 COMPARISON WITH EARLIER WORK

As with the results found from single-sided ventilation in the wind tunnel the results from the outdoor experiments will be compared to earlier design expressions.

Originally the outdoor experiments were meant to be used for correction of the expression found from the wind tunnel experiments. Since only a limited variety of incidence angles was obtained during the outdoor experiments, the measurements will instead be used as a control of the design expression found from the wind tunnel experiments. This decision will be discussed further in the conclusion in the next section.

In Figure 5.63 the measured values are compared to the calculated values. The measured values are corrected by the estimated error caused by leakage of the testoffice (see chapter 4). The comparison is made between measurements and calculations from Warren & Parkins, exp. (5.5), De Gids & Phaff, exp. (5.3), and the new design expression found in exp. (5.17). For the calculations from the new design expression, C_p-values are found from tables in /AIVC96/. $\Delta C_{p,opening}$ is found from the expression in (5.18).

In the comparison it is seen that almost all values calculated from Warren & Parkins are too low. The average deviation is 21%. The main reason for this is probably that the temperature difference is not included, since the same tendency was found for the experiments in the wind tunnel. Another reason can be the shape of the opening, but according to the window description in /Warren et al. 85/ the window seems alike. In the work of Warren and Parkins it is mentioned as a final comment that the constant in their expression is chosen so that the expression will give predictions that might be too small.

The results found from De Gids & Phaff and the new design expression are both giving reasonable results with some values too high and some

values too low. The averaged deviation calculated from absolute values (as described in 5.2.6) are 16% with De Gids and Phaff and 14% with the new expression. If the signs of the deviations are included the averages are found to be -6% with De Gids and Phaff and -7% with the new expression. This must be concluded as good for both expressions. However, the expression made by De Gids & Phaff does not include the incidence angle of the wind which also has an influence on the air change rate, but since the wind in most of the cases is coming directly towards the window it is not possible to show the effect of this difference in the two expressions. This is instead shown in the results from the wind tunnel experiments.

5.4 CONCLUSION – NEW DESIGN EXPRESSION FOR SINGLE-SIDED NATURAL VENTILATION

During the work with single-sided ventilation in the wind tunnel and outdoors a lot of experiments have been made and thereby knowledge about this type of ventilation is obtained.

Before the work started the aim was to find a new design expression for single-sided ventilation that included the shape of the building and the incidence angle of the wind. A design expression was found from the wind tunnel experiments (203 different cases) and the idea with the outdoor experiments was to be able to correct the expression from the results obtained outdoors, since it was suspected that the two types of wind were different.

Unfortunately, it was not possible to have a large variety of incidence angles during the outdoor experiments and, therefore, instead these experiments (48 different cases) were used as a control of the new design expression. The result from this showed good agreement with an average deviation of 14%.

At this point the question is then whether it is possible to use the results from the wind tunnel directly as done here - in fact with a good result! In chapter 3 a comparison between the characteristics of natural and mechanical wind was made. Here it was found that the dominating frequencies in mechanical wind were higher than the ones found in natural wind. This means that larger eddies are found in the natural wind which corresponds well to the fact that the limits for eddies is much bigger outdoors where they are set by other buildings or large obstacles. The differences between the two types of wind are shown in Figure 5.64 and Figure 5.65.

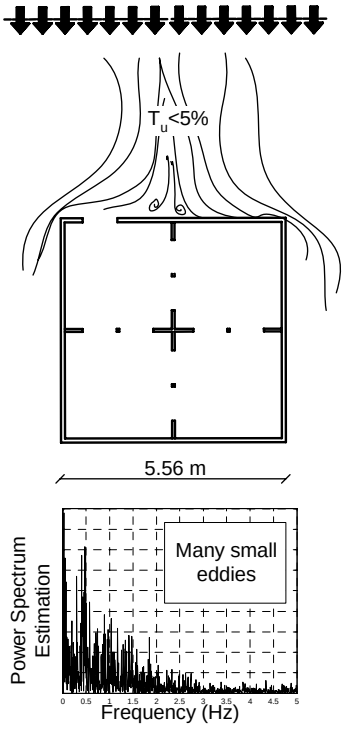

Figure 5.64. *Characteristics found for mechanical wind – building length = 5.56m..*

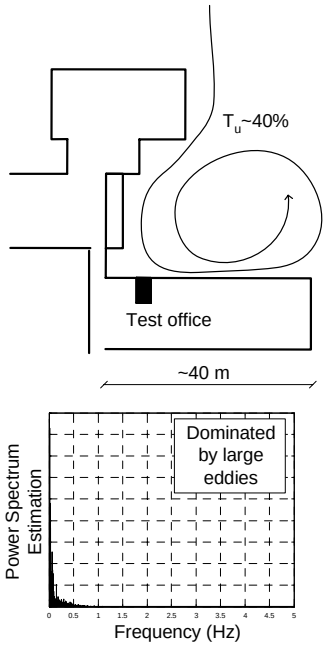

Figure 5.65. *Characteristics found for natural wind – test office building length = 40m.*

The differences in the two types of flows indicate that the airflow in single-sided ventilation is also driven by different forces depending on whether the wind is mechanical or natural. In the wind tunnel case the airflow through the opening is induced by pressure differences at the opening area (either by height or width) and by the small eddies in the wind that are smaller than the opening.

In the outdoor experiments it is shown that larger eddies are present than in mechanical wind, but at the same time the turbulence intensity is approximately 40% which shows that the direction and speed often changes. Therefore, the airflow in this case is mainly driven by the pulsations caused by wind gusts and changing wind direction.

Since it is shown that it is two different phenomena that mainly drive the airflow through the opening in mechanical wind and natural wind, it is interesting that good results are obtained anyway with the expression found from the wind tunnel experiments. The reason for this is, that all these unsteady parameters in the flow are included in the same term of the design expression and somehow have the same value in both situations.

NEW DESIGN EXPRESSION FOR SINGLE-SIDED NATURAL VENTILATION

From the above description of the differences between natural and mechanical wind it is concluded that the design expression found from wind tunnel experiments can be used without any corrections to predict airflows in single-sided ventilation in outdoor buildings.

The design expression is shown in (5.19).

$$Q_v = A \cdot \sqrt{C_1 \cdot num(C_p) \cdot U_{ref}^2 + C_2 \cdot \Delta T \cdot H + C_3 \cdot \frac{\Delta C_{p,opening} \cdot \Delta T}{U_{ref}^2}} \quad (5.19)$$

where the constants C_1, C_2 and C_3 are defined as:

	C_1	C_2	C_3
Windward:	0.0012	0.0006	-0.0006
Leeward:	0.0026	0.0006	0.0273
Parallel:	0.0012	0.0004	0.0097

and $\Delta C_{p,opening}$ is calculated from

$$\Delta C_{p,opening} = 9.1894 \cdot 10^{-9} \cdot \beta^3 - 2.626 \cdot 10^{-6} \cdot \beta^2 - 0.0002354 \cdot \beta + 0.113 \quad (5.20)$$

It is seen that the level of the constants C_1, C_2 and C_3 depends on the wind direction. This is due to the fact that the flows in the three cases (windward, leeward and parallel) are very different from each other and

therefore also have different weighting of the terms including wind pressure, thermal forces and fluctuating forces. Contrary to what was expected, C_1 does not have the largest weight factor at windward side, but it is the most dominating factor in this case. In the case where the opening is in the leeward side of the building the fluctuating term is the most dominating. This is also the case in the parallel situations, but here the difference is not as big as in the leeward case.

CHAPTER 6

Conclusion

As a summary of the results found in this thesis a conclusion is made. This is done for the results and ideas for future research found through this work are discussed.

6. CONCLUSION

During the experimental and analytical work with natural ventilation made in connection with this thesis, a lot of results have been found, but at the same time also a lot of new questions have appeared that need to be analysed further in the future. The results found in this work are described in section 6.1 and afterwards a discussion of the ideas and topics for further analysis is made in section 6.2.

6.1 RESULTS FROM THIS WORK

Even though natural ventilation is more and more often used for building ventilation, the design of openings for this type of ventilation still includes some uncertainties.

During studies of earlier work made in the area of natural ventilation, some different and unsolved questions popped up regarding the parameters that influence the airflow through openings in natural ventilation. One of the main questions was how the incidence angle of the wind can be included in predictions of the airflow through the openings. Earlier work by e.g. Warren & Parkins and Crommelin & Vrins has proven that some dependence exists, but neither has the wind direction included in their design expressions made for single-sided ventilation.

Figure 6.1. *The building in the wind tunnel at BRI.*

To analyse which parameters that affect the air change rate, experiments were made with cross-ventilation and single-sided ventilation in a full-scale building in a wind tunnel and with single-sided ventilation in an outdoor office. The two test facilities are shown in Figure 6.1 and Figure 6.2, respectively.

Figure 6.2. *The office building used for the outdoor experiments.*

CHARACTERISTICS IN NATURAL AND MECHANICAL WIND

By doing the experiments both in wind tunnel and outdoors it was necessary to know if any difference exists between the mechanical wind from the wind tunnel and the natural wind outdoors. This was analysed by spectral analysis and lagged scatterplots in chapter 3. Here it was found that the characteristics in mechanical wind differ from natural wind by having a larger variety of frequencies in the power spectrum. This means that mechanical wind consists of eddies in many different sizes contrary to natural wind which is mainly dominated by large eddies (low frequencies). One of the main reasons for this difference is the difference in scales of the surroundings. Outdoors the eddies are shaped by other buildings or very large scales in the atmosphere contrary to mechanical wind where the edges of the wind tunnel set the limit of eddies. By analysing the airflow in the opening it was found that also here the origin from either natural or mechanical wind can be traced in the power spectrum.

In this comparison of natural and mechanical wind the pressure distribution on the buildings was also compared. Here it was found that the only wind direction where the C_p-values differed was when the wind was coming directly towards the wall with the opening. Here the pressure near the ground in the wind tunnel was higher than outdoors because of the uniform velocity profile in the tunnel. In the area with the opening the

pressure distribution had the same tendencies and, therefore, it was decided that a comparison between the two different types of wind was feasible.

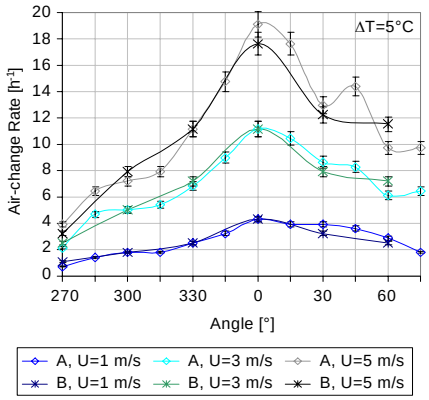

Figure 6.3. *The air change rate in cross-ventilation as a function of incidence angle in the case where ΔT=5°C.*

RESULTS FROM CROSS-VENTILATION

From the experiments with cross-ventilation a clear dependence of the incidence angle of the wind was found on the measured air change rates. An example of this is shown in Figure 6.3.

It was also investigated whether the position of the outlet opening influenced the airflow through the openings. This was done with two different cases where air was either crossing the room or going straight through the room. It was found that the air change rate was independent of the position, but the result will always depend on the shape of the building through the C_P-values.

Since the opening height in cross-ventilation was quite small (15 cm) and positioned at the same height in both sides of the building on effect from an increase in temperature difference was found. To investigate this effect, higher openings or openings in different heights were needed and, therefore, it was not included in this work.

From the measured air change rates the discharge coefficient (C_D) defined from the orifice equation was calculated in all cases. Here it was found that the assumptions concerning constant pressure and velocity distribution across the opening made in connection with the use of the orifice equation was not obtained in this work, since the C_D-values were varying at different incidence angles. The reason for this may be found in the porosity of the building (ratio between opening area and surface area) which was found as 0.95%. Earlier work by Jensen True, described in chapter 2 & 5, found that the limit between purely pressure driven flow and flow affected by the kinetic energy in the wind is around 1% porosity.

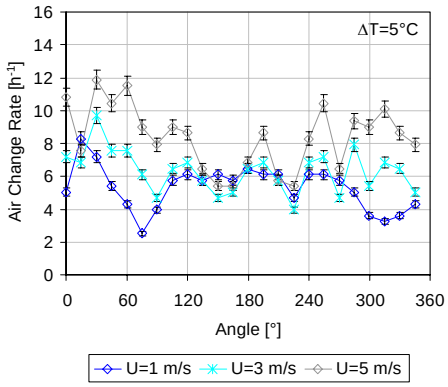

Figure 6.4. *The air change rate in single-sided ventilation as a function of incidence angle in the case where ΔT=5°C.*

RESULTS FROM SINGLE-SIDED VENTILATION

From the experiments made with single-sided ventilation in the wind tunnel it was seen that the air change rate also in this type of ventilation depends on the incidence angle. This is shown in Figure 6.4. It was also shown that the airflow through an opening does not depend on the volume behind the opening, which makes a design expression independent of this parameter.

In Figure 6.4 it is seen that the effect from increasing the wind velocity is different depending on the incidence angle. This shows that the dominating force (wind pressure or temperature difference) changes as a function of incidence angle. It was also found that it depends on the level of either the temperature difference or the wind velocity.

The same variation between temperature dominated and wind dominated cases was found in an analysis of the velocity profiles measured in these cases. An example of different shapes is shown in Figure 6.5.

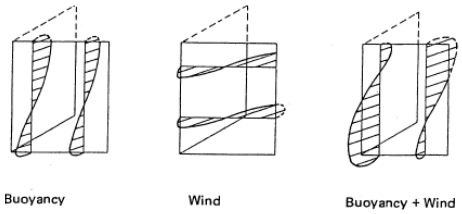

Figure 6.5. *Flow patterns through open windows in single-sided ventilation /De Gids et al. 82/.*

From the results found in the experiments and also by comparing them with earlier work with single-sided ventilation made by Warren & Parkins and De Gids & Phaff, it was found that to have a more accurate prediction of the airflow through an opening, it was necessary to include the incidence angle of the wind in a new design expression for single-sided natural ventilation that also included the combination of wind pressure and temperature difference.

From the wind tunnel experiments a new design expression was set up in chapter 5. The expression makes it possible to predict the airflow in single-sided ventilation. The design expression is divided into three cases because of different flow patterns near the opening. These cases depend on whether the opening is at the windward or the leeward side or has the flow direction parallel with the opening. The uncertainty in the predictions is found to be 19%, which is an improvement of the expression found by De Gids and Phaff who had an uncertainty of 29%. The new design expression can be seen in chapter 5.4.

As a final control of the design expression found through results from the wind tunnel experiments, 48 outdoor experiments were made and compared to the predictions obtained from the design expression. The deviation was in these cases found to be 14% which is considered satisfactory.

6.2 IDEAS FOR FUTURE WORK

Through the analyses and discussions in this work, some ideas for further research have arisen.

An area that needs more research is the difference between natural and mechanical wind. A lot of research within natural ventilation is made as wind tunnel experiments, since the conditions are much easier controlled inside a wind tunnel than outdoors where you really can feel the unsteadiness of the nature. The uncertainty with these kinds of experiments is more or less unclear, since the difference in mechanical and natural wind is a more or less unexplored area.

In the analysis with different characteristics of mechanical and natural wind in this work it was concluded that a difference exists between the two types of wind, but still after this work it seems unclear how this difference affects the obtained results. It was also found that the mechanical airflow just in front of the building in the wind tunnel had nearly natural characteristics, but the reason for this stays unclear.

In chapter 5.4 it was discussed whether the airflow through the opening in natural and mechanical wind is actually driven by two different parameters. It was suggested that the airflow in the wind tunnel case is induced by pressure differences at the opening area (either by height or width) and by the small eddies in the wind that are smaller than the

opening. In the outdoor case the airflow is mainly driven by the pulsations caused by wind gusts and changing wind directions.

In the new design expression found from this work the unsteady effects are all included in the same term of the expression. An idea for future work is to divide these effects into two different terms – one including the effect from turbulence in the wind and one including the pulsations in pressure in the opening. If this is done the expression will probably be more precise in the predictions, but still the uncertainty can never be cancelled out, since an uncertainty also lies within the decision of C_p-values, wind velocity and also the pressure difference in the opening ($\Delta C_{p,opening}$).

Another topic for future work was found during the work with cross-ventilation. Here calculations of the discharge coefficient (C_D) were made. From the calculations it was found that the C_D-value varied with the incidence angle of the wind. The reason for this variance is undefined and could come from a variation in pressure or velocity profile in the opening. Another reason can be that the C_D-value not is constant as suggested until now, but instead depends on the incidence angle. This assumption seems reasonable at least for deep openings where the airflow through the opening can be compared to an airflow through a duct. The question is just how deep the opening should be before this tendency will appear?

DANISH SUMMARY

Det følgende er et kort referat af ph.d. afhandlingen "Natural ventilation driven by wind and temperature difference".

Hovedemnet i rapporten er naturlig ventilation drevet af vindtryk og temperaturforskelle. Som det første gennemgås i kapitel 1 de parametre, der påvirker den naturlige ventilation i en bygning. Her er gennemgået, hvordan vejrdata inddrages i beregninger, og hvilken betydning det har, hvilke data der bruges. Bl.a. diskuteres det, om det er reelt kun at have ét vejrdatasæt for beregninger i hele Danmark. De karakteristiske træk ved vinden er også gennemgået, og der lægges op til en diskussion af forskellen mellem den vind, man oplever udendørs, og den vind, som findes under målinger i vindtunnel, hvor en del af målingerne i dette projekt er foretaget. Endelig defineres de drivkræfter, der driver den naturlige ventilation.

I kapitel 2 gennemgås beregningsgangen i naturlig ventilation sammen med tidligere forskning inden for området. Gennemgangen er opdelt i tværventilation og ensidet ventilation, da beregningerne er forskellige afhængigt af det princip, der ventileres efter. Beregning af luftstrømmen gennem en åbning i tværventilation er efterhånden veldefineret, og her ligger usikkerheden mest i bestemmelse af C_p- og C_D-værdier. I forbindelse med vurdering af C_D-værdien er tidligere arbejde af Jensen True gennemgået. I dette arbejde er det bl.a. undersøgt, om forudsætningerne om konstant tryk og hastighed i åbningen er opnået, når C_D beregnes, /True03/ & /Heiselberg et al. 05/. Det foreslås her, at strømningen gennem åbningen er afhængig af facadens porøsitet (forhold mellem åbningsareal og vægareal), og grænsen mellem rent trykdrevet flow og flow påvirket af den kinetiske energi i strømningen ligger i dette arbejde omkring 1%.

Ved beregning af ensidet ventilation bliver beregningerne mere komplicerede, da ventilationsmængden her påvirkes af turbulensen i vinden og trykændringer i åbningen forårsaget af fx vindstød og ændringer i vindretning. Da disse påvirkninger ikke er stationære, bliver usikkerheden ved beregning af luftmængder i ensidet ventilation væsentligt større. Desuden er der ikke noget entydigt svar på, hvordan luftmængden beregnes, men nogle forskellige udtryk gennemgås. Bl.a. medtages et beregningsudtryk opstillet af Warren & Parkins, som kun inddrager vindens hastighed samt åbningsarealet i deres udtryk. De foreslår samtidig, at der i tilfælde med både vind og temperaturforskel beregnes

som to separate bidrag, og herefter bruges det største bidrag som resultat. Et andet beregningsudtryk opstillet af De Gids & Phaff medtager både temperaturforskel og vindhastighed samt et konstant bidrag fra turbulensen i vinden. Det besluttes, at disse to udtryk senere vil blive sammenlignet med de resultater, der opnås fra målingerne i dette projekt, da det er interessant at se, hvilken betydning det har, om temperaturforskellen er inddraget eller ej. Ingen af de gennemgåede udtryk inddrager vindens indfaldsvinkel, selv om det tidligere er påvist, at denne også vil påvirke ventilationsmængden.

Ud fra gennemgangen i kapitel 2 opstilles målet for dette ph.d. arbejde som følgende:

> *Det ønskes at opstille et nyt designudtryk for ensidet naturlig ventilation, som inddrager vindens indfaldsvinkel. For at kunne opstille dette udtryk laves en række forsøg i vindtunnel. Forsøgene foretages både med ensidet ventilation og tværventilation, da det også ønskes undersøgt, om der findes afhængighed af vinklen ved tværventilation.*
> *Da forsøgene foretages i en vindtunnel, skal det desuden undersøges, om der evt. er nogen forskel på den type vind, der forekommer i en vindtunnel (mekanisk vind skabt af ventilatorer), og naturlig vind.*

I kapitel 3 foretages først en analyse af den nødvendige længde til en måleserie, når der foretages målinger af vindretning og hastighed udendørs. Denne periode skal minimum være 20 minutter lang, og målefrekvensen skal minimum være 5 Hz. Herefter sammenlignes den naturlige og mekaniske vind via spektralanalyse og en korrelationsmetode kaldet ”lagged Scatterplot”. Begge undersøgelser viser forskel i mekanisk og naturlig vind, og det konkluderes, at den dominerende hvirvelstørrelse i den naturlige vind er væsentligt større end i den mekaniske. Den mekaniske vind er mere præget af mange forskellige hvirvler med højere frekvenser – dvs mindre hvirvler. En endelig diskussion af betydningen af denne forskel foretages sammen med resultaterne af målingerne i kapitel 5.

I kapitel 4 er måleudstyr og testfaciliteter beskrevet med detaljer om hvordan forsøgene er gennemført. Der er i forsøgene brugt både sporgasmålinger (decay og constant-injection method) og hastighedsmålinger i åbningen til bestemmelse af luftskiftet i de enkelte forsøg. Usikkerheden ved disse metoder er diskuteret sidst i kapitlet. Her nævnes det bl.a., at den væsentligste forudsætning for korrekte sporgasmålinger er fuldstændig opblanding mellem sporgassen og rumluften. Desuden er der ved brugen af ”konstant-tilførsels-metoden”, som er brugt i forsøgene udendørs, risiko for at sporgassen forsvinder fx gennem vinduet uden at være blandet med rumluften. Disse fejl vil resultere i en overvurdering af luftskiftet. Det antages, at den samlede fejl ved sporgasmålingerne er ca. 5%.

I kapitel 5 gennemgås resultaterne af forsøgene lavet i vindtunnelen samt udendørs. I forbindelse med gennemgang af resultaterne for tværventilation konstateres det, at denne type ventilation afhænger af vindens indfaldsvinkel, og at hastigheden over åbningen i de fleste tilfælde varierer. Ved beregning af C_D-værdien for åbningen konstateres det, at denne varierer med indfaldsvinklen, og dermed ikke er konstant, som det ellers normalt antages. Årsagen til dette skyldes, at antagelserne om konstant tryk og hastighed over åbningen ikke er opfyldt. Desuden diskuteres det, om dybden af åbningen (som i disse forsøg var 10 cm) har nogen betydning for C_D-værdien, da åbningens karakteristik vil ændres når indfaldsvinklen ændres i tilfælde af en dyb åbning. Hermed vil der også opstå forskellige C_D-værdier afhængigt af indfaldsvinklen.

Ud fra resultaterne opnået med ensidet ventilation i vindtunnelen ses også her, at det fundne luftskifte er afhængigt af indfaldsvinklen. Desuden ses i disse forsøg, at størrelsen af påvirkningen fra henholdsvis vind og temperaturforskel også afhænger af vindens indfaldsvinkel. I de tilfælde hvor vinden er rettet mod åbningen, er det hovedsageligt vinden, der dominerer, men når åbningen er i læsiden, er det temperaturforskellen, der bliver den drivende kraft i luftstrømningen gennem åbningen. Analysen af resultaterne fra ensidet ventilation i vindtunnelen afsluttes med at opstille et nyt beregningsudtryk for denne type ventilation. I udtrykket inddrages vindens indfaldsvinkel indirekte via C_p-værdien for bygningen. Desuden defineres en ny parameter kaldet $\Delta C_{p,opening}$, som beregnes som den maksimale forskel i C_p-værdier på åbningsarealet beregnet enten lodret eller vandret, alt efter hvor værdierne findes. Ved brug af denne parameter inddrages variansen i trykket i åbningen. Der er i kapitel 5 også opstillet et udtryk til beregning af $\Delta C_{p,opening}$.

Ud fra beregninger foretaget med det nye beregningsudtryk findes frem til en usikkerhed i beregningerne på +/-19%. Foretages samme beregning med udtrykket fra De Gids og Phaff, findes en fejl på +/- 29%, så det ses her, at en inddragelse af indfaldsvinklen giver en mere præcis beregning af den forventede ventilationsmængde gennem åbningen.

Som en kontrol af det nye beregningsudtryk foretages 48 udendørs forsøg i en kontorbygning med et ensidet ventileret kontor. Da det danske vejr ofte har vindretninger fra vest, blev det under forsøgene svært at opnå andre retninger end denne, som svarede til vind direkte ind mod åbningen. De temperaturforskelle og vindhastigheder, der blev registreret, stemmer forholdsvis godt overens med de værdier, der er brugt i vindtunnelforsøgene. Ud fra beregninger af kontrolforsøgene blev der fundet frem til en fejl på 14% med det nye beregningsudtryk. Ved beregninger foretaget med udtrykket af De Gids og Phaff blev afvigelsen 16%, så i disse kontrolforsøg er der ikke stor forskel på nøjagtigheden af de to udtryk. Dette skyldes sandsynligvis, at der ikke er nogen variation i vindretningen, som det var tilfældet under vindtunnelforsøgene, hvor der blev fundet større forskel i nøjagtigheden af de to udtryk.

Efter denne kontrol af udtrykket konkluderes det, at udtrykket fundet i vindtunnelen også kan bruges i udendørstilfælde. Det diskuteres i denne sammenhæng, hvilken betydning det har, at forsøgene er lavet i vindtunnel med ”mekanisk” vind. Det blev fra resultaterne af

spektralanalysen konkluderet, at der er forskel på de to typer vind (mekanisk og naturlig vind), men effekten af denne forskel er ukendt. Sammenlignes trykfordelingen i de to tilfælde på området omkring åbningen, er der derimod ikke nogen stor forskel. Det besluttes derfor at bruge udtrykket uden korrigering af værdierne.

Ved opstilling af det endelige beregningsudtryk er der foretaget en diskussion af hvilke drivkræfter, der hovedsageligt driver vinden i vindtunnel-forsøgene og i de udendørs fuldskalaforsøg. Ud fra en vurdering af resultaterne fra spektralanalysen samt en vurdering af turbulensintensiteten konkluderes det, at de væsentligste drivkræfter for luftstrømningen gennem åbningen i vindtunnel-forsøgene er de små hvirvler i vinden ved mekanisk vind samt variationen i tryk på åbningsarealet. Turbulensintensiteten i vindtunnel-forsøgene er under 5%. Ved fuldskala-forsøgene, hvor turbulensen er oppe på ca. 40%, drives ventilationen hovedsageligt af vindstødene og hastighedsændringerne udenfor åbningen.

Til trods for denne forskel i drivkræfter i de to typer af vind opnås alligevel tilfredsstillende resultater ved brug af det samme designudtryk både for mekanisk og naturlig vind. Dette skyldes, at effekterne fra disse ikke stationære parametre alle er inkluderet i det samme led i designudtrykket og tilsyneladende har samme størrelse i de to situationer. En ide til fremtidigt arbejde er at opdele disse påvirkninger i to forskellige led for muligvis at forbedre nøjagtigheden ved beregningerne af ensidet ventilation, men foreløbig vælges det at benytte udtrykket med et enkelt led til at udtrykke de ikke stationære påvirkninger.

BIBLIOGRAPHY

/AIVC96/, Air Infiltration and Ventilation Centre
A Guide to Energy Efficient Ventilaiton, Annex V, AIVC, 1996, ISBN 0 946075 85 9

/ASHRAE01/
2001 ASHRAE Fundamentals, American Society of Heating, Refrigerating and Air-Conditioning Engineers, 2001, ISBN 1-883413-88-5

/By og Byg 202/, K.T. Andersen, P. Heiselberg, S. Aggerholm
By og Byg Anvisning 202: Naturlig ventilation i erhvervsbygninger. Beregning og dimensionering, Statens byggeforskningsinstitut, 2002, ISBN 87-563-1128-1

/Cockroft et al. 76/, J.P. Cockroft, P. Robertson.
Ventilation of an Enclosure Through a Single Opening, Building and Environment, Vol. 11, pp. 29-35, 1976

/Crommelin et al. 88/, R.D. Crommelin, E.M.H. Vrins.
Ventilation Through a Single Opening in a Scale Model, Air Infiltration Review, Volume 9, No. 3, 1988

/Dai et al. 03/, W. Dai, Y. Zhu, Q. Ouyang.
Research on the Fluctuating Characteristics of Mechanical Airflow, In proceedings of The 4th international Symposium on HVAC, Beijing, China, 2003

/Dascalaki 99/, E. Dascalaki, M. Santamouris, D.N. Asimakopoulos.
On the use of deterministic and intelligent techniques to predict the air velocity distribution on external openings in single-sided natural ventilation configurations, Solar Energy, Vol. 66, No. 3, pp. 223-243, 1999.

/De Gids et al. 82/, De Gids & Phaff.
Ventilation rates and energy consumption due to open windows: A brief overview of research in the Netherlands. Air infiltration review, 4(1), pp. 4-5, 1982

/DMI 99/, J. Cappelen & B. Jørgensen.
Technical report 99-13: Observed Wind Speed and Direction in Denmark - with Climatological Standard Normals, 1961-90, Danish Meteorological Institute, 1999

/Etheridge et al. 96/, D. Etheridge, M. Sandberg.
Building Ventilation – Theory and measurement, John Wiley & Sons Ltd., 1996, ISBN 0 471 96087 X

/Etheridge 02/. D. Etheridge.
Nondimensional methods for natural ventilation design. Building and Environment, Vol. 27, pp. 1057-1072, 2002.

/Haghighat et al. 00/, F. Haghighat, H. Brohus, J. Rao.
Modelling air infiltration due to wind fluctuations – a review,. Building and environment 35, pp. 377-385, 2000.

/Hara et al. 97/. T. Hara, M. Shimizu, K. Iguchi, G. Odagiri.
Chaotic Fluctuation in Natural Wind and its Application to Thermal Amenity, Nonlinear Analysis, Theory, Methods & Applications, Vol. 30, No. 5, pp. 2803-2813, 1997

/Heiselberg 05/. P. Heiselberg.
Natural and Hybrid Ventilation Notes, lecture notes from the PhD-course "Modelling natural and hybrid ventilation, Aalborg University, august 2005.

/Heiselberg et al. 05/. P. Heiselberg, M. Sandberg.
Wind Driven Natural Ventilation – Evaluation of the Classical Approach, 2nd International Workshop on Natural Ventilation, Tokyo, Japan, December 1-2, 2005

/Li et al. 05/, HJ. Li, XC. Chen, Q. Ouyang, YX. Zhu.
Wavelet Analysis on Fluctuating Characteristics of Airflow in Building Environments, In Proceedings of Indoor Air 2005, pp. 160-164.

/Matlab/, Matlab help file

/Ouyang et al. 03/, Q. Ouyang, Y. Zhu, W. Dai.
Study on Spectral Characteristics of Natural Wind in Built Environments, In proceedings of The 4th international Symposium on HVAC, Beijing, China, 2003

/Zhu et al. 03/, Y. Zhu, Q. Ouyang.
Airflow Fluctuations and Thermal Environment: A Literature Review, In proceedings of The 4th international Symposium on HVAC, Beijing, China, 2003

/Sandberg et al. 85/, M. Sandberg, C. Blomqvist.
A Quantitative Estimate of the Accuracy of Tracer Gas Methods for Determination of the Ventilation Flow Rate in Buildings, Building and Environment, Vol. 20, No.3, pp. 139-150, 1985.

/Sandberg et al. 89/, M. Sandberg, H. Stymne.
The Constant Tracer Flow Technique, Building and Environment, Vol. 24, No.3, pp. 209-219, 1989.

/Smith 97/, Steven W. Smith.
The Scientist and Engineer's Guide to Digital Signal Processing, California Technical Publishing, 1997, ISBN 0-9660176-3-3

/Stoica 97/, Petre Stoica & Randolph L. Moses.
Introduction to Spectral Analysis, Prentice-Hall, 1997, ISBN 0-1325841-9-0

/Straw 00/. M.P. Straw.
Computation and Measurement of Wind Induced Ventilation. Ph.D. thesis, University of Nottingham, 2000

/True 03/, J. P. Jensen True.
Openings in Wind Driven Natural Ventilation, PhD-thesis, Dept. of Building Technology and Structural Engineering, Aalborg University, Denmark, 2003

/Warren 77/, P.R. Warren.
Ventilation through openings on one wall only, Int. Conf. Heat and Mass Transfer in Buildings, Dubrovnik, Yugoslavia. In: Energy conservation in heating, cooling and ventilating buildings, Vol 1. eds. C. J. Hoogendorn and N. H. Afgar, pp 189-209. Hemisphere, Washington DC, 1977.

/Warren et al. 85/, P.R. Warren, L.M. Parkins.
Single-sided ventilation through open windows. In conf. Proceedings, Thermal performance of the exterior envelopes of buildings, Florida, ASHRAE SP 49, pp. 209-228, 1985

APPENDICES

APPENDIX 1 – MATLAB PROGRAMMES

All Matlab programmes, data files (.mat) and text files (.txt) used in the project can be send from the author if necessary. Here the content of the programs, data files and text files will shortly be described.

PROGRAM FILES

CompareFreq.m	Plot measurements made with different frequencies in the same graph.
Cp-matrice.m	This file contains C_p-values measured at 60 points at the closed building as a function of the incidence angle of the wind.
FrkvAnalyseTP.m	Compares measurements made at different frequencies.
LagScatOut.m	This file calculates the lagged scatterplots for experiments made outdoors. The calculations are made both with measurements in the free wind and measurements at four points in the opening.
LagScatWT.m	This file calculates the lagged scatterplots for experiments made in the wind tunnel. The calculations are made both with measurements in the free wind and measurements at a point in the opening.
pressure.m	Plots the distribution of C_p-values as a function of the incidence angle of the wind.
MeasureTime.m	Calculates the necessary duration for the measurements. Mean value and standard deviation are plotted as a function of the length of the measurement period.
SpectralOutFree.m	This program calculates the power spectrum for wind measurement made in the free wind during the outdoor measurements.
SpectralOutOpening.m	This program calculates the power spectrum for wind measurements made in the opening in the outdoor experiments.
SpectralWTFree.m	This program calculates the power spectrum for wind measurements made in the free wind in the BRI wind tunnel. The measurements are made at four different positions and five different heights
SpectralWTOpening.m	This program calculates the power spectrum for wind measurements made in the opening in the BRI wind tunnel. The calculations are made for three different points.

WindDirection.m	Loads the data of wind direction and plots it with respect to time. An averaged line with one minute values is also plotted in the graph.
WindSpeed.m	Loads the wind data and plots it with respect to time. An averaged line with one minute values is also plotted in the graph.
Zeropad.m	Gives an example of the effect of zero-padding.

.MAT FILES

analysetime.mat	This file contains all the data for direction and speed in a nine hour test period.
Openings20.mat	Data from the opening at case 20 outdoors.
Openings62.mat	Data from the opening at case 62 outdoors.
Openings89.mat	Data from the opening at case 89 outdoors.
Pos15.mat	Data from free wind at wind tunnel point 15 (in front of the building)
Pos43.mat	Data from free wind in wind tunnel point 43 (right side of the building)
Pos57.mat	Data from free wind in wind tunnel point 57 (left side of the building)
Pos70.mat	Data from free wind in wind tunnel point 70 (behind the building)
WindSpeed53.mat	Wind speed measured outdoors in case 53.

.TXT FILES

Case20 – out.txt	Data from the opening in case 20 outdoors.
Case62 – out.txt	Data from the opening in case 62 outdoors.
Case89 – out.txt	Data from the opening in case 89 outdoors.
Hast53.txt	Wind speed measured outdoors in case 53.

APPENDIX 2 – "DO-IT-YOURSELF" BUILDING MODEL

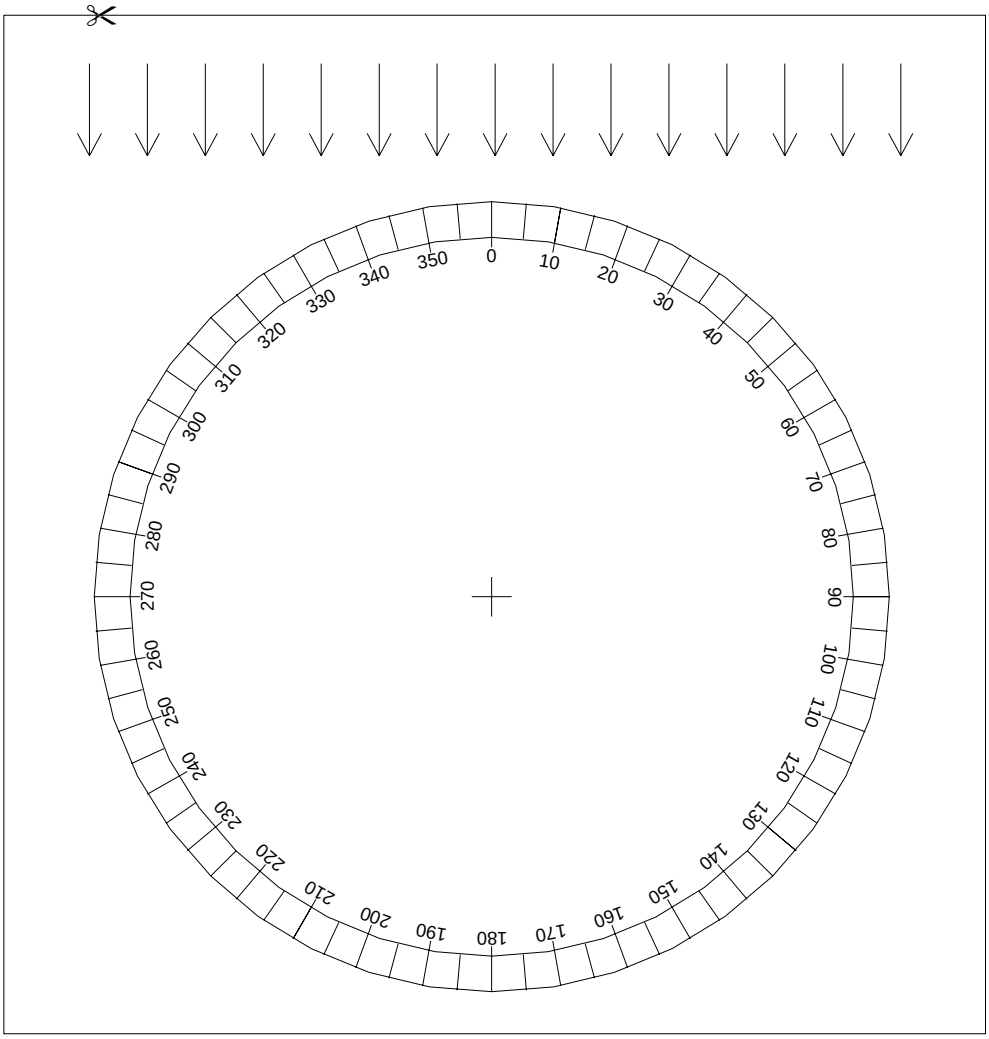

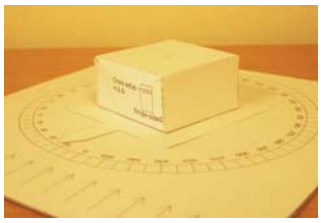

DESCRIPTION

Cut along the edges. Bend the building model along the dashed lines and fix it to the small square with the arrow. Fix the "wind tunnel" floor to a piece of cardboard and put a paper clip through the mark in the middle. The building model is then put onto this clip.

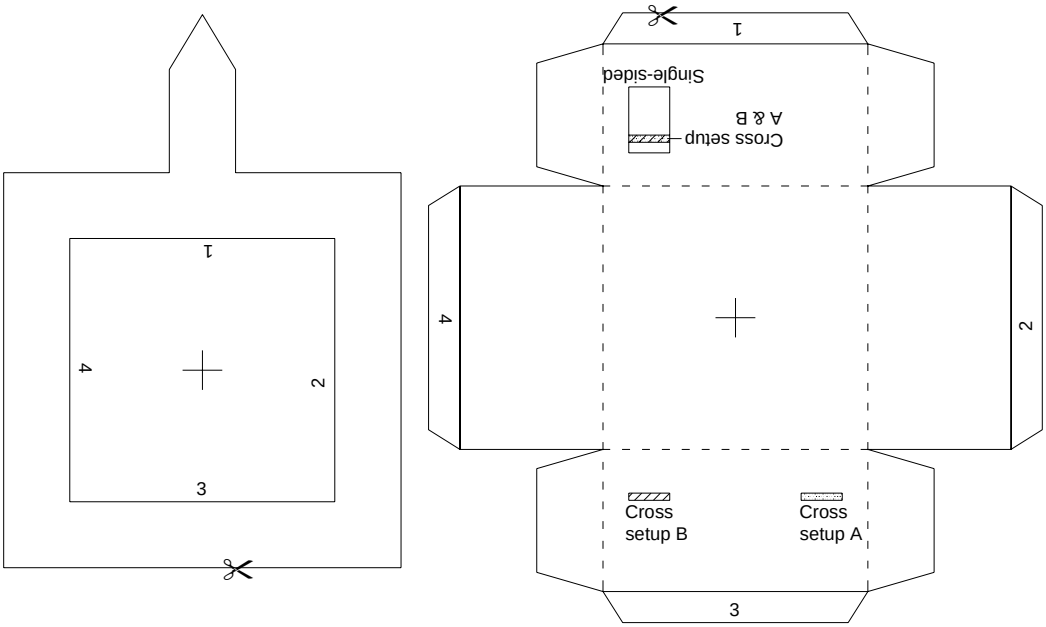

APPENDIX 3 – TEST PLAN FOR WIND TUNNEL EXPERIMENTS

Test		S1	S2	S3	S10	S11
Set-up		1A	1A	1A	1B	1C
Temperature difference	[°C]	0	0	0	0	0
Angle	[°]	0..30..330	0..15..345	0..30..330	0..30..330	0..30..330
Velocity	[m/s]	1	3	5	3	3
Number of sequences pr test		11	23	11	11	11
Total number of sequences				67		
Estimated days				12		

Test		S4	S5	S6
Set-up		1A	1A	1A
Temperature difference	[°C]	5	5	5
Angle	[°]	0..15..345	0..15..345	0..15..345
Velocity	[m/s]	1	3	5
Number of sequences pr test		23	23	23
Total number of sequences		69		
Estimated days		12		

Test		S7	S8	S9	S12	S13
Set-up		1A	1A	1A	1B	1C
Temperature difference	[°C]	10	10	10	10	10
Angle	[°]	0..30..330	0..15..345	0..30..330	0..30..330	0..30..330
Velocity	[m/s]	1	3	5	3	3
Number of sequences pr test		11	23	11	11	11
Total number of sequences				67		
Estimated days				11		

Measurements made during experiments with single-sided ventilation.

Test		C1	C2	C3	C4	C5	C6
Set-up		2A	2A	2A	2A	2A	2A
Temperature difference	[°C]	0	0	0	5	5	5
Angle	[°]	0..30..150	0..15..165	0..30..150	0..15..165	0..15..165	0..15..165
Velocity	[m/s]	1	3	5	1	3	5
Number of sequences pr test		6	12	6	12	12	12
Total number of sequences			24			36	
Estimated days			4			6	

Test		C7	C8	C9	C10	C11	C12
Set-up		2A	2A	2A	2B	2B	2B
Temperature difference	[°C]	10	10	10	0	0	0
Angle	[°]	0..30..150	0..15..165	0..30..150	0..30..150	0..30..150	0..30..150
Velocity	[m/s]	1	3	5	1	3	5
Number of sequences pr test		6	12	6	6	6	6
Total number of sequences			24			18	
Estimated days			4			3	

Test		C13	C14	C15	C16	C17	C18
Set-up		2B	2B	2B	2B	2B	2B
Temperature difference	[°C]	5	5	5	10	10	10
Angle	[°]	0..30..150	0..30..150	0..30..150	0..30..150	0..30..150	0..30..150
Velocity	[m/s]	1	3	5	1	3	5
Number of sequences pr test		6	6	6	6	6	6
Total number of sequences			18			18	
Estimated days			3			3	

Measurements made during experiments with cross ventilation.